Technische Universität München
Fakultät für Chemie
Professur für Zelluläre Proteinbiochemie

Folding and quality control of the cytokines interleukin 12 and interleukin 23

SUSANNE MEIER

Vollständiger Abdruck der von der Fakultät für Chemie der Technischen Universität München zur Erlangung des akademischen Grades eines

Doktors der Naturwissenschaften (Dr. rer. nat.)

genehmigten Dissertation.

Vorsitzende: Prof. Dr. Kathrin Lang

Prüfer der Dissertation: 1. Prof. Dr. Matthias J. Feige

2. Prof. Dr. Johannes Buchner

Die Dissertation wurde am 01.04.2019 bei der Technischen Universität München eingereicht und durch die Fakultät für Chemie am 03.06.2019 angenommen.

Parts of this thesis have been published in peer-reviewed journals:

Assembly-induced folding regulates interleukin 12 biogenesis

Susanne Reitberger, Pascal Haimerl, Isabel Aschenbrenner, Julia Esser-von Bieren and Matthias J. Feige

J Biol Chem. 2017;292(19), pp 8073-8081

Parts of this thesis have been presented at scientific conferences:

27th Faltertage

21th – 23th October 2016, Halle an der Saale, Germany

oral presentation

3rd Sino-German Symposium on Protein Folding, Redox Regulation and Quality Control

18th – 19th October 2017, Beijing, China

oral presentation

All things are difficult before they are easy.

Thomas Fuller

ACKNOWLEDGEMENTS

At first, I would like to thank Prof. Dr. Matthias Feige for giving me the opportunity to conduct my Ph.D. studies in his research group and for his trust in hiring me as one of his very first students. His guidance, inspiration and patience helped me in all difficult situations during my Ph.D. studies.

Furthermore, I am very thankful to Prof. Dr. Johannes Buchner for agreeing to be the second reviewer of this thesis. I would also like to thank Prof. Dr. Kathrin Lang for chairing on my defense committee.

I want to thank all the people I collaborated with during the last years. Pascal Haimerl, Julia Esser-von Bieren, Abraham Lopez, Christian Choe, Philipp Schmid, Florian Rührnößl, Martin Haslbeck, Michael Sattler and Po-Ssu Huang contributed with their expertise and ideas to the success of my projects. It has been a pleasure working with you!

I am also very grateful to all CPB lab members who contributed with theoretical and psychological support on very hard days in the lab. I will miss every one of you! I am going to miss João, whistling Fado; Yonatan´s surprising “Oh really???”; Stephie´s “Dos & Don´ts” labels in the lab; Karen´s Wednesday question: “Do we bring our running cloths tomorrow? “ (I´m very glad you did this); Nico, telling me about his holiday plans every three months; Anna always coming to our lab, closing the centrifuge; putting back the milk into the fridge after Matthias had his afternoon cappuccino. Besides the CPB group members, I also found friends in other research groups. You always cheered me up! Thanks for that!

My interns, bachelor and master students, Marie-Lena Jokisch, Isabel Aschenbrenner, Carolin Klose, Anna Folz and Sina Bohnacker deserve special thanks for their hard and enthusiastic work and I wish you all the best for the future. I always enjoyed working with you, also on a personal level! I am very proud of having had the chance to contribute to what kind of scientists you are now!

Additionally, I want to thank Anna and Carolin who supported my work and the whole lab by their technical assistance.

Furthermore, my thanks go to Münchner Verkehrsgesellschaft, you gave me the opportunity to read a lot of papers, while I was waiting for one of your trains or when I was stuck in a tunnel. That made me a better scientist for sure!

Finally, I would like to give special thanks to my family who always supported me and believed in me, although they did not really know what I was actually doing! Above all I thank my husband Robin who spent so many Saturdays together with me in the lab! I am looking forward to all future Saturdays, as long as you are with me!

ABSTRACT

Interleukins are small immunoregulatory proteins, circulating in the tissue environment. The interleukin (IL) 12 family is of particular interest due to its unique structural properties. The heterodimeric IL-12 family members show extensive subunit sharing within the family: four functionally distinct heterodimers (IL-12, IL-23, IL-27, IL-35) are produced from only five subunits (IL-12α, IL-23α, IL-27α, IL-12β, EBI3). For instance, IL-12 and IL-23 are composed of one shared IL-12β and individual IL-12α or IL-23α subunits. Due to their wide functional spectrum, IL-12 family members are intimately involved in multiple pathologies from autoimmunity to cancer. As secreted proteins interleukins cotranslationally enter the endoplasmic reticulum (ER) where they obtain folding and pass ER quality control (QC) prior to secretion. While the major setup of the ER folding machinery has been described in recent years, mechanistic insights into protein folding and quality control (QC) pathways are still missing *in vivo*. Furthermore, it remains unclear how cells discriminate unassembled proteins *en route* to the native state from misfolded ones that need to be degraded.

This thesis shows that assembly-induced folding is key for the biogenesis of IL-12 and IL-23. Isolated α subunits fail to form their native structure but instead misfold, including formation of incorrect disulfide bonds. Co-expression of their designate β-subunit inhibits misfolding and thus allows biologically active heterodimeric ILs to be secreted. Based on these findings, we identified the cysteine residues in IL-12α and IL-23α that are critical for assembly-induced secretion and biological activity *versus* misfolding and degradation.

Furthermore, we found that a single helix in the IL-23 α-subunit remains incompletely structured until assembly with its β-subunit occurs. Incomplete folding of this substructure is recognized by different chaperones along the secretory pathway, regulating sequential assembly control. Structural optimization of the chaperone recognition site allows to overcome quality control checkpoints and results in a secretion-competent IL-23α subunit, which can still form functional heterodimeric IL-23. Additionally, we show that simplified yet functional IL-12 and IL-23 cytokines are possible which may also provide attractive opportunities for pharmacological interventions.

Our detailed molecular analysis of IL-12 and IL-23 biogenesis contributed to the understanding, how small single domain proteins regulate and combine folding, degradation, quality control and interaction signals within a spatial limited topology.

ZUSAMMENFASSUNG

Interleukine sind kleine immunoregulatorische Proteine, die frei im Gewebe zirkulieren. Ein einzigartiges Merkmal der IL-12 Familie ist ihre heterodimere Struktur und das Verwenden von gleichen Untereinheiten in mehreren Familienmitgliedern: vier Heterodimere (IL-12, IL-23, IL-27, IL-35) werden von nur fünf unterschiedlichen Untereinheiten (IL-12α, IL-23α, IL-27α, IL-12β, EBI3) gebildet. IL-12 und IL-23 bestehen beispielsweise aus der gleichen β Untereinheit aber individuellen α Untereinheiten. Ihre vielfältigen Funktionen führen dazu, dass die IL-12 Familie an einer Vielzahl von Erkrankungen beteiligt ist, unter anderem an Autoimmunreaktionen und Krebs. Interleukine werden cotranslational in das ER transportiert, wo sie eine native Struktur ausbilden können und einer Qualitätskontrolle unterzogen werden, die es nur vollständig gefalteten Proteinen erlaubt die Zelle zu verlassen. Obwohl ein Großteil der Proteine, die an der Qualitätskontrolle beteiligt sind bereits bekannt ist, ist das mechanistische Verständnis dieses Prozesses auf zellulärer Ebene noch unvollständig. Des Weiteren ist noch nicht vollständig geklärt, wie Zellen es bewerkstelligen zwischen korrekt gefalteten aber noch nicht assemblierten Proteinen und ungefalteten Proteinen zu unterscheiden.

Die folgende Arbeit zeigt, dass eine Interaktions-basierte Faltung ein Schlüssel-mechanismus in der Biogenese der IL-12 Familie ist. Die α-Untereinheiten von IL-12 und IL-23 können keine vollständige Faltung in der Zelle ausbilden, was mit einer falschen Verknüpfung von Disulfidbrücken einhergeht. Erst die Interaktion mit IL-12β induziert vollständige Faltung und führt zur Sekretion des biologisch aktiven IL-Komplexes. Darauf aufbauend konnten Disulfidbrücken in IL-12α und IL-23α identifiziert werden, die entweder essentiell für die Assemblierung und biologische Aktivität sind oder aber an der Fehlfaltung der Proteine beteiligt sind. Außerdem konnte ein Bereich in IL-23α identifiziert werden, der ungefaltet vorliegt und von unterschiedlichen Chaperonen in der Zelle erkannt wird, solange bis die Interaktion mit der β-Untereinheit stattfindet. Strukturelle Optimierung beider Interleukine hat es ermöglicht vereinfachte Varianten der IL-12 und IL-23 Komplexe und ebenso einer stabilen IL-23α Untereinheit herzustellen, die weiterhin biologisch aktiv bzw. neue potenzielle biologische Aktivitäten aufweisen könnten.

LIST OF ABBREVIATIONS

β-Me	β-mercaptoethanol
APC	antigen presenting cell
AUC	analytical ultracentrifugation
BiP	heavy chain binding protein
BSA	bovine serum albumin
°C	degree Celsius
CD	circular dichroism
CHX	cycloheximide
CNX	calnexin
CRT	calreticulin
DC	dendritic cell
DTT	dithiothreitol
DUB	deubiquitinating enzyme
DMEM	Dulbecco´s modified Eagle´s medium
EBI3	Epstein-Barr virus-induced gene 3
EDEM	ER degradation-enhancing α-mannosidase-like protein
EDTA	ethylenediaminetetraacetic acid
ER	endoplasmic reticulum
ERGIC	ER-Golgi intermediate compartment
ERMan	ER mannosidase
Ero1α	endoplasmic reticulum oxidoreductin-1α
Fn	Fibronectin
GI	α-glucosidase
GSH	reduced glutathione
GSSG	oxidized glutathione
h	hour(s)
HC	heavy chain
HDX	hydrogen/deuterium exchange
HGMR	HMG-CoA reductase
HMW	high molecular weight
hPBMC	human peripheral blood mononuclear cells
HSQC	heteronuclear single quantum coherence
IFN-γ	interferon- γ
Ig	immunoglobulin
IL	interleukin
IP	immunoprecipitation
Jak	Janus kinase
L	lysate
LC	light chain
LMW	low molecular weight
M	medium
(m)M	(milli) molar
min	minute
mL	milliliter
MW	molecular weight
NEM	N-Ethylmaleimide
NK	natural killer
nm	nanometer
NMR	nuclear magnetic resonance
OST	oligosaccharyltransferase
P	pellet
PBS	phosphate buffered saline
PDI	protein disulfide isomerase
PPIase	peptidyl-prolyl *cis-trans* isomerases
QC	quality control
RNC	ribosome-nascent chain
RORγt	retinoic acid receptor-related orphan receptor- γt
RT	room temperature
S	soluble
SEM	standard error of the mean
SERCA	sarcoplasmic/endoplasmitic-Ca^{2+} ATPase
SD	standard deviation
SRP	signal recognition particle
SS	disulfide bond
STAT	signal transducers and activators of transcription
$t_{½}$	half-life
T_H1	type 1 T-helper
T_H17	type 17 T-helper
Tm	tunicamycin
Trx	thioredoxin
UGGT	UDP-glucose:glycoprotein glucosyltransferase
UPR	unfolded protein response
UV	ultraviolet
wt	wild type

TABLE OF CONTENTS

1 Introduction

1.1 The interleukin 12 family

1.1.1 Interleukins are key messengers of the human immune system

It is our immune system that allows survival in the everyday competition with invaders such as viruses, bacteria, parasites and toxins. The immune system is an incredibly complex, interconnected multi-layered system that expands with every single challenge, making it unique for every human being. A fundamental feature of our immune system is the discrimination between self and non-self[1]. This ability allows the immune system to attack foreign substances without damaging the host. As a first line of defense physical (skin) or chemical barriers and the innate immune system respond to different threats. The innate immune system is one of the first defense mechanisms, which becomes activated upon pathogen encounter. An innate immune response exists in vertebrates and invertebrates, as well as in plants, and the basic mechanisms are conserved within this evolutionary old system. Secreted molecules like the complement system and cellular components of the innate immune system are the first defense mechanism of the body that encounter invading pathogens. In humans, leukocytes like mast cells, phagocytes, dendritic cells (DC) or natural killer (NK) cells patrol the tissues of our body, recognizing invaders by molecular patterns typically associated with pathogens. The innate immune system provides an immediate and fast immune response, eliminating pathogens that might cause infection and activates the second major layer of our immune system, the adaptive immunity[1,2]. The latter is evolutionary younger and only present in vertebrates. Once activated, it guarantees a highly specific reaction to the particular pathogen and provides a long-lasting protection by establishing an immunological memory. Adaptive immune responses are carried out by two main classes of leukocytes: B- and T-cells. Activated B cells secrete antibodies that specifically recognize a certain pathogen, leading to its inactivation and mark it for phagocytosis. T cells are part of the cell-mediated immune response of the adaptive immune system and a subset of T cells directly recognize and eliminate infected host cells. Furthermore, T cells produce signals that either further enhance, regulate or dampen inflammations[2]. An effective and fast immune response upon pathogen encounter requires an efficient and reliable immune cell

communication. Key messengers of this communication are a class of structurally diverse secreted proteins, the interleukins (ILs). So far, approximately 60 different ILs and IL-like proteins are known, eliciting all kinds of immunomodulatory functions in cells and tissues, thereby connecting the innate and adaptive immune system[3]. ILs regulate pro-*versus* anti-inflammatory responses by modulating development, expansion, activation or inactivation of immune cells. ILs are secreted proteins, which initiate a response by binding to receptors exposed on the surface of immune cells and act in an endocrine fashion to transmit information between immune cells. Classification of ILs into different subgroups is confusing and difficult due to little sequence homology even between evolutionary related ILs[4]. As a result of host-pathogen co-evolution, genes of the immune system are under constant pressure to adopt. As a consequence, gene mutations are heavily favored in ILs and they are among the most highly divergent genes within mammals[5]. Due to low sequence homology, ILs were classified based on structural similarities and receptor usage. A classification system was established dividing the majority of ILs into seven distinct groups and subgroups[4]. The IL-6/12-like cytokines constitute one of those groups which can be further subdivided into the monomeric IL-6-like and the heterodimeric IL-12 family. The IL-12 family of interleukins is of special interest since its members have pleiotropic functions and play critical roles in multiple immune responses. It is the only strictly heterodimeric IL family, and despite structural similarities within the family its members have highly diverse or even opposing biological functions[6].

1.1.2 The interleukin 12 family: Functional diversity *versus* structural similarity

The IL-12 family consists of four established heterodimeric members, named IL-12, IL-23, IL-27 and IL-35, which can all be produced by similar or even identical immune cells[6]. Although the founding member IL-12 was already discovered in 1988[7], two potential new IL-12 family members were recently discovered: IL-Y and IL-39[8,9]. The fact that new IL-12 family members are still discovered can be explained by a unique structural feature of this IL family: each IL-12 family molecule consists of one α-chain and one β-chain which are shared between the family members[6,10]. The three different α (p19, p35 and p28) and two β subunits (p40 and Epstein-Barr virus induced gene 3 (EBI3)) thus give rise to six possible combinations of α and β subunit pairing[11] (Fig. 1.1).

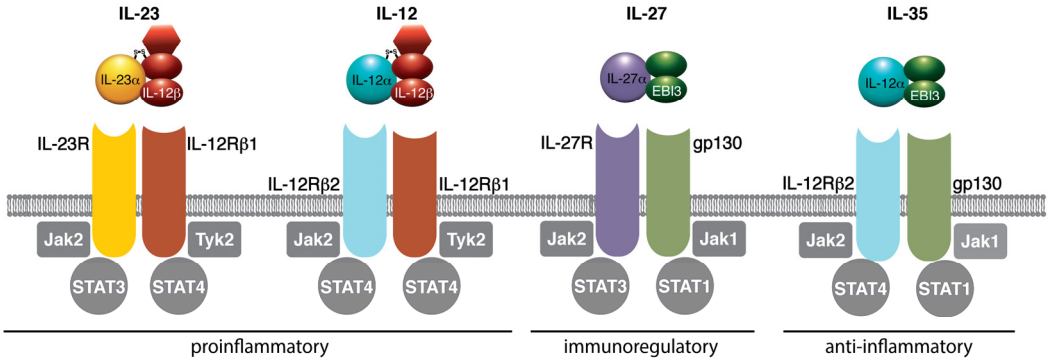

Figure 1.1: The four established IL-12 family members and their receptors. Each IL-12 family cytokine signals *via* heterodimeric receptors, which, like the cytokines themselves, use shared building blocks. Downstream signaling is propagated via Janus kinases (Jak/Tyk2) and members of the signal transducer and activator of transcription (STAT) protein family. IL-12 and IL-23 function mainly proinflammatory, IL-27 immunoregulatory and IL-35 anti-inflammatory. Immunological functions strongly depend on the environmental conditions and may be more diverse as depicted here.

Besides the traditional IL-12 family heterodimers, unconventional subunit-pairings like in IL-Y and IL-39 were investigated during the past years[8,9,12]. If those recently identified IL combinations are relevant in the biological context of immune reactions remains yet to be determined. Furthermore, the chain-sharing theme extends to receptor usage, with several IL-12 interleukins indeed signaling *via* the same receptor chains (Fig. 1.1) but inducing different biological outcomes[13]. The IL-12 family α-subunits have a characteristic four-helix bundle structure, whereas the β-chains comprise immunoglobulin (Ig) and/or fibronectin (Fn) domains (Fig. 1.2) and are structurally related to the soluble receptors of the IL-6 family[6]. Despite their structural similarity, the IL-12 family spans a broad range of distinct or even opposing biological functions. IL-12 (p35 + p40) and IL-23 (p19 + p40) which are the only two IL-12 family members with disulfide bridged subunits are highly proinflammatory molecules with key roles in the development of helper T cells[14]. In contrast IL-27 (p28 + EBI3) can exert both, stimulation and inhibition of immune reactions dependent on the cytokine milieu[15,16] and IL-35 (p35 + EBI3) acts strictly immune-suppressive[17,18]. Thus, all possible immunological functions are combined in one structurally closely related IL family. This raises the question, if an immune balance is established within the IL-12 family itself. Interestingly, the pairing efficiency and ability of the individual subunits to be secreted alone or in combination with other cytokines are vastly different. Of

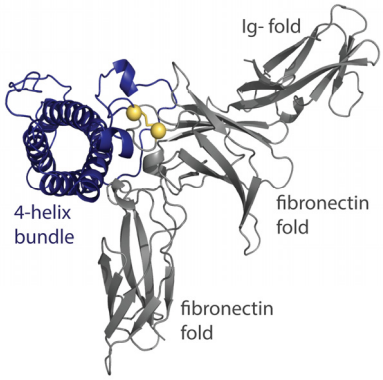

Figure 1.2: Structure of heterodimeric IL-23. Cysteines from IL-23α (blue) and IL-12β (grey) that form an intermolecular disulfide bond are shown in yellow. IL-23α shows a 4-helix bundle structure, whereas IL-12β is comprised of two fibronectin and one immunoglobulin - like domain. (Crystal structure is based on 3DHU pdb entry.)

note, the secretion efficiency of disulfide-linked proinflammatory IL-12 and IL-23 is much higher than for the not covalently linked immunoregulatory or anti-inflammatory IL-27 and IL -35. If this is a coincidence or a valid structure–function relationship remains to be determined. Recent studies indicate that the function of the IL-12 family is not only restricted to the action of IL-12 heterodimers but that unpaired IL-12 family subunits can have autonomous activities under certain conditions[19-24]. This raises the question if the IL-12 family members should be further expanded by unpaired α and β subunits in the near future, what would render the structural and functional properties of this family even more complex.

1.1.3 Function and immunological signaling of the cytokines IL-12 and IL-23

IL-12 and IL-23 are mainly produced by antigen presenting cells (APC) like macrophages, dendritic cells or monocytes after pathogen encounter[14]. For efficient secretion of biologically active IL-12 or IL-23, both subunits of the heterodimeric complexes need to be expressed within the same cell. Once secreted, ILs function in an endocrine manner on a different set of immune cells exposing the corresponding receptor. IL-12 and IL-23 engage a heterodimeric receptor complex of IL-12Rβ1 and IL-12Rβ2 or IL-12Rβ1 and IL-23R, respectively (Fig. 1.1)[6]. Although IL-12/IL-23 signaling is very well established, less is known about how receptor binding of the IL-12 family members is accomplished. Models have been proposed during the last decade based on IL-6 signaling receptor formation, which follows a “site I-II-III” paradigm. This model predicts site I of the α-subunits to be required for complex formation with IL-12β, followed by a conformational shift which subsequently allows binding of site II and site III of p35/p19 to IL-12Rß1 and IL-12Rß2/IL-23R[25-27]. However, more recent studies suggest a non-canonical binding mechanism for IL-23 and its receptor chains where IL-12β is predicted to be involved in IL-12βR1 receptor chain binding as well[25,27,28]. After receptor binding, signal transduction proceeds via the JAK (Janus kinase)–STAT (signal transducer and activator of transcription) pathway. Whereas IL-12 induces STAT4 activation, IL-23 leads to STAT3 and STAT4 activation, resulting in a different biological outcome.

IL-12 is secreted during the early stages of immune reactions by activated APCs and was shown to mediate development and maintenance of type 1 T-helper cells (T_H1), $CD8^+$ cytotoxic T lymphocytes and natural killer cells which play critical roles in proinflammatory reactions, fighting intracellular bacteria or parasites. IL-12 furthermore stimulates, in synergy with other

cytokines (e.g. IL-18 or IL-1) NK and T_H1 cells to produce IFN-γ, which is a highly inflammatory cytokine (Fig. 1.3). Thus, IFN-γ mediates many of the proinflammatory functions of IL-12[29-31]. In addition, IL-12 is known to support DC maturation and cytotoxicity, to enhance B cell production of immunoglobulins and to affect the more recently described regulatory T cells and innate lymphoid cells (Fig. 1.3)[29,32,33]. Since IL-12-producing APCs express IL-12 receptor chains on their surface, they respond in a positive feedback loop to increased IL-12 levels, further enhancing IL-12 function (Fig. 1.3)[14,29]. Due to its strictly proinflammatory effects on APCs as well as on T- or B-cells IL-12 can be considered an important inflammation mediator connecting the innate and adaptive immune system.

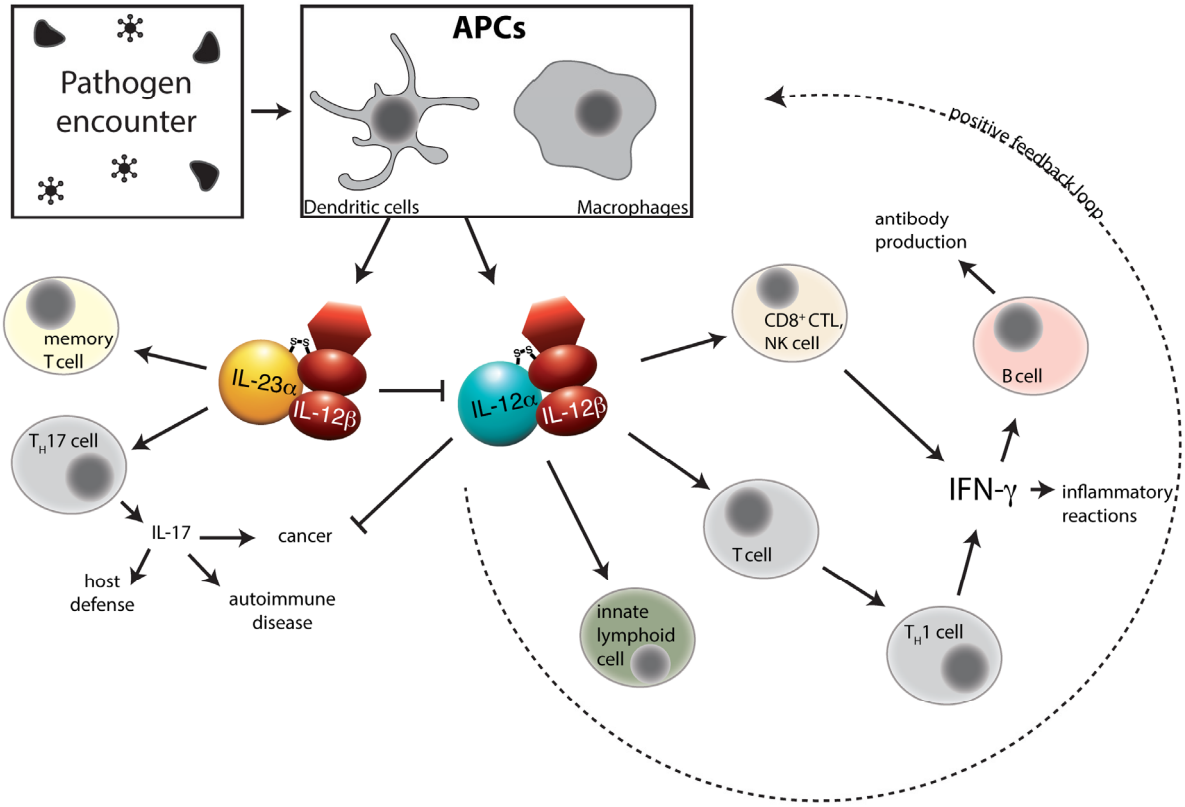

Figure 1.3: Immunological functions of IL-12 and IL-23. After pathogen encounter antigen producing cells (APCs) like macrophages or dendritic cells produce high amounts of proinflammatory IL-12 and IL-23 in order to eliminate invaders. IL-12 induces proliferation of innate lymphoid cells (e.g. ILC1 cells), increases cytotoxicity and proliferation of natural killer (NK) cells or $CD8^+$ cytotoxic T cells ($CD8^+$ CTL) and supports differentiation and maintenance of T_H1 cells. Altogether, IL-12 function results in high levels of IFN-γ which further increases pro-inflammatory responses and antibody production in B cells. A positive feedback loop is established between IL-12 and APCs which results in increased IL-12 production. IL-23 mainly functions on the proliferation and survival of T_H17 cells which drive host defense and autoimmune diseases as well as cancer. Tumor-promoting functions of IL-23 are counteracted by IL-12. Additionally, IL-23 is capable to reduce IL-12 expression and to stimulate memory T cells.

IL-12 and IL-23 are both known for their proinflammatory effects in fighting intracellular pathogens during early immune reactions. Whereas IL-12 functions via activation of T_H1 cells, IL-23 regulates maintenance and survival of type 17 immune cells (T_H17). T_H17 cells regulate

host defense by recruiting neutrophils and macrophages to infected tissues[34]. During the past decades it has been shown that IL-23 is involved in the progression of various autoimmune diseases like inflammatory bowel disease, rheumatoid arthritis, psoriatic skin inflammation or experimental autoimmune encephalomyelitis (EAE) by the activation of T_H17 cells (Fig. 1.3)[35-37]. T_H17 cells are composed of a variety of different cell types, including subsets of γδ T cells, natural killer T cells, innate lymphoid cells and natural T_H17 cells which are all characterized by retinoic acid receptor-related orphan receptor-γt (RORγt) transcription factor regulated IL-17 expression[36]. Activated T_H17 cells produce high amounts of IL-17 which augments inflammation by regulating expression of inflammatory genes in mostly non-hematopoietic cells[38]. Besides its effect on T_H17 cells, the first function of IL-23 was reported by Oppman *et al*.[39] and referred to its activity on memory T cells (Fig. 1.3). Memory T cells that encountered antigens already during prior infections are able to induce a faster and stronger immune reaction upon a second encounter with the same pathogen. IL-23 assists in their reactivation by promoting proliferation and secretion of a proinflammatory cytokine cocktail[39,40].

Interestingly, several studies have suggested independent functions for unpaired IL-12 family members. IL-12β was the first single IL-12 family subunit with individual functions reported. IL-12β can be secreted in absence of its interaction partners from macrophages and dendritic cells as monomer or as homodimer and was shown to act as an antagonist in IL-12 and IL-23 signaling[25,41,42]. This dual effect can be explained by subunit and receptor chain pairing within the IL-12 family. Furthermore, the IL-12β homodimer was shown to induce expression of nitric oxide synthase in microglia cells and thereby promoting neurodegenerative diseases[43]. Its effect on NO production further leads to suppression of regulatory T cells in mouse splenocytes[44]. IL-12β homodimers additionally promote migration of dendritic cells and macrophages during respiratory infections[45,46]. IL-12α on the other hand has been predicted to possess independent intrinsic immunoregulatory functions on regulatory B cells[47] and proinflammatory functions in a mouse model of herpes stromal keratitis[20]. To complete independent functions of IL-12/IL-23 subunits, IL-23α has been shown to be produced by endothelial cells in absence of IL-12β, executing proinflammatory functions. It has been suggested, that IL-23α intracellularly binds to gp130 and induces gp130-STAT3 signaling, which increases the abundance of adhesion molecules on the cell surface, promoting endothelial cell migration during infection. Thus, IL-23α has been shown to increase proinflammatory effects during infection, independently of IL-23[48]. Strikingly, the

intracellular activity of IL-23α shows strong similarity to viral IL-6. Both proteins share about 16% sequence similarity and signal via gp130 to promote inflammation[48,49].

Nevertheless, subunit sharing within the IL-12 family and the existence of potential, yet unknown interaction partners makes it challenging to discriminate between immunological functions of unpaired *versus* paired subunits as demonstrated by early studies on IL-12, where several effects were mistakenly attributed to IL-12 but induced by the later identified IL-23[50]. As a consequence of IL-12, IL-23 and even its unpaired subunits affecting various cell types and different layers of our immune system they are ultimately involved in different diseases as well.

1.1.4 Targeting IL-12 and IL-23 in human diseases

The broad functional spectrum of IL-12 and IL-23 is reflected in the large number of diseases they are associated with, ranging from the eradication of bacterial pathogens to contributing to autoimmunity and cancer. Due to its strong activation of the cellular immune response IL-12 is a very promising target in anti-cancer therapies. IL-12, together with its effector IFN-γ promote and increase response of the immune system against malignant cells[30,51]. IL-12 leads to the destruction of tumor cells by activating cytotoxic cells and macrophages, inhibiting neo-angiogenesis as well as induction of tumor cell surface marker expression that enables recognition by immune cells[52]. Unfortunately, first clinical trials in the 1990s reported problematic results due to strong systemic toxicity of recombinant IL-12 in cancer immunotherapy[53,54]. Thus, new strategies to restrict IL-12 function by local delivery have been established during the last years, restoring IL-12 as a promising anti-cancer agent. Local delivery of IL-12 into the tumor environment can be achieved by adenoviral or electroporation delivery of IL-12 encoding vectors directly into the tumor tissue[55,56]. Other approaches making use of IL-12-fused antibodies or nanoparticles to achieve a tumor-restricted delivery[57-59]. In concert with novel biotechnological tools that allow local delivery of cytokines and in combination with conventional cancer therapies IL-12 is one of the most prominent candidate in cancer immunotherapy nowadays.

Besides its destructive effect on cancer cells, IL-12 was thought to be the key driver of various inflammatory diseases for many years. Upon discovery of IL-23, many disease phenotypes were reattributed to IL-23, instead. Nowadays, IL-23 is the accepted main driver of several autoimmune diseases whose function is only supported by IL-12[30,60,61]. By

promoting the survival and maintenance of T_H17 cells, IL-23 induces tissue pathology and chronic inflammation like psoriasis, inflammatory bowel disease, multiple sclerosis or rheumatoid arthritis. Currently several promising approaches targeting the IL-23/IL-17 immune axis are under clinical testing or already in therapy. Among them the first monoclonal specific IL-23α and IL-17 neutralizing antibodies[36,62]. Although IL-12β targeting antibodies like Ustekinumab which neutralize IL-12 and IL-23 function by blocking its shared β subunit are still used in psoriasis treatment, design of specific IL-23α anti- or nanobodies are of great advantage due to less side effects[63,64]. Moreover, IL-23α neutralizing antibodies may not only be beneficial in treatment of autoimmune diseases but also in cancer. Whereas IL-12 shows impressive anti-tumor activity, IL-23 function promotes cancer formation[65-67]. IL-23, via IL-17, contributes to angiogenesis, expression of matrix metalloproteinases and infiltration of tumor associated macrophages which are known to potentiate tumor growth and metastasis[68-71]. Furthermore, IL-23 inhibits IL-12 functions on tumors and thereby negatively regulates the function of cytotoxic cells which have the potential to eliminate tumor cells[72]. Although the role of IL-23 in tumor progression is still under investigation it is already an attractive target in the treatment of various types of cancers.

As reported for IL-12, natural cytokines are often highly pleiotropic and exert severe side effects. Thus, engineered cytokines which are generally considered to be more effective and may lead to fewer side effects are becoming a powerful tool to modulate immune functions, as previously reported e.g. for IL-2, IL-15, IL-27, IL-12 and others[73-78]. Therefore, engineered IL-12 family cytokines, as well as their single-chain subunits might represent a new class of therapeutic cytokines in the future.

1.2 Protein folding and quality control in the human endoplasmic reticulum

In order to acquire their biologically active form, interleukins undergo folding and assembly in the endoplasmic reticulum (ER). Protein folding is a highly complex process that requires conversion of a two dimensional amino acid chain into a functional three dimensional topology. Since protein production comes along with high energy costs and accumulation of misfolded proteins may lead to aberrant cell functions or diseases, cells must guarantee an efficient system to support proper folding. The ER with its chaperones, folding catalysts or protein-modifying enzymes presents an optimal environment for productive protein folding. The ER provides a sorting mechanism that allows only mature proteins to enter the downstream secretory pathway and furthermore retains proteins that terminally failed to fold and targets them for ER-associated degradation (ERAD).

1.2.1 Translation of ER-targeted proteins

Approximately one third of all human proteins reside or are processed within the ER and thus depend on effective targeting and entry to the ER. This is achieved by a proteinaceous pore, called Sec61 in the ER membrane that allows co-translational transport of a nascent polypeptide chain directly into the ER[79]. Post-translational entry into the ER is reported for small secretory proteins or tail-anchored proteins and basically follows the same principle as co-translational import. It uses the Sec61 channel as well but under assistance of different co-factors[80-82]. Co-translational translocation begins in the cytosol during early stages of translation, when N-terminal residues start to emerge from the ribosomal exit tunnel, providing a conserved hydrophobic signal sequence which assigns the protein to the ER, *via* recognition by the signal recognition particle (SRP)[83,84]. One of the major tasks of SRP is to halt translation and thereby keep the nascent polypeptide in a translocation-competent state[85]. SRP, together with the ribosome-nascent chain (RNC) complex subsequently binds to the SRP receptor on the ER membrane and after docking of the RNC complex to the translocon, translation resumes[86]. Recent structural studies have revealed detailed insights into how cells accomplish co-translational localization of ER proteins. After docking of the RNC complex to the translocon a two-step channel opening process is proposed in which the RNC docking primes the channel and the intruding signal peptide induces complete opening. Complete opening is achieved by the intercalation of the signal sequence helix between transmembrane

helices of Sec61 what leads to formation of a lateral gate and displacement of a helical plug which is otherwise anchored in the central pore of the Sec61 channel. Subsequently, translation is continued and delivers the polypeptide to the ER lumen or membrane, which is achieved by lateral opening of the translocon[87-89]. The Sec61 channel is assisted by several proteins or protein complexes, which influence protein import, transmembrane protein topology and insertion or early protein maturation[90-93]. Among those is the ER resident molecular chaperone immunoglobulin heavy-chain binding protein (BiP), which assists Sec61 channel functions and facilitate protein import. Since movement of the nascent polypeptide is reversible within the Sec61 channel, translocation is facilitated by BiP which binds incoming hydrophobic peptides and thus inhibits back-sliding of the translocated peptide[94].

Already during protein translocation, signal peptide cleavage occurs as one of the first modifications in protein maturation. Signal peptides are cleaved, mostly co-translationally, by the translocon-interacting signal peptidase complex[79]. However, signal peptide cleavage is also reported to occur post-translationally for some proteins as described for the HIV envelope protein gp160 where delayed cleavage supports folding[95]. Furthermore, in the case of the ER quality control factor EDEM1, inefficient signal peptide cleavage results in a soluble and a membrane bound topology, with a different spectrum of clients[96]. Several studies suggest, that signal peptides are more than simple cellular postcodes but further influence protein folding, localization as well as N-glycosylation[97].

N-glycosylation occurs mainly co-translationally *via* the translocon interacting oligosaccharyltransferase (OST) complex. Sugar moieties composed of three glucoses, nine mannoses, and two N-acetylglucosamines ($Glc_3Man_9GlcNAc_2$) (Fig. 1.4) are transferred *en bloc* from a lipid carrier to an asparagine residue within an Asn-Xaa-Ser/Thr (Xaa: any amino acid except proline) motif on the emerging polypeptide chain[98].

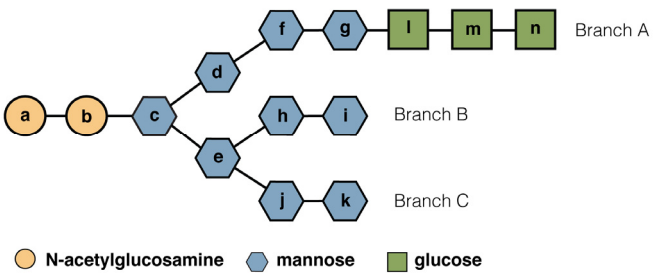

Figure 1.4 Schematic representation of N-linked oligosaccharides. The oligosaccharide, co-translationally attached to nascent polypeptide chains consists of two N-acetylglucosamines moieties (yellow cycles), nine mannose residues (blue hexagons) and three glucoses (green squares). The core oligosaccharide shows a tree like topology, composed of three branches. Letters indicate the order of carbohydrates added during assembly.

Protein N-glycosylation possesses intrinsic as well as extrinsic effects on the protein stability and maturation. Addition of hydrophilic carbohydrates changes the physical properties of a protein and can influence folding kinetics. The presence of oligosaccharyl moieties furthermore targets the protein to carbohydrate binding molecular chaperones (lectins) of the calnexin/calreticulin (CNX/CRT) cycle, which promote efficient protein folding or target terminally misfolded proteins for degradation[79].

1.2.2 Protein folding by chaperones

1.2.2.1 Recognition and processing of N-glycan structures in the ER

Of all modifications taking place inside the ER, attachment of carbohydrates as described before is one of the most prevalent ones. Almost simultaneously with glycan-transfer, glucosidase and mannosidase activity leads to the removal of the outermost glycan units from the oligosaccharide tree. The composition of the attached glycan tag subsequently serves as a signal, communicating the folding status of a protein. Removal of the first glucose from branch A generates a binding site for a more recently discovered ER-membrane-bound lectin called malectin (Fig. 1.5) which is reported to associate with immature or misfolded proteins early after or during their entry to the ER[99-101]. Further investigation is required to answer the question how malectin is already able to distinguish natively from non-natively folded proteins as early as during protein maturation. Additional removal of a glucose unit from branch A results in a monoglucosylated polymannose structure which is able to enter the CNX/CRT cycle (Fig. 1.5). Whereas calnexin is attached to the ER membrane by its transmembrane domain, calreticulin resides within the ER lumen. Both lectins share a globular N-terminal carbohydrate lectin domain, followed by a flexible prolin rich domain which serves as a binding platform for additional ER chaperones[102-104].

Among those are oxidoreductases, which are discussed later in this chapter and peptidyl prolyl *cis-trans* isomerases (PPIases). The latter catalyzes the isomerization of Xaa-Pro peptide bonds which are initially inserted in the *trans* configuration into the nascent polypeptide. Intrinsic proline isomerization is very slow and hence can be rate-limiting for folding. PPIases accelerate this process and thereby facilitate protein folding[79]. Thus CNX/CRT not only support folding themselves but additionally recruit folding factors, which support the folding process of the client proteins. Despite strong similarities and 39% sequence homology between CNX and CRT, differences have been observed in regard to substrate binding[105].

Whereas some glycosylated proteins are able to interact with both, others preferentially interact with either CNX or CRT. However, human CNX or CRT knock out cell lines do not show severe phenotypes, indicating that CNX/CRT act in a synergistic manner with interchangeable substrate binding[106]. Removal of the last remaining glucose from branch A inhibits rebinding to CNX/CRT and liberates the protein from the lectin cycle. Properly folded glycoproteins subsequently undergo secretion (Fig. 1.5) whereas deglucosylated proteins that still show hydrophobic/unfolded regions are reintegrated into the CNX/CRT folding cycle. Reintegration of immature proteins is accomplished by transferring a single glucose residue to the earlier trimmed A chain, catalyzed by UDP-glucose:glycoprotein glucosyltransferase (UGGT) (Fig. 1.5). Hence, UGGT represents one of the major folding sensors of the ER by specifically recognizing near-native intermediates and orphaned subunits and commits them to another round of folding. How many cycles of CNX/CRT binding are necessary for proper folding highly depends on the substrate itself[107]. Taken together, CNX/CRT promote efficient folding by preventing protein aggregation and facilitating interaction with additional chaperones.

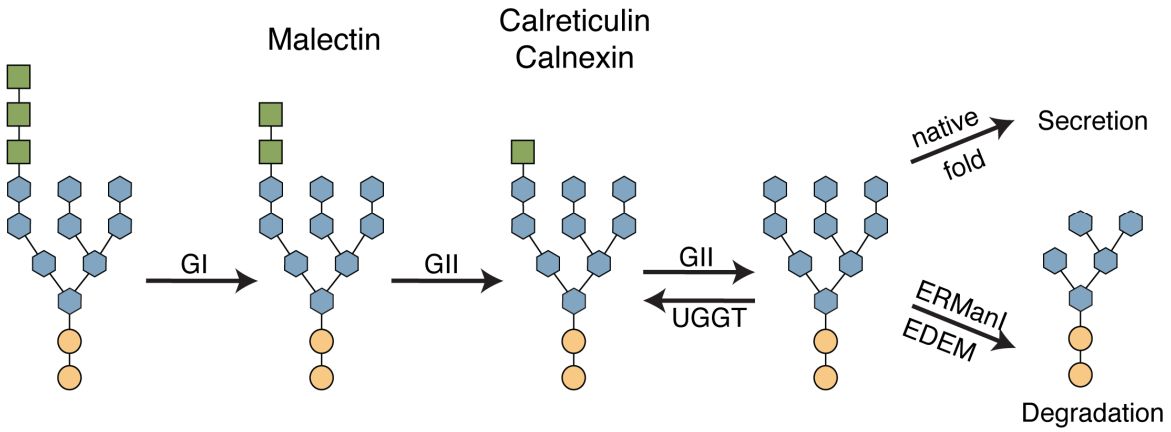

Figure 1.5 Glycan processing inside the ER. After attachment of the core oligosaccharide tree processive glycan trimming communicates the folding state of the protein and allows chaperone recognition. The first glucose from branch A is cleaved by α-glucosidase I and generates a binding site for malectin. Further removal of glucose*s* by α-glucosidase II enables the protein to enter the CNX/CRT cycle. Cleavage of the last remaining glucose by the same enzyme excludes the protein from the lectin cycle and is followed by secretion of natively folded secretory proteins. If folding is incomplete, reglucosylation by UGGT dedicates the protein to another round of folding within the CNX/CRT cycle. Terminally misfolded proteins are not reintroduced to the lectin cycle but extensive mannose trimming by ERManI and EDEM proteins leads to degradation by the ERAD machinery.

Terminally misfolded proteins are not recognized by UGGT but by mannose trimming enzymes instead which assign the protein for degradation. Mannose trimming seems to be a time dependent effect where proteins, which need extended periods of time or which cannot achieve proper folding become substrates of ER mannosidase I (ERManI) or ER degradation-

enhancing α-mannosidase-like proteins (EDEM) which remove mannose residues from different branches of the co-translationally transferred N-glycan structure (Fig. 1.5). De-mannosylation ultimately excludes the protein from re-entering the CNX/CRT cycle and provides a unidirectional pathway towards destruction. Recent evidence suggests that removal of more than one mannose residue is necessary to target the protein for degradation[108,109]. Altogether, attachment of N-glycans to proteins constitute a unique mechanism that enables the cell to discriminate between natively folded and misfolded proteins. However, the extent to which cells depend on CNX/CRT function is not yet understood, due to controversial phenotypes in CNX/CRT knock out in mice and humans[106].

1.2.2.2 BiP and its co-factors as master regulators of ER protein folding

BiP is at the center of the second major class of ER chaperones besides lectins. It is part of the Hsp70 family of chaperones and is the only conventional family member inside the ER. Unlike CNX/CTR, which recognize a combination of glycan modification and hydrophobic stretches, BiP binds exclusively to the latter and can thus assist folding of unglycosylated proteins, which would be missed by the CNX/CTR system[110]. BiP preferentially binds to aliphatic side chains, which become buried in the native protein and occur approximately every 16-34 residues in a polypeptide chain[111,112]. Binding of incompletely folded substrates by BiP is tightly regulated by a cycle of ATP binding and hydrolysis, which is fine-tuned by different co-factors. BiP is composed of one nucleotide-binding (NBD) and one substrate-binding domain (SBD). Client binding to the SBD is regulated by an extended lid whose conformation depends on the nucleotide bound. Binding of ATP to the NBD leads to increased compaction of NBD and SBD onto each other and information on the nucleotide state is transmitted to the SBD what ultimately results in lid opening and substrate release (Fig. 1.6)[113]. BiP in the ATP state shows low substrate affinity and high on-off rates and only ATP hydrolysis leads to tight binding and SBD lid closure over the bound substrate, preventing premature folding or aggregation (Fig. 1.6). Subsequently, the intrinsic ATPase activity of BiP is catalyzed by the substrate binding itself and is further stimulated by BiP co-chaperones, the ERdjs[113,114]. In order to release the substrate and to re-enter the ATPase cycle, exchange of the nucleotide needs to be achieved. Since nucleotide exchange is the rate limiting step of the BiP ATPase cycle *in vivo*, assistance of nucleotide exchange factors (NEFs) is required. Two NEFs are currently known to participate in the BiP cycle: Grp170 and Sil1. Both bind mainly to

the NBD in the ADP state and destabilize BiP binding to ADP, resulting in nucleotide release and another cycle of substrate binding (Fig. 1.6)[110].

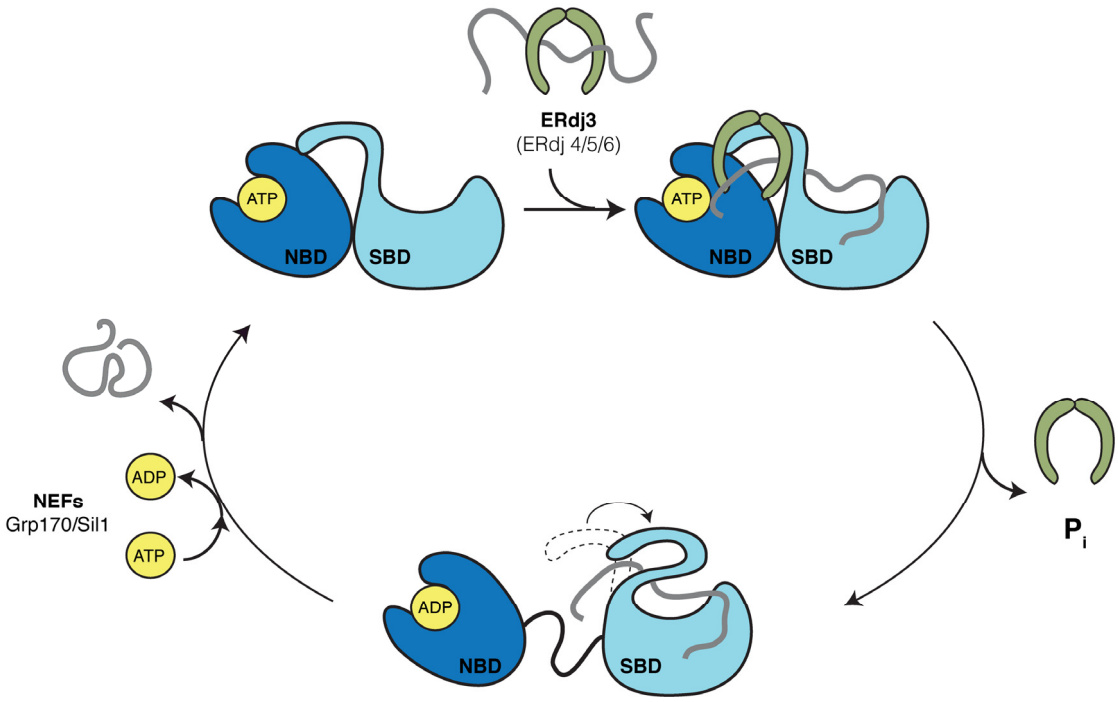

Figure 1.6 Model of the ATPase cycle of BiP. The Hsp70 chaperone BiP consists of two domains: The nucleotide binding domain (NBD) (dark blue) and the substrate binding domain (SBD) (light blue). In the ATP-bound state, NBD and SBD are in close proximity and the lid of the SBD is in an open conformation, which allows low affinity substrate binding. Substrates are delivered to BiP by different ERdj proteins (ERdj 3,4,5,6), which additionally increase the ATPase activity of BiP. ATP hydrolysis induces lid closure over the bound client, resulting in strong client binding and less compaction of the two domains over each other. To regenerate BiP activity, nucleotide exchange is performed with the aid of Grp170 or Sil1. ATP loading to BiP results in release of the bound client.

BiP has been referred to be the master regulator of the ER because of its broad role in ER processes and functions. It is known to facilitate protein folding in the ER, to maintain the permeability barrier of the ER during translocation, to assist in retrograde transport of terminally misfolded protein into the cytosol and to regulate the unfolded protein response (UPR), which deals with an increased load of unfolded proteins accumulating in the ER[115]. In order to regulate and execute all those different functions, BiP highly depends on action of its co-chaperones. ERdjs are part of the J-domain protein family often also referred to as Hsp40. J proteins are highly diverse but all have the conserved J-domain in common which is crucial for interaction with Hsp70 and to induce ATPase activity of Hsp70[116]. To date, 6 out of 7 ERdjs are known to support BiP function in the ER. Whereas ERdj1 and 2 reside within the ER membrane and connect BiP function to co-translational translocation, ERdj3 and 6 directly bind substrates and deliver them to BiP for folding[117-122]. Besides pro-folding activities of ERdjs, there is also evidence that ERdj5 and 4 support BiP function in the recognition of

misfolded proteins, which are subsequently targeted for retrograde transport and degradation[123]. Furthermore, BiP independent functions are reported for some ERdjs as well[116].

Additionally BiP activity can be regulated by calcium concentration or post-translational modifications such as ADP-ribosylation, AMPylation and oxidation. Some of the mentioned modification lead to BiP inactivation, generating an inactive pool of protein, which can be rapidly reactivated to cope with an increased ER folding burden[124-127]. Altogether, several layers of regulation work synergistically in order to guarantee efficient and rapid performance of the various functions of BiP.

1.2.2.3 Grp94: A highly abundant but enigmatic folding helper of the ER

Although the Hsp90-like chaperone Grp94 is one of the most abundant proteins in the ER and despite extensive research on its cytosolic homologue, its precise working mechanism is still enigmatic. The Grp94 is supposed to support folding of a variety of secreted proteins or cell surface receptors by ATP-driven conformational changes during the maturation of bound client proteins. Grp94 topology resembles that of cytosolic Hsp90 which is composed of one N-terminal nucleotide binding domain, a middle domain that is needed for ATP hydrolysis and a C-terminal domain that regulates homo-dimerization of the chaperone[128]. Furthermore, recent structural insights revealed important functions of a pre-N-domain in substrate binding and ATP-hydrolysis. Interestingly, this domain is unique to Gpr94 and may lead to functional differences that are key to adaptations of Grp94 to the ER[129]. In terms of client binding, Grp94 is more selective than many of the ER chaperones. Among its known clients are various immune proteins such as Toll-like receptors, integrins or immunoglobulins, what explains the essential role of Grp94 during immune responses[130-133]. Which regions within Grp94 participate in substrate binding has not yet been elucidated, arguing for a large and diverse interaction surface, as described for Hsp90[128,134].

Another topic of debate is the existence of Grp94 co-chaperones. So far no co-chaperones have been identified to assist the Grp94 folding cycle, whereas a plethora of co-factors are known to regulate functions of cytosolic Hsp90. Only few examples exist, where specialized proteins assist folding of a certain Grp94 client[135,136]. Co-chaperones not only regulate Hsp90 chaperone-client interaction in the cytosol but also facilitate Hsp90-Hsp70 interaction. Numerous studies have shown a functional interplay between those chaperones

with Hsp70 acting upstream of Hsp90. Recent data indicate that BiP in the ADP conformation with a stably bound substrate is able to directly recruit Grp94 in order to allow substrate transfer, without any help of co-chaperones[137]. Although recent studies thus contributed to sharpen our understanding of Grp94 function, still several important questions need to be answered.

1.2.3 Oxidative protein folding in the ER

The extracellular milieu is a very rough environment for proteins. In order to increase protein survival outside the cell, cysteines are preferentially introduced into secreted polypeptides[138]. Cysteines can form covalent linkages between distant regions of a protein *via* an oxidative reaction with another cysteine residue, resulting in the formation of a disulfide bond, which ultimately stabilizes the native structure of the protein. In accordance with this, disulfide forming cysteines are the most highly conserved residues in a protein[139]. Since disulfide bond formation is an error prone process, it is facilitated by a chaperone and catalysis system, provided by the ER.

1.2.3.1 PDI enzymes: Catalysts of disulfide bond formation

ER protein disulfide isomerases (PDIs) assist formation of disulfides in proteins. The name was derived from the founding member, which is still simply referred to as PDI. Up to date 20 different human PDIs are known which catalyze the controlled formation, rearrangement or reduction of disulfide bonds. The type of reaction these proteins catalyze, depends on the redox potential of the enzyme[140]. The hallmark of PDI function is their thioredoxin (Trx)-like domain, which contains the catalytically active motif CXXC, where two reactive cysteines are separated by two amino acid residues, which strongly influence the redox activity of the active site cysteines[141]. PDI itself contains two enzymatically active (a & a') and two inactive Trx-domains (b & b') in an abb'a' configuration (Fig. 1.7a). Due to an U-shaped overall structure, the active site domains are facing each other across a central substrate binding cleft[142]. There is also a small interdomain region known as the x-linker, located between b' and a' which has been recently reported to modify the redox state of the active sites and to enhance the catalytic activity of PDI (Fig. 1.7a)[143]. PDI is able, dependent on its redox state to catalyze oxidation, reduction or isomerization of disulfides in a wide range

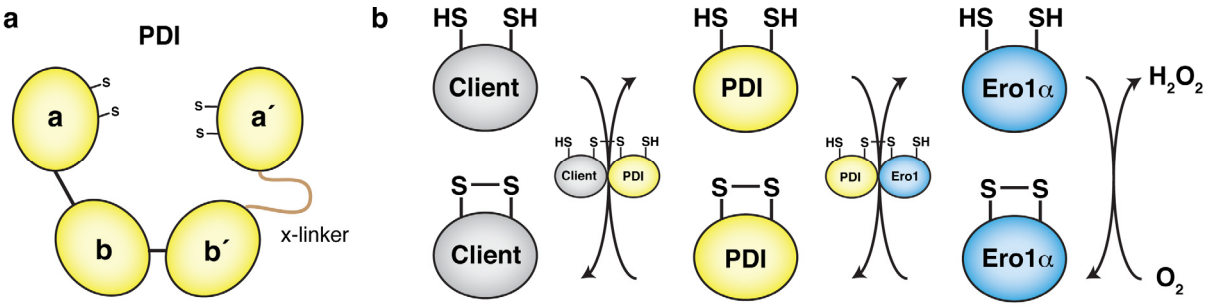

Figure 1.7 PDI structure and activity. **a** Model of the PDI structure. PDI is composed of four domains a a' b and b'. The a domains are catalytically active and involved in client disulfide oxidation (a') or PDI regeneration (a) whereas b domains are involved in client binding. The highlighted x-linker region, connecting the b' and a' domain has been recently reported to modify the redox state of the active sites and to enhance PDI's catalytic activity. **b** PDI activity cycle. PDI catalyzes disulfide formation in client proteins via the formation of a mixed disulfide. The transfer of electrons from PDI to the client protein results in client oxidation and PDI reduction. To allow iterative cycles of PDI activity, PDI is re-oxidized by Ero1α under formation of a mixed disulfide. Ero1α uses O_2 as the final electron acceptor, resulting in H_2O_2 formation.

of substrates. During these reactions, the catalytic vicinal active site thiols (-CXXC-) undergo sequential oxidation and reduction reactions. Oxidative as well as reductive activity of PDIs is essential during protein folding since non-native disulfides may form during the maturation process, which require reduction to restore the native fold. However, in some cases the formation of non-native disulfides facilitates the formation of productive folding intermediates that are essential for successful folding[144]. Consequently, free PDI is present in different oxidation states in the ER[145]. It is suggested that the cycle of PDI activity begins with the oxidized a-domain which catalyzes the oxidation of the reduced substrates and subsequently becomes reduced. The N-terminal cysteine of the catalytic motif then reacts with the substrate to form a mixed disulfide while the C-terminal cysteine releases the substrate (Fig. 1.7b)[146]. The a-domain is then oxidized by the a'-domain back to a disulfide through intramolecular reactions[147]. Crystal structures revealed a conformational switch of PDI, dependent of its redox state. Oxidized PDI shows a more open conformation than the reduced form[148]. This redox-dependent conformational switch may play a role in regulating substrate affinity and specificity of PDI. Interestingly, recent investigations showed that besides its activity on disulfides PDI further possesses chaperone activity, which is independent of its redox activity and predominantly executed by its b' domain[149-151].

In order to allow cycles of substrate oxidation, PDI needs to be re-oxidized after disulfide transfer. Re-oxidation of the a'-domain is catalyzed by the protein endoplasmic reticulum oxidoreductin-1α (Ero1α), which uses O_2 as the final electron acceptor and generates hydrogen peroxide as a by-product (Fig. 1.7b)[152]. Ero1α is bound in a substrate-like

manner in a hydrophobic cleft within the b' domain and is easily replaced upon substrate binding[153]. Different PDIs are oxidized by Ero1α but binding occurs with lower affinities, which could ultimately influence redox reactions in the ER[141]. Besides Ero1α, several upstream oxidoreductases, like peroxiredoxin-4 as well as the more reducing PDIs like ERdj5 are known to oxidize or reduce and recycle PDIs in mammalian cells[154]. Interestingly, peroxidases recycle hydrogen peroxide, produced by Ero1α to introduce disulfides in their clients, thereby, clearing a potentially harmful reagent, which is a source of reactive oxygen species and thus oxidative stress from the ER and guarantee proper ER function[154].

Disulfide bond formation can occur during very early stages of protein maturation, as demonstrated by ERp57. ERp57 is a PDI family member and closely resembles PDI. As the only known active PDI, it associates with CNX/CRT during early protein maturation by binding to the P-domain of CNX/CRT. It catalyzes disulfide formation and isomerization in glycoproteins during early protein folding[155]. Whereas PDI and ERp57 are known for oxidizing and reshuffling disulfide bonds, ERdj5 is mainly known as a reducing PDI family member. When associated with BiP or EDEM proteins, it reduces disulfide bonds in misfolded proteins, targeted for ERAD, in order to prepare them for retrotranslocation[156]. Furthermore, a recent study revealed a novel function of ERdj5 as modulator of calcium concentration in the ER. Calcium concentration within the ER is tightly regulated by Ca^{2+} transport activity of sarcoplasmic/ER Ca^{2+} ATPase-2b (SERCA2b) whose activity is regulated by a disulfide bond catalytic switch. If the catalytic disulfide bond becomes oxidized by ERp57, Ca^{2+} transport is inhibited, whereas reduction by ERdj5 activates SERCA activity. ERdj5 activates SERCA only under low luminal calcium levels. Its Ca^{2+} dependent oligomeric state prevents binding to and activation of the SERCA pump at high Ca^{2+} concentrations[157,158].

Another PDI family member with unique structural and functional features is ERp44. ERp44 travels between the ER and the ER-Golgi intermediate compartment (ERGIC) and thereby retrieves incompletely folded or unassembled proteins back to the ER where they obtain folding assistance. Furthermore, ERp44 does not exclusively recognize incompletely folded proteins in the ERGIC. It induces ER tethering of proteins that lack an ER targeting signal, like Ero1α[159]. Its active Trx-domain contains a unique CRFS motif, where the C-terminal active site cysteine is missing, indicating that ERp44 possesses an unusual client binding mechanism. Erp44 client binding and release relies on a pH-dependent regulation, which is triggered by conformational changes in its C-terminus. Inside the ER at neutral pH, the client

binding surface of ERp44 gets blocked by its C-terminus. Upon transport towards the Golgi, the pH becomes more acidic, leading to protonation of a histidine cluster in ERp44, inducing a conformational shift of its C-terminal tail. This is followed by the exposure of the client binding interface and an ER retention signal. After formation of a mixed disulfide with its substrate, ERp44 travels back to the ER with its cargo[160,161]. Thus, members of the PDI family not exclusively use their PDI activity to promote disulfide bond formation but also for quality control purposes or to regulate protein functions.

1.2.3.2 ER redox homeostasis

The ER represents a specialized protein folding factory, which strongly supports oxidative protein folding by numerous disulfide-generating enzymes and optimized redox conditions. Compared to the cytosol, the ER lumen provides a much more oxidizing environment, which is required for disulfide formation. If the ER would be as reducing as the cytosol, disulfide formation would be strongly inhibited, whereas hyperoxidizing ER conditions would also impair productive folding through extensive mispairing of cysteines. Therefore, a balanced ER redox milieu is key for oxidative protein folding. In the ER (and the cytosol) the redox potential is provided by a redox couple comprising reduced glutathione (GSH) and its oxidized dimer (GSSG). A recent study estimated a GSH:GSSG ratio inside the ER of about 35:1, compared to 100:1 in the cytosol[162-164]. GSH is used, within ER reductive pathways, as an electron donor for Ero1α or thioredoxins, which subsequently transfer the electron to PDIs. To date, it is not known how the thereby produced GSSG is recycled in the ER[165].

Furthermore, the role of GSH as the ultimate electron donor in disulfide formation is subject of ongoing discussion since a recent study revealed that GSH is dispensable for oxidative folding of some cysteine rich proteins[166]. This study emphasized the existence of a compensatory mechanism, regulating ER redox homeostasis. A subsequent study connected the cytosolic thiodredoxin system to disulfide formation in the ER, presenting cytosolic NADPH as the ultimate electron donor. NADPH is produced in the cytosol and is subsequently used to reduce thioredoxins. How electrons are further transferred from thioredoxins into the ER is unknown but most likely requires action of a membrane protein[167]. This newly proposed mechanism closely resembles the reductive pathway present in bacteria[168].

1.2.4 Folding and assembly of protein complexes

Analyses in yeast revealed that over half of all proteins produced in cells are part of stable protein complexes[169]. This makes a protein assembly control system, regulating efficient complex formation, indispensable for proper cell function. In the cytoplasm, recent studies have shown that protein translation and assembly can be intimately coupled, increasing efficiency of these processes by spatial constraints[170,171] or translational pausing[172]. During co-translational folding, aggregation of an incompletely folded nascent polypeptide can be inhibited by the interaction with its already fully synthesized partner[170]. Such a scenario has not been described for secretory pathway proteins in the ER, since translation and assembly in the ER are spatially separated. Before being transported to their final destination from the ER, cells still have to make sure that proteins are correctly assembled and simultaneously secured from premature degradation[173]. Furthermore, as opposed to the cytosol, quality control proteases or ubiquitin conjugating systems are absent from the lumen of the ER, rendering assembly control highly dependent on recognition by the generic ER chaperone machinery. The main underlying principle in protein assembly is that unassembled subunits of a complex are retained by assembly factors until they get replaced by the actual assembly partner[174,175]. Only few examples exist which have elucidated the folding pathway of secretory proteins in detail. Among them are IgM antibodies, whose assembly process has been extensively studied during the last decades. IgM biogenesis can be divided into sequential steps and checkpoints, beginning with the assembly of two heavy (H) and light (L) chains, forming an IgM monomer in the ER. Domains of the H chain fold vectorially with aid from BiP and PDI as they emerge from the translocon. However, one domain within the heavy chain is not able to form a stabilizing disulfide bond and stays unfolded. This unstructured region is recognized by BiP, which leads to ER retention of the H chain[176]. Only upon assembly with the autonomously folded L chain BiP is released and folding can be completed inducing formation of the intramolecular disulfide bond[176]. This process is followed by the formation of an intermolecular disulfide bond between two H-L hemimers, resulting in an IgM monomer which is now able to exit the ER (Fig.1.8). After passing this first folding checkpoint further assembly control is required to allow only oligomerized IgMs to leave the cell. In order to leave the ER, IgM monomers are bound by the transmembrane lectin ERGIC-53, providing a platform for oligomerization and escorting IgM to the Golgi (Fig.1.8)[177]. While bound to ERGIC-53, IgM monomers can oligomerize by the formation of an intermonomer disulfide bond[178].

In the slightly more acidic pH of the Golgi, ERGIC-53 releases its cargo and correctly assembled IgMs can exit the cell[179]. IgM is secreted as pentamers, under assistance of a joining (J) chain, which connects the first and the fifth monomeric IgM unit or as hexamers without the J chain. Within a second quality control checkpoint, the cysteine which usually forms the intermonomer disulfide bond in the oligomer but stays free and exposed in unassembled intermediates, is recognized by ERp44. ERp44 retrieves unassembled IgM monomers to the ER for another chance of being incorporated into a secretion-competent IgM oligomer (Fig.1.8)[177]. Taken together, the early QC checkpoint within the ER relies on folding of heavy chain domain whereas formation of an intermolecular disulfide bond is key for escaping later QC induced retention. Biogenesis of IgM therefore exemplifies an assembly induced folding and thiol-dependent QC pathway, where oxidative folding is intimately coupled to folding checkpoints.

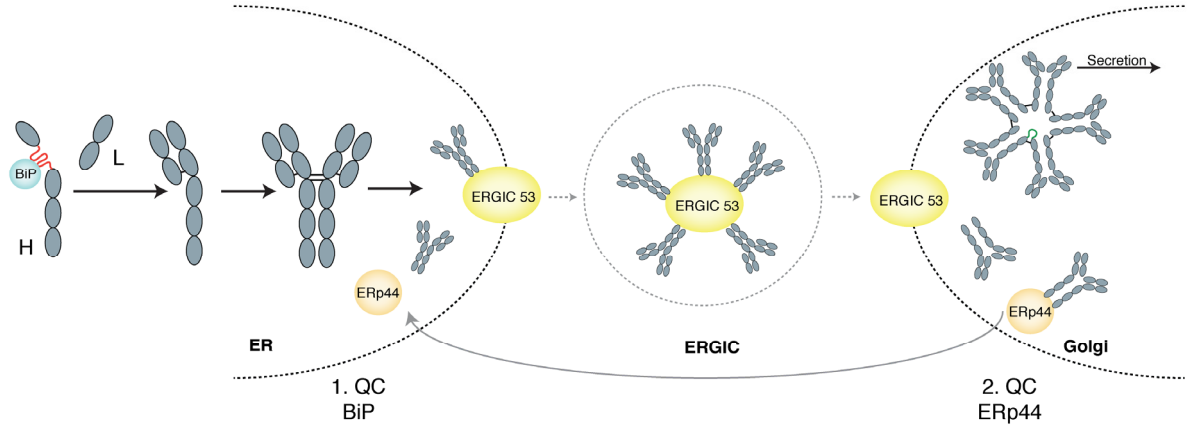

Figure 1.8 IgM biogenesis. IgM is composed of five or six IgM monomers which are further build up by two IgM heavy chains (H) and light chains (L). In a first quality control checkpoint, IgM monomer formation is regulated by an unfolded domain within the H chain which is recognized by BiP. Only upon interaction with the independently folded L-domain, complete folding of this domain is induced. Correctly folded monomeric IgM associates with ERGIC-53 which constitute a polymerization platform for IgM oligomer formation. ERGIC-53 further is responsible for IgM transport towards the Golgi. The pH conditions inside the Golgi lead to dissociation of IgM and ERGIC-53 and fully oligomerized IgM can leave the cell as pentamers, containing a connecting joining (J) chain (green loop) or as hexamers. Assembly of IgM and the J chain occurs late during oligomerization. Unassembled IgM monomers are recognized by ERp44 by an exposed cysteines which form intermonomer disulfides in the IgM pentamer. Retranslocation to the ER provides another chance for IgM monomers to be incorporated into a secretion competent oligomer. Black lines within assembled antibody monomers indicate disulfide bonds.

In many cases, the precise order of protein complex assembly is important, like for the T cell receptor (TCR), which consists of eight polypeptide chains. Prior to interaction with each other, the clonotypic α and β transmembrane chains form complexes with their dedicated co-receptors. TCR biogenesis further includes an assembly-induced folding QC mechanism, where the α chain only obtains its native fold upon assembly with the β chain, similar to the described

IgM monomer formation[180]. Although protein complex assembly is tightly controlled within the ER, unassembled protein subunits constitute a major fraction of proteins targeted for degradation.

1.2.5 ER associated degradation of terminally misfolded proteins

Although a well-functioning system of chaperones and folding factors evolved to facilitate protein maturation in the ER, protein folding is still an error-prone process. Proteins which irreversibly fail to obtain their native structure are potentially harmful for cells and the organism and must be cleared from the ER in a process referred to as ER-associated degradation (ERAD). Since an ubiquitin-proteasome system (UPS) is absent in the ER, proteins dedicated to destruction need to be retrotranslocated into the cytosol where they are finally degraded. ERAD can be divided into three major steps: initial substrate recognition, retrotranslocation with simultaneous ubiquitination and proteasomal degradation[181]. Attachment of ubiquitin occurs at the ER membrane and is executed by transmembrane E3 ligases, which play a key role in connecting ERAD substrate recognition inside the ER to the cytosolic UPS. In yeast, ERAD substrates, depending on the localization of the misfolded region, use different ERAD pathways. Proteins with defective ER luminal portions or misfolded transmembrane regions use the ERAD-L or ERAD-M route *via* the E3 ligase Hrd1. ER proteins with misfolded cytosolic domains are degraded *via* the E3 ligase Doa10 (ERAD-C). Hrd1 and Doa10 are both evolutionally conserved, yet mammalian cells use an extended set of different E3 ligases with a unique or redundant substrate spectrum. Furthermore, a differentiation between distinct ERAD pathways is not as simple as in yeast due to increased complexity in mammals[182,183].

The most extensively studied and discussed topic in the ERAD field is the retrotranslocation channel. There is ample evidence that Hrd1 forms a protein conducting channel within the ER membrane and thereby accomplishes retrotranslocation of its substrates prior to ubiquitination[184-188]. A recently solved cryo-EM structure shows that Hrd1 adopts a pore-like topology inside the ER membrane by forming an aqueous cavity extending from the cytosol almost to the ER lumen[188]. How Hrd1-associating factors may contribute to channel formation and regulation still needs to be elucidated. Additionally, a role of Sec61 in retrotranslocation is still discussed due to reported interactions with ERAD substrates and yeast Sec61 mutants, which are defective in retrotranslocation[189,190]. However, structural

studies on Sec61 homologues revealed a narrow channel architecture which makes is unlikely that partially folded domains or bulky N-linked oligosaccharides are able to traverse through the tunnel[181].

ERAD pathways not only rely on the action of E3 ligases but on further assistance of a variety of ER luminal, membrane and cytosolic co-factors. One major task of the ERAD machinery is to discriminate between folding intermediates and terminally misfolded proteins. This is an especially complex challenge to assess since both protein species may only be discriminated by subtle structural differences. Timing and on-off rates of ERAD and folding factors seem to play important roles[174]. A well-established example of time dependent protein degradation is the afore-mentioned glycan trimming of newly synthetized proteins. Upon a prolonged residence time in the ER, mannose trimming of the glycan core structure by EDEM proteins creates a binding site for Os9. Os9 is a lectin of the ERAD-L pathway which is able to transfer misfolded proteins to Derlin1. The latter is a multispanning transmembrane ER protein which transfers its substrates to Hrd1 for retrotranslocation and ubiquitination[191]. Non-glycosylated proteins can enter the ERAD-L pathway *via* extended interaction with BiP[181]. During retrotranslocation, substrates become ubiquitinated by autoubiquitinated Hrd1[184]. Ubiquitin chains on the substrate and Hrd1 recruit the p97 complex, which extracts the substrate from the ER lumen by its ATPase activity. The p97 complex consists of the p97 AAA+ ATPase, which provides the pulling force for retrotranslocation, adaptor proteins (Ufd1, Npl4) which recruit p97 to the polyubiquitinated substrate/Hrd1 and deubiquitinating enzymes (DUBs)[181,192]. DUBs are absent in yeast but may function indirectly on retrotranslocation activity in mammals, by increasing Hrd1 stability or modulating substrate-E3 affinity[193-196]. After successful ER extraction the proteins become deglycosylated and are maintained in a soluble form by different cytosolic chaperones (e.g. Bag6, Ubl4A, Trc35, Rad23) before being transferred to the proteasome for degradation[181].

ERAD-M follows the basic rout of ERAD-L but its substrates are predicted to enter the Hrd1 translocation channel through a lateral gate which opens in Hrd1 upon substrate binding[185,188,197]. The predicted mechanism is similar to how Sec61 releases TM proteins into the membrane during translation[198].

Certain folded and perfectly active proteins are also targeted for ERAD. However, their degradation does not lead to destruction but to formation of a signaling factor under specific environmental conditions. One well-studied example is HMG-CoA reductase (HMGR), a key

enzyme in sterol synthesis whose degradation by ERAD is part of a negative feedback loop, preventing the accumulation of sterol metabolites[199]. An alternative ERAD pathway exist for ER membrane proteins. Here, an intermembrane rhomboid protease RHBDL4 recognizes ubiquitinated type I membrane proteins with a positive charge inside their transmembrane region. Cleavage results in liberation of a cytosolic and an ER luminal portion with the latter becoming a substrate of the ERAD-L pathway[200]. Interestingly, the Derlin1 transmembrane protein involved in ERAD-L/M shows structural homology to rhomboid proteases but no protease activity is reported. This illustrates how rhomboid proteases evolved for ERAD and how these two processes are still connected[181,201].

Taken together, ERAD provides an effective system to eliminate accumulating misfolded proteins from the ER to allow cell survival. In recent years there has been tremendous progress in understanding ERAD processes. However, further studies are needed to complete our understanding, how ERAD substrates are recognizes and how different ERAD branches work together. Furthermore, mechanistic insights are required to understand these processes.

1.3 Aims of this work

The ER is chemically similar to the extracellular environment and possesses a machinery that allows various posttranslational modifications to occur, which convey functional diversity and/or structural stability to secreted proteins. To allow reliable production of secreted proteins, the ER is equipped with a large variety of molecular chaperones that aid in protein folding and quality control, which secures secretion only of correctly folded and modified proteins. As secretory proteins, interleukin folding and assembly into specific heterodimers takes place in the ER. Despite their biological importance, folding and IL-12 α/β-heterodimerization are only poorly understood[6]. All of the human IL-12 family α-subunits are retained in the ER when expressed alone and require assembly into a heterodimeric interleukin to allow secretion[202-205]. For IL-12/23 folding and assembly evidence of chaperone assistance exists[206,207]. The aforementioned structural features together with their important biological roles render the IL-12 family a very appealing model system to study determinants of protein folding, assembly and quality control in the ER. The different biological roles of IL-12 family members despite their structural similarities furthermore highlight the need for a tight regulation and control of their biosynthesis in the cell. A deeper understanding of the biosynthesis of IL-12 family members may also provide attractive opportunities for pharmacological interventions into these processes. We used an interdisciplinary approach, combining *in vitro* and *in vivo* techniques to elucidate characteristics of IL-12/23 folding and assembly as well as chaperone assistance in the folding process. We aim to achieve an understanding, why the IL-12 family α subunits misfold in the ER and how this is inhibited by their interaction partner. We further asked the question, how incompletely folded α subunits communicate their folding status to the cell.

2 Assembly-induced folding regulates interleukin 12 biogenesis[208]

Susanne Reitberger[1], Pascal Haimerl[2], Isabel Aschenbrenner[1], Julia Esser-von Bieren[2] and Matthias J. Feige[1]*

[1] Center for Integrated Protein Science at the Department of Chemistry and Institute for Advanced Study, Technical University of Munich, Lichtenbergstr. 4, 85748 Garching, Germany
[2] Center of Allergy & Environment (ZAUM) , Technical University of Munich and Helmholtz Zentrum München, Biedersteiner Str. 29, 80802 Munich, Germany,
*Corresponding author: matthias.feige@tum.de

Author Contributions

SR, PH, JEvB and MJF designed experiments. SR, PH, IA and MJF performed experiments. Data was analyzed by SR, PH, IA, JEvB and MJF and the paper was written by SR and MJF.

Published in The Journal of biological chemistry **292**, 8073-8081, doi:10.1074/jbc.M117.782284 (2017)

2.1 Introduction

For proteins of the secretory pathway, folding and assembly have to be coordinated in the endoplasmic reticulum (ER) to guarantee functionality of in total one third of all human proteins[209]. This poses a challenge to the cell as assembly intermediates may already resemble native states of proteins and are thus difficult to discriminate from mature proteins[175].

Different principles are realized in oligomeric proteins to safeguard assembly. Insights into underlying principles have, among others, been obtained for proteins of the immune system where assembly control is particularly critical in quantitative as well as qualitative terms to maintain immune homeostasis. Accordingly, quality control mechanisms have evolved that specifically fulfil the demands of certain immune proteins. For immunoglobulin G (IgG) antibodies, domain folding is coupled to heavy chain (HC) / light chain (LC) interaction and thus allows the ER chaperone machinery to efficiently discriminate native tetrameric IgG (HC_2LC_2) from immature assembly states[176,210,211]. For the oligomeric IgM, pentamerization of HC_2LC_2 tetramers has to be assessed additionally. This is particularly challenging, as HC_2LC_2 tetramers are already well-folded[212,213]. Free cysteines within not yet pentamerized IgM allow the cell to perform this critical quality control step and allow the recovery of HC_2LC_2 tetramers from the Golgi *via* the chaperone ERp44[159,214]. For oligomeric membrane-embedded B cell receptors, assembly within the membrane can be directly scrutinized[215] and for an even more complex membrane protein in the immune system, the αβT cell receptor, multiple checkpoints exist that couple folding, membrane integration and shielding of retention motifs to scrutinize assembly of in total eight polypeptide chains and thus guarantee correct receptor functionality[180,216-221].

For one important family of proteins in the immune system, the interleukin-12 (IL-12) family, which comprises IL-12, IL-23, IL-27 and IL-35[6], principles of assembly control are not yet understood but are particularly intriguing: each family member is a heterodimer composed of one α and one β subunit. The α subunits are four-helix bundle proteins; β subunits are composed of fibronectin and Ig domains and are related to IL receptors[222,223]. Furthermore, the four heterodimeric family members are made up of only five shared subunits, three α (IL-12α/p35, IL-23α/p19 and IL-27α/p28) and two β subunits (IL-12β/p40 and EBI3), adding a layer of combinatorial complexity to assembly regulation and control in the cell; in particular since certain immune cells produce all five subunits simultaneously

(see e.g.[224]) and the family members perform highly distinct immunoregulatory roles: IL-12 and IL-23 are mostly pro-inflammatory cytokines, and targeting IL12 and IL23 has emerged as an important therapeutic avenue to treat immune-mediated inflammatory diseases[225]. In contrast, IL-27 and IL-35 act immunomodulatory or immunosuppressive, respectively[6,226].

To dissect molecular principles of IL-12 family assembly, within this work we focused on the founding member IL-12/p70[203,227,228]. IL-12 is produced by antigen presenting cells and can stimulate T cell differentiation into pro-inflammatory T_H1 cells that secrete IFNγ, which further increases T_H1 cell differentiation in a positive feedback loop[14,229]. As such, IL-12 is critical for the eradication of intracellular pathogens and has gained interest in stimulating anti-tumor responses and regulating autoimmunity[6,226,230]. IL-12 is a disulfide-bridged heterodimeric glycoprotein composed of IL-12α and IL-12β[223,228]. Both subunits need to be expressed simultaneously in order to secrete bioactive IL-12[203,231]. Of note, isolated IL-12β can be secreted as a monomer or homodimer[228,232,233], whereas isolated IL12α is retained in cells and its secretion depends on IL-12β expression[204,234]. Why IL-12α as opposed to IL-12β is retained and how IL-12β induces secretion of IL-12α, and thus biologically active IL-12, has remained unclear but is critical to understand IL-12 family-mediated immune reactions as well as principles of cellular protein assembly control.

Here we show that in isolation IL-12α fails to fold properly, accumulating non-native protein redox species. Misfolding is inhibited by IL-12β, giving rise to the native IL-12 heterodimer. Furthermore, we identify which of the seven cysteine residues in IL-12α contribute to folding and heterodimerization *versus* misfolding and degradation. This study thus establishes assembly-induced folding as a general mechanism in IL-12 family biogenesis.

2.2 Results

2.2.1 IL-12β releases IL-12α from ER retention

The secretion of IL-12 depends on the expression of both subunits of the IL-12 heterodimer (Fig. 2.1a), IL-12α and IL-12β[203,231]. It has been shown that IL-12α is retained in the cell in isolation, whereas isolated IL-12β is readily secreted and its expression is limiting for the secretion of heterodimeric IL-12[204]. In agreement with these findings, our data show that human IL-12α is retained in 293T cells, an established model cell line for studying IL-12 family assembly[17,39,204,205], and its secretion is induced by human IL-12β (Fig. 2.1b). In contrast, IL-12β alone is readily secreted (Fig. 2.1c). Although IL-12 is a covalent heterodimer (Fig. 2.1a), mutation of the cysteine residues in IL-12α and IL-12β that form the interchain disulfide bond in the heterodimer to Ser (IL-12α^{C96S} and IL-12β^{C199S}, respectively) neither significantly affected IL-12β-induced secretion of IL-12α (Fig. 2.1b)[223,235] nor secretion of IL-12β^{C199S} alone (Fig. 2.1c).

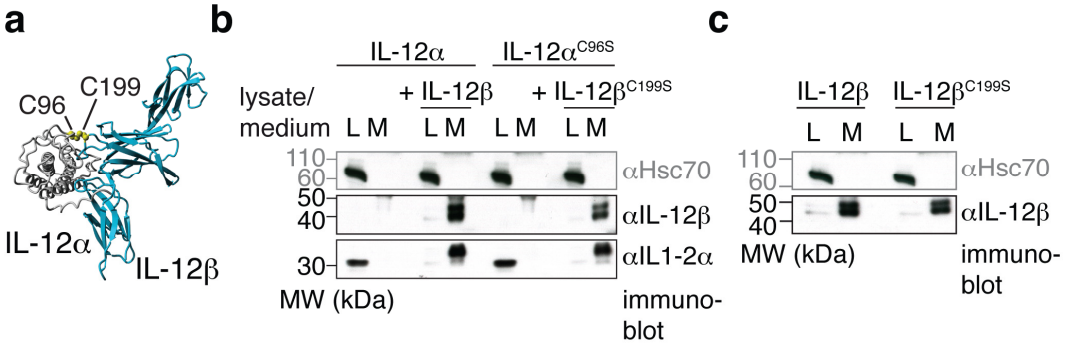

Figure 2.1 IL-12α secretion depends on IL-12β co-expression. a IL-12 structure. IL-12 is composed of two covalently linked subunits (IL-12α and IL-12β, structure based on pdb entry 3HMX). The IL-12α subunit is depicted in grey, the IL-12β subunit in blue. The intermolecular disulfide bond between IL-12α C96 and IL-12β C199 is shown in a yellow CPK representation. **b** IL-12α secretion analyzed by immunoblotting. IL-12α is retained in the cell if expressed in isolation (L, lysate) and co-expression of IL-12β induces its secretion (M, medium) independent of the presence or the absence of the cysteine residues that form the IL-12α-IL-12β disulfide bridge. 1% lysate or medium were applied to the gel and blotted with the indicated antibodies. Hsc70 served as a loading control. **c** IL-12β secretion analyzed by immunoblotting. The same as in b), only that isolated IL-12β and its C199S mutant were analyzed.

2.2.2 Misfolding of isolated IL-12α is inhibited by IL-12β

To assess the molecular basis for ER retention of IL-12α we analyzed its redox status in the cell, as an indicator for its folding state[236]. IL-12α possesses seven cysteines, six of which form three intramolecular disulfide bonds in the native state and one forms an intermolecular disulfide bridge with IL-12β[223]. Analysis of the redox status of IL-12α by non-reducing SDS-PAGE coupled to immunoblotting revealed multiple redox species for IL-12α expressed in

isolation, which collapsed into a single species upon treatment of cells with the reducing agent dithiothreitol (DTT) (Fig. 2.2a). These species included one with a higher electrophoretic mobility than the reduced protein, a species with the same mobility as the reduced protein and a prominent species at approximately the size of an IL-12α dimer as well as several higher molecular weight forms (Fig. 2.2a).

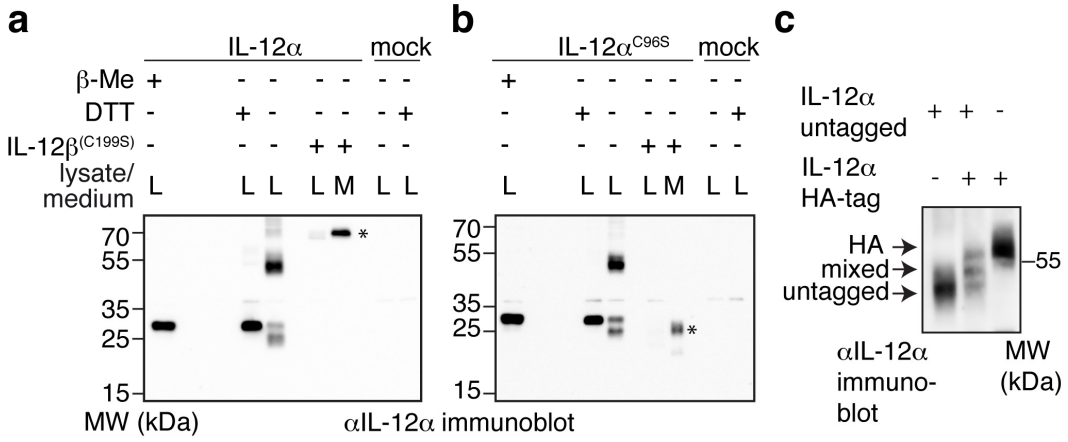

Fig. 2.2 Misfolding of isolated IL-12α is inhibited by IL-12β. **a** IL-12α redox state in the cell. The oxidation state of IL-12α was analyzed by non-reducing SDS-PAGE. Where indicated, samples were treated with β-mercaptoethanol (β-Me) after cell lysis to provide a standard for completely reduced protein or cells were treated with DTT for 1 h before lysis to reduce disulfide bonds in cells. Alternatively, IL-12β was co-expressed to analyze its effect on the redox state of IL-12α. 293T cells were (co-)transfected with the indicated IL-12α-/β-subunits and 2% lysate (L) or medium (M) were applied to the gel and blotted with the indicated antibodies. IL-12 heterodimers are highlighted with an asterisk. **b** IL-12α^{C96S} redox status in the cell. The same as in a), only that IL-12α^{C96S} was analyzed in the absence or presence of IL-12β^{C199S} as indicated. Secreted IL-12α^{C96S} is highlighted with an asterisk. **c** IL-12α oligomerization in the cell. Possible IL-12α dimerization was assessed by co-expression of untagged and HA-tagged IL-12α subunits. IL-12α untagged/HA-tagged only samples served as size standard in comparison to the co-transfected sample. 1% lysate was analyzed by non-reducing SDS-PAGE (8% gel) and blotted with the indicated antibodies.

Under the IL-12α/IL-12β expression ratio of our experiments, co-expression of IL-12β led to secretion of the covalent IL-12α-IL-12β heterodimer concomitant with the disappearance of all intracellular redox species except for the heterodimer (Fig. 2.2a). Of note, when IL-12α^{C96S} was analyzed analogously, a very similar mispairing behavior of its disulfide bonds was observed (Fig. 2.2b). This argues that the multiple redox species of IL-12α are not caused by its C96 residue, which is unpaired in the absence of IL-12β. Similar to the wild type (wt) pair, IL-12β^{C199S} induced secretion of IL-12α^{C96S}, which, once secreted, migrated with an electrophoretic mobility in between the species observed in the lysate (Fig. 2.2b). This suggests the formation of intrachain disulfide bonds and further modification of the N-linked glycans in the Golgi in IL-12α^{C96S}, as expected to occur upon its secretion induced by IL-12β^{C199S}. The different redox species observed for IL-12α could either be due to covalent IL-

12α oligomerization, interaction with other cysteine-containing proteins, e.g. ER oxidoreductases, or both. To discriminate between these scenarios for the major IL-12α species of ca. 50-60 kDa (Fig. 2.2a and b), we co-expressed HA-tagged and untagged IL-12α. If the α subunit was able to form homodimers, a mixed complex of untagged and HA-tagged α subunits with a size in between the homogenous complexes was expected. Indeed, in these experiments three bands at the expected sizes of the possible IL-12α dimers were present (Fig. 2.2c). Thus, in absence of the IL-12β subunit, IL-12α is prone to form disulfide-bridged homodimers.

2.2.3 Impact of disulfide bonds in IL-12α on IL-12 folding, assembly and secretion

Our data reveal that isolated IL-12 family α-subunits populate non-native redox species in the cell whose formation is suppressed by IL-12β. To assess the impact of the different cysteine residues in IL-12α on this behavior, we individually replaced each of the disulfide bond-forming cysteine pairs in IL-12α (SS1-3) against serines (Fig. 2.3a), denoted as ΔSS1/2/3. Our data show that all IL-12α mutants individually lacking one disulfide bridge had a qualitatively comparable redox pattern to wt IL-12α, including monomers, dimer and larger species (Fig. 2.3b, left). However, the relative amount of the species varied significantly for the different mutants in comparison to wt. To assess the extent of covalent misfolding of the different disulfide mutants, we quantitatively compared the percentage of high molecular weight (HMW) and low molecular weight (LMW) species, defined as species migrating above or below 35 kDa, respectively (Fig. 2.3b, left). Remarkably, all disulfide mutants showed significantly less HMW species than the wt, with mutants ΔSS1 and ΔSS2 having a particularly strong impact (Fig. 2.3b, right). All mutants were still retained in the cell when expressed in isolation and thus unable to pass ER quality control (Fig. 2.3c). Upon IL-12β co-expression, IL-12α ΔSS1 and ΔSS2 were secreted to a very similar extent as IL-12α wt whereas IL-12α ΔSS3 showed no secretion upon co-expression of IL-12β (Fig. 2.3c). Furthermore, all secretion-competent IL-12α disulfide mutants were still able to form the heterodimeric IL-12 complex inside the cell, albeit with an apparently slightly reduced efficiency as judged by the presence of different IL-12α redox species even in the presence of IL-12β (Fig. 2.4). To further analyze the secretion behavior of our mutants we co-transfected them with IL-12β^{C199S}, which cannot form the intermolecular disulfide bond resulting in a non-covalent IL-12 complex.

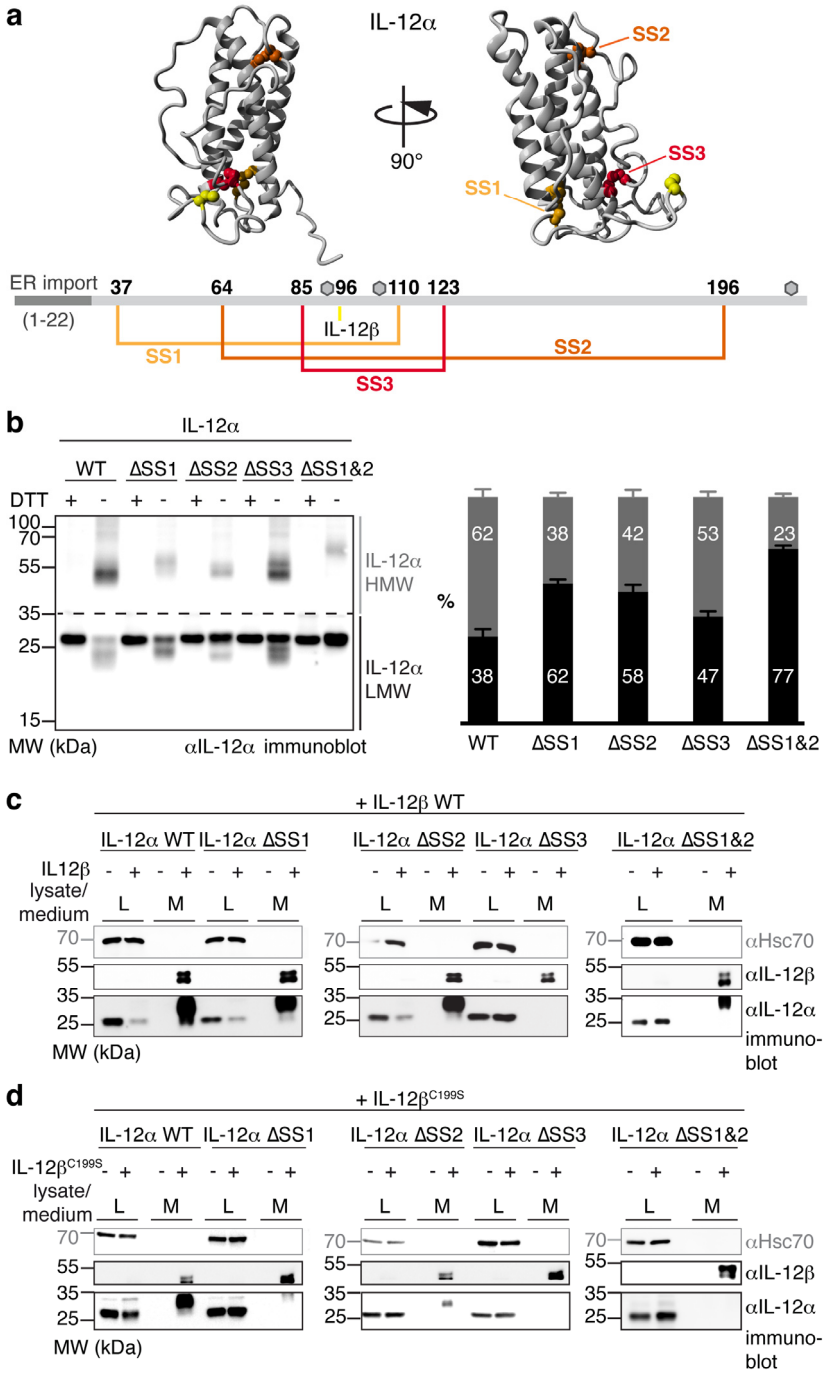

Figure 2.3 Disulfide bonds differently affect IL-12α misfolding and secretion. a Disulfide bonds within IL-12α. Cysteines forming intra- or intermolecular disulfide bridges are highlighted in IL-12α (structure based on the pdb file 3HMX), numbered and depicted in the corresponding colors in IL-12α. Grey hexagons indicate predicted glycosylation sites. **b** Impact of intramolecular disulfide bonds on the IL-12α redox state. IL-12α subunits individually lacking one disulfide bridge (ΔSS1-3, respectively; cysteine pairs were mutated to Ser) or a combination of two mutants (ΔSS1&2) were analyzed by non-reducing SDS-PAGE (left). 293T cells were transfected with the different IL-12α subunits, where indicated treated with DTT and 2% lysate (L) were applied to the gel and blotted with IL-12α antibody. A quantitative analysis (right) indicates the percentage of high molecular weight (HMW) and low molecular weight (LMW) IL-12α species (N=4±SEM). LMW species (black) were defined as smaller than 35 kDa, HMW species (grey) as larger than 35 kDa. **c** Secretion behavior of IL-12α disulfide bond mutants. 293T cells were transfected with the indicated constructs and 2% lysate (L) or medium (M) were applied to the gel and blotted with the indicated antibodies. Hsc70 served as a loading control. **d** Secretion behavior of IL-12α disulfide bond mutants. Same as in c), only that IL-12α constructs were co-transfected with IL-12β^{C199S}.

IL-12α ΔSS1 and ΔSS2 were still secreted with IL-12β^{C199S}, but much less efficiently than the IL-12α wt/IL-12β^{C199S} pair (Fig. 2.3d), revealing an interplay between the different disulfide bonds. Again, no secretion of IL-12α ΔSS3 could be detected (Fig. 2.3d), which is in agreement with the observed redox species (Fig. 2.4). Since our data revealed that disulfide bonds 1 and 2 in IL-12α were dispensable for secretion of a covalent IL-12α-IL-12β heterodimer (Fig. 2.3c), in a next step we combined these deletions (ΔSS1&2), giving rise to an IL-12α mutant with only three cysteine residues. This mutant populated the least amount of HMW species of all mutants tested (Fig. 2.3b). Of note, it was the only mutant, which showed exclusively one monomeric species, migrating the same as the reduced protein (Fig. 2.3b, left). Furthermore, efficient secretion of IL-12α ΔSS1&2 could still be induced by IL-12β wt but not by IL-12β^{C199S} (Fig. 2.3c, d)

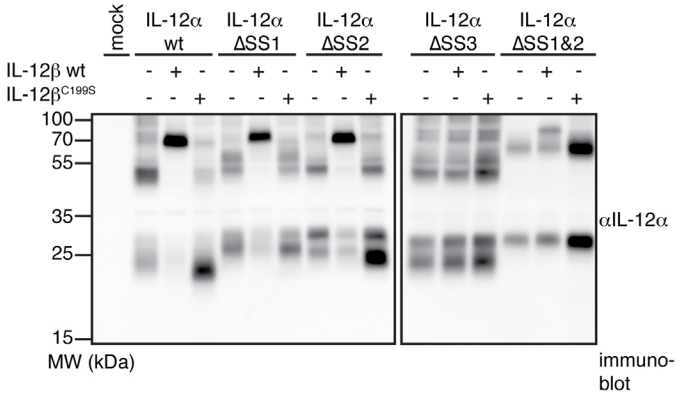

Figure 2.4 Influence of IL-12α disulfide bonds on IL-12α redox status in the presence of IL-12β. The redox status of IL-12α alone and in the presence of IL-12β or IL-12β^{C199S} was analyzed by non-reducing SDS-PAGE. Samples were treated with brefeldin A for 1 h before lysis to inhibit protein secretion. 293T cells were co-transfected with the indicated IL-12α-/β-subunits and 2% lysate was applied to the gel and blotted with anti-IL-12α antibody

2.2.4 Assessing determinants of IL-12α degradation

The reduction of disulfide bonds can be rate-limiting in ER-associated protein degradation (ERAD)[156]. Since we had observed covalent misfolding for IL-12α, we assessed the half-life of our IL-12α disulfide mutants by cycloheximide (CHX) chase experiments combined with quantitative immunoblots. For wt IL-12α we observed a half-life of ~1.6 h (Fig. 2.5a), in agreement with a previous study that reported a half-life of ~2 h[204]. Unexpectedly, our data revealed no significant differences in the half-lives of all IL-12α disulfide mutants in comparison to wt IL-12α (Fig. 2.5a). Taken together, these data suggested an overall limited role of disulfide bridges on the stability of unassembled IL-12α in the cell, which is in agreement with the only slightly faster degradation kinetics of IL-12α HMW species *versus* LMW species (Fig. 2.5b).

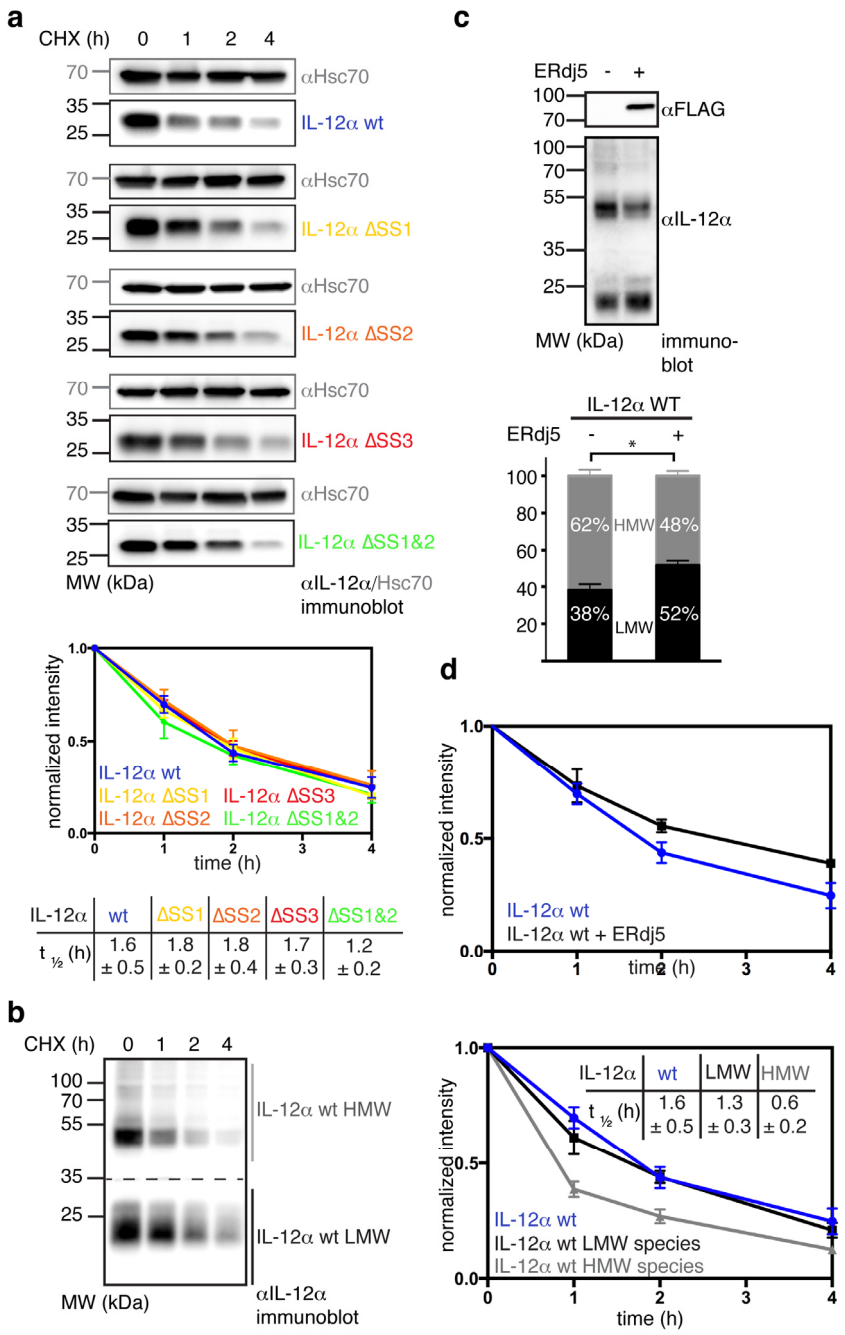

Figure 2.5 Influence of intramolecular disulfide bridges and ERdj5 on IL-12α degradation. a Measurement of IL-12α turnover by cycloheximide (CHX) chase assays. 293T cells were transfected with the indicated IL-12α subunits and incubated with CHX for up to 4 h. Cell lysates were analyzed by immunoblotting with anti-IL-12α antibody. The anti-IL-12α immunoblot signal was normalized to the signal present at the beginning of the chase for the respective IL-12α constructs (N=4± SEM). Half-lives from exponential fits of the curves (±SD) are shown below the graph. **b** Degradation behavior of HMW and LMW IL-12α species. Same as in a) but cell lysates were analyzed under non-reducing conditions. The anti-IL-12α immunoblot signal was normalized to the signal of high molecular weight (HMW) (larger than 35 kDa) and low molecular weight (LMW) species (smaller than 35 kDa) which were present at the start of the chase. Half-lives of LMW and HMW species were compared with IL-12α wt from a), (N=4±SEM). Half-lives from exponential fits of the curves (±SD) are shown in the table. **c** Influence of ERdj5 over-expression on the IL-12α redox state. The amount of HMW and LMW IL-12α species in the absence or presence of ERdj5 overexpression was analyzed (N=3±SEM; the asterisk indicates $p<0.05$). Expression of FLAG-tagged ERdj5 was verified by immunoblotting. **d** Influence of ERdj5 overexpression on IL-12α degradation. IL-12α turnover by CHX chase assays in the absence (data taken from a)) or presence of ERdj5 overexpression (N=3±SEM).

Nevertheless, IL-12α HMW species most likely need to be reduced prior to degradation. Thus, to further understand the biological fate of mis-assembled IL-12 α-subunits we assessed if the BiP co-chaperone ERdj5[237] was involved in their degradation. For the truncated α1-antitrypsin mutant NHK, which aberrantly forms disulfide-bridged dimers, ERdj5 accelerates its degradation[156]. Interestingly, overexpression of ERdj5 shifted the HMW/LMW ratio of IL-12α towards the monomeric species, arguing that ERdj5 can indeed reduce covalent IL-12α assemblies (Fig. 2.5c). Degradation of IL-12α in the presence of ERdj5, however, was not accelerated but rather appeared slightly decelerated, indicating that reducing the disulfide bonds in mis-assembled IL-12α is not rate-limiting for its degradation (Fig. 2.5d).

2.2.5 A simplified, biologically active IL-12

Since our data revealed that two out of three disulfide bonds in IL-12α are dispensable for secretion and did not change the rate of IL-12α degradation, we next investigated their impact on the stability and biological activity of IL-12. Towards this end we incubated supernatants of 293T cells co-transfected with IL-12β and either IL-12α wt, ΔSS1, ΔSS2 or ΔSS1&2 for extended times at 37 °C (IL-12α ΔSS3 was excluded since it was not secreted with IL-12β). None of the constructs showed detectable aggregation within 48 h and all revealed a stability comparable to wt IL-12 (Fig. 2.6a).

Next, to assess the impact of the different cysteine deletions in IL-12α on IL-12 activity, we used supernatants of 293T cells co-transfected with IL-12β wt and all different IL-12α mutants and assessed their effect on IFNγ induction in human peripheral blood mononuclear cells (hPBMCs). For all the mutants that were secreted in the presence of IL-12 (Fig. 2.3c) we also observed induction of IFNγ in hPBMCs (Fig. 2.6b) indicating that most cysteines within IL-12α are dispensable for IL-12 activity.

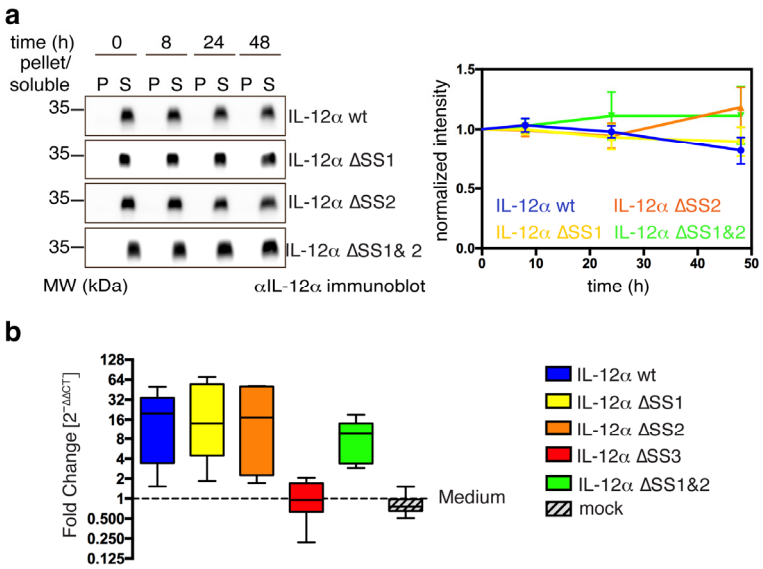

Fig. 2.6 Influence of intramolecular disulfide bonds on IL-12α extracellular stability and biological activity. a For stability tests, 293T cells were transfected with IL-12β and the indicated IL-12α subunits. 24 h after transfection, supernatants were withdrawn and incubated at 37 °C for the indicated times. 2% pellet (P) and soluble (S) material was analyzed by SDS-PAGE and blotted with IL-12α antibody. The anti-IL-12α immunoblot signal for soluble protein was normalized to the signal at 0 h incubation for the respective IL-12α constructs (N=4±SEM). **b** Biological functionality of different IL-12 disulfide mutants. To assess the biological activity of IL-12 complexes containing different IL-12α mutant subunits, hPBMCs (from 6 blood donors) were stimulated with supernatants from 293T cells expressing IL-12β and one of the different IL-12α constructs as indicated. The relative expression of IFNγ was determined by qPCR, normalized to IFNγ expression in hPBMCs in the presence of medium from mock-transfected cells and calculated as described in the experimental part.

2.3 Discussion

Since its discovery, IL-12 has gained particular interest due to its heterodimeric nature[203,227,228]. Early on, it had been speculated that its β subunit could potentially act as a scaffold for more than one co-subunit because IL-12β could not only be secreted in complex with IL12α but also alone[228,231]. This idea was proven correct when IL-23 was discovered[39] and more recently has come into focus again when mass spectrometric studies revealed several IL-12β-interacting proteins in mouse plasma[238]. This interaction promiscuity is a general theme within the IL-12 family, where at least four heterodimers (IL-12, IL-23, IL-27 and IL-35) are made up by only five subunits[6]. Since IL-12α as well as IL-23α secretion are dependent on IL-12β[39,203,204,231], and secreted IL-12β can compete with IL-12 signaling[232,239], important questions arise about how IL-12β can induce the secretion of multiple α-subunits and how this process, and thus downstream immune reactions, are regulated and controlled in the ER. The IL-12 family thus extends assembly-induced secretion as a principle in ER quality control[209,240] by important questions.

Our data show that assembly-induced folding of IL-12α is key: isolated IL-12α misfolds and forms non-native disulfide bonds. IL-12β inhibits these side reactions in the ER and induces formation of native IL-12. It is noteworthy that isolated IL-12α predominantly forms covalent homodimers. Such a well-defined interaction suggests a certain degree of structure in isolated IL-12α. In other proteins of the immune system, where assembly-induced folding underlies ER quality control, no such well-defined non-native covalent assembly states have been observed[180,211,241].

In more general terms, the formation of non-native disulfide bonds is often an initial step in oxidative protein folding and it is often assumed that folding drives correct disulfide bond formation[144,242,243]. Since IL-12α depends on IL-12β for proper folding, oxidation can be separated from folding. It remains to be seen if IL-12β can rescue IL-12α from misfolding, as has been observed for the αβTCR upon assembly *in vitro*[180], or if assembly has to occur early on to inhibit otherwise irreversible IL-12α misfolding. In addition to their effects on folding, non-native disulfide bonds can decelerate degradation by ERAD. Interestingly, we find that over-expression of ERdj5, an ER oxidoreductase involved in ERAD[156] but also in disulfide isomerization during productive folding[244], reduces the amount of non-native covalently assembled IL-12α but does not accelerate IL-12α degradation. In combination with our

findings that the half-life of the different IL-12α disulfide mutants was unaltered, this argues that ERAD factors downstream of ERdj5/IL-12α reduction are likely rate-limiting for its degradation.

Native IL-12α possesses three intramolecular and one intermolecular disulfide bond connecting it with IL-12β[223]. Whereas the intermolecular disulfide bridge is dispensable for the secretion of bioactive IL-12[223,235], our data show that an interplay exists between the various disulfide bonds within IL-12α and the IL-12 heterodimer. Surprisingly, two out of the three disulfide bond within IL-12α can be deleted while still allowing secretion of IL-12 - yet only if these IL-12α mutants can form covalent dimers with IL-12β. If not, IL-12β-induced secretion of IL-12α lacking any one of its disulfide bonds is drastically reduced arguing for a mutual stabilization by intra- and intermolecular disulfide bridges in IL-12. Previous studies had shown that Tunicamycin (Tm), which globally inhibits N-linked glycosylation, significantly reduces IL-12 secretion[233]. Often an interplay between glycosylation and oxidative folding exists, e.g. by chaperone recruitment to or exclusion from certain sites within a polypeptide as well as mediated by CNX/CRT recruited PDIs[209,245]. Abolishment of IL-12 glycosylation by Tm treatment may thus also impact on correct oxidative folding of IL-12α, which we now report to be important in IL-12 biogenesis. However, our findings also show that a simplified IL-12 heterodimer is possible. Deleting two out of the three disulfide bonds in IL-12α did not significantly reduce secretion efficiency and stability of IL-12 while biological activity was maintained and covalent misfolding within cells was reduced. We cannot exclude however, that biological activity under limiting concentrations of IL-12 was reduced or stability under more drastic conditions or in the more complex environment of the blood was compromised. Nevertheless, the combination of these beneficial traits may render this simplified IL-12α an interesting molecule, as IL-12 has regained interest in immunotherapy[246,247]. Of note, this simplified IL-12 also shows that population of a more compact IL-12α species, which argues for disulfide bond formation within the subunit (see Fig. 2.3b), is not a prerequisite for IL-12 secretion. This highlights intriguing questions regarding the structural biology of IL-12 cytokines: which extent of structure within IL-12α and IL-23α is necessary for specific recognition by IL-12β to form the similar but structurally distinct IL-12 or IL-23 heterodimers[26,223]? And how, being incompletely structured, does IL-12α specifically recognize even a second interaction partner, EBI3, to give rise to IL-35[17,202]? Answers to these questions, building on our findings (Fig. 2.7), will depend on more detailed *in vitro* studies as

well as insights into which ER chaperones regulate and control these processes[248] to reveal how folding and assembly of IL-12 family members is orchestrated in immune cells to shape immune responses.

2.4 Graphical summary

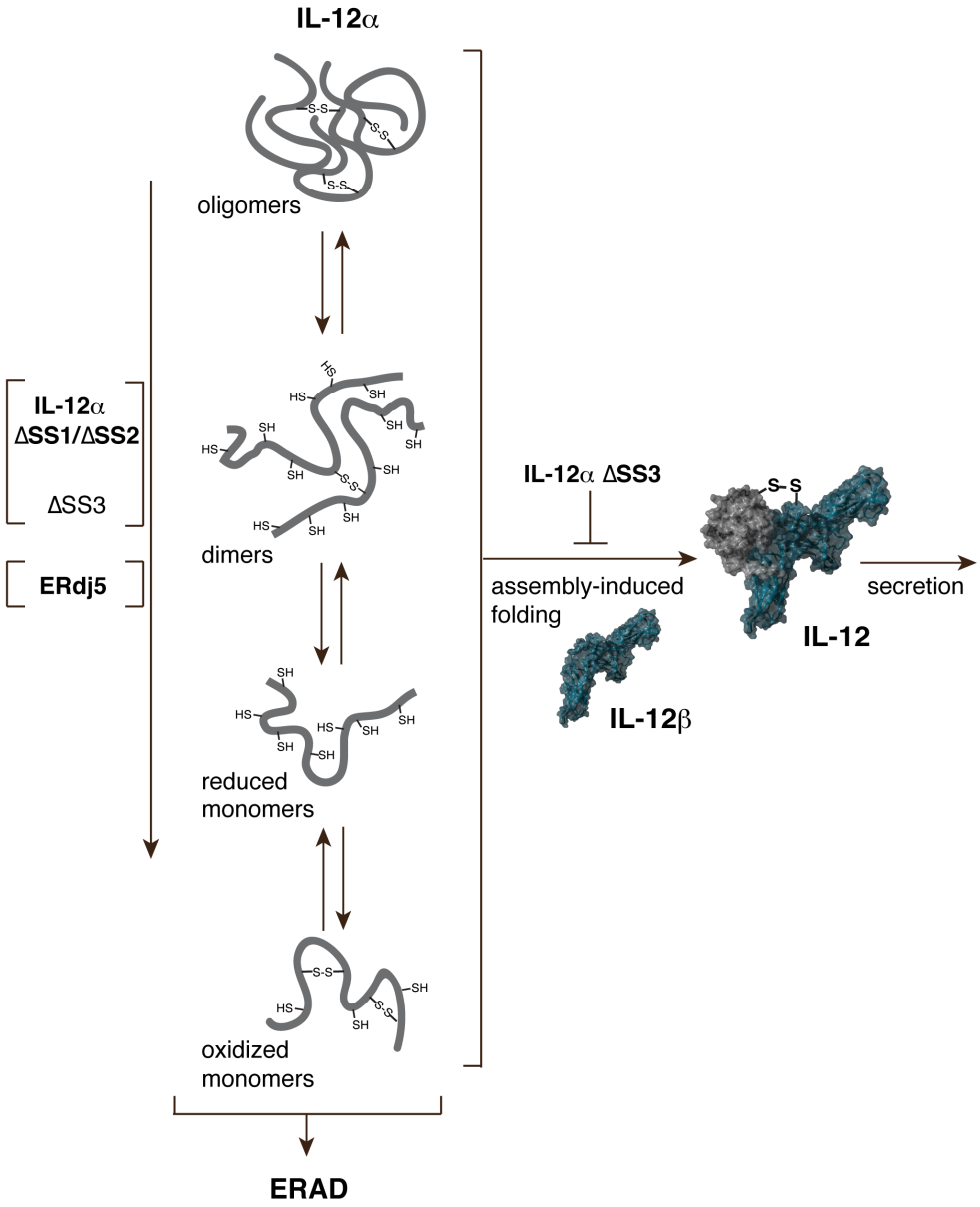

Figure 2.7 A model for IL-12 biogenesis. In isolation, IL-12α covalently misfolds including a prominent homodimeric species. Assembly with IL-12β inhibits misfolding and allows secretion of bioactive IL-12. Disulfide bond 3 within IL-12α is essential for IL-12β-induced secretion, whereas disulfide bonds 1 & 2 are dispensable. Their deletion, as well as ERdj5 overexpression, leads to a reduced amount of covalently misfolded IL-12α, which is ultimately targeted for ERAD if no IL-12β is present.

2.5 Experimental part

Constructs

Human interleukin cDNAs were obtained from Origene (Rockville) and cloned into the pSVL (Amersham) vector for mammalian expression. FLAG-tagged murine ERdj5 [156] and was a kind gift from Kenji Inaba, Tohoku University. Mutants were generated by site-directed mutagenesis. All constructs were sequenced.

Cell culture and transient transfections

293T cells were grown in Dulbecco's modified Eagle's medium (DMEM) containing L-Ala-L-Gln (AQmedia, Sigma-Aldrich) supplemented with 10% (v/v) fetal bovine serum (Biochrom) at 37 °C and 5% CO_2. Medium was complemented with a 1% (v/v) antibiotic-antimycotic solution (25 µg/ml amphotenicin B, 10 mg/ml streptomycin, and 10,000 units of penicillin; Sigma-Aldrich). Transient transfections were carried out for 24 h in either p35 or p60 poly D-lysine coated dishes (Becton Dickinson) using GeneCellin (BioCellChallenge) according to the manufacturer's protocol. In p35 dishes, always 1 µg of IL-12α DNA and 2 µg of IL-12β DNA were (co-)transfected, in p60 dishes, always 2 µg of IL-12α DNA and 4 µg of IL-12β DNA were (co-)transfected if not stated otherwise. For ERdj5 experiments, 1 µg of IL-12α DNA were co-transfected with 1 µg of ERdj5 DNA.

Immunoblotting experiments

For secretion experiments by immunoblotting, cells were transfected for 8 h in p35 dishes, washed twice with PBS and then supplemented with 0.5 ml fresh medium for another 16 h. For CHX chase assays cells were treated with 50 µg/ml CHX (Sigma-Aldrich) for times indicated in the figures before lysis. Prior to lysis, if indicated, cells were treated with 10 mM DTT or 1 µg/ml brefeldin A (Sigma-Aldrich) for the last hour, washed twice in ice cold PBS, supplemented with 20 mM NEM if samples were to be run on non-reducing SDS-PAGE gels. Cell lysis was carried out in RIPA buffer (50 mM Tris/HCl, pH 7.5, 150 mM NaCl, 1.0% Nonidet P40 substitute, 0.5% sodium deoxycholate, 0.1% SDS, 1x Roche complete Protease Inhibitor w/o EDTA; Roche Diagnostics). 20 mM NEM was added to the lysis buffer for non-reducing SDS-PAGE gels. To analyze secreted proteins, the medium was centrifuged for 5 min, 300 g, 4 °C. Subsequently, samples were supplemented with 0.1 volumes of 500 mM Tris/HCl, pH 7.5,

1.5 M NaCl (and 200 mM NEM in the case of non-reducing SDS-PAGE) and protease inhibitor and centrifuged for 15 min, 20,000 g, 4 °C. Samples were supplemented with 0.2 volumes of 5x Laemmli containing either β-Me for reducing SDS-PAGE or 100 mM NEM for non-reducing SDS-PAGE. For the stability assay, samples were treated like described above for secretion experiments and subsequently incubated at 37 °C for the times indicated in the figures, recentrifuged (15 min, 20,000 g, 4°C) and pellet or supernatant were supplemented with equal amounts of 1x Laemmli containing β-Me. For immunoblots, samples were run on 12% SDS-PAGE gels, transferred to PVDF membranes and blotted with anti-IL-12α (abcam ab133751, 1:1,000 in TBS, 0.05% Tween, 5% milk), anti-IL-12β (abcam ab133752, 1:500 in TBS, 0.05% Tween, 5% milk), anti-Myc Tag (millipore 05-724, 1:500 in TBS, 0.05% Tween, 5% milk), anti-FLAG (Sigma-Aldrich F1804, 1:1,000 in TBS, 0.05% Tween, 5% milk) or anti Hsc70 (Santa Cruz sc-1059, 1:1,000 in gelatin buffer (0.1% gelatine, 15 mM Tris/HCl, pH 7.5, 130 mM NaCl, 1 mM EDTA, 0.1% Triton X-100, 0.002% NaN_3). Species-specific HRP-conjugated secondary antibodies (in TBS, 0.05% Tween, 5% milk or gelatin buffer) were used to detect the proteins (Santa Cruz). Blots were detected using Amersham ECL prime (GE, Freiburg, Germany) and a Fusion Pulse 6 imager (Vilber Lourmat).

Quantification and statistics

Western blots were quantified using the Bio-1D software (Vilber Lourmat). Statistical analyses were performed using Prism (GraphPad Software). Where indicated, data were analyzed with two-tailed, unpaired Student's *t*-tests. Differences were considered statistically significant when $p<0.05$. Where no statistical data are shown, all experiments were performed at least three times, and one representative experiment was selected.

PBMA stimulation assays

Whole blood was collected from six healthy volunteers at the Center of Allergy and Environment Munich (ZAUM) after informed written consent and after ethical approval by the internal ethics review board at the University Hospital of the Technical University of Munich (internal reference number: 5156/11) in S-Monovette® tubes with EDTA (Sarstedt, Nümbrecht, Germany). PBMCs were isolated by gradient centrifugation using Polymophoprep (Axis Shield, Oslo, Norway) and depleted of CD14 positive monocytes by using human CD14 MicroBeads (Miltenyi Biotec) according to the manufacturer's protocol. CD14 negative PBMCs

were cryopreserved until further use. Frozen PBMCs were rapidly thawed at 37 °C and resuspended in RPMI 1640 media (Thermo Fisher Scientific) supplemented with 10% heat-inactivated FBS (GE Healthcare) and 100 units/mL penicillin, 100 µg/mL streptomycin, 1 µg/mL gentamicin, 2 mM L-glutamine (Thermo Fisher Scientific). The different IL-12 constructs were expressed in 293T cells as described above. IL-12-containing 293T supernatants were centrifuged for 30 min, 2,000 g and 4 °C before use. Thawed PBMCs were seeded at a density of $1x10^6$ /mL and stimulated with 20 µL of supernatant from 293T cells expressing the different IL-12 constructs or 293T media as control and incubated for 24 h at 37 °C and 5% CO_2. After centrifugation (2,000 rpm, 3 min, 4 °C), PBMCs were rinsed with cold PBS and lysed in RLT buffer (Qiagen) supplemented with 1% β-mercaptoethanol at room temperature. Cell lysates were stored at -70 °C or directly used for RNA isolation. Total RNA was isolated using QuickRNA™ MicroPrep (Zymo Research) by following the manufacturer's instructions. cDNA was synthesized using the High-Capacity cDNA Reverse Transcription Kit (Thermo Fisher Scientific) following the manufacturer's instructions. cDNA was diluted in DEPC Treated Water (Thermo Fisher Scientific) to a concentration of 1.25 ng/µL. qPCR was performed in 384-well plates (4titude) in duplicates using FastStart Universal SYBR Green Master (Rox) (Roche) and forward and reverse target gene primer in a final concentration of 640 nM (18S forward: 5'-GTA ACC CGT TGA ACC CCA TT-3'; reverse: 5'-CCA TCC ATT CGG TAG TAG CG-3'; IFNγ forward: 5'-TCA GCC ATC ACT TGG ATG AG-3'; reverse: 5'-CGA GAT GAC TTC GAA AAG CTG-3'; metabion) Data were collected in a ViiA™ 7 Real-Time PCR System (Thermo Fisher Scientific) following the conditions: 50 °C x 2 min (1x), 95 °C x 10 min (1x), followed by 40 cycles of 95 °C x 15 s and 60 °C x 1 min. Samples exceeding a cycle threshold (Ct) of 35 were excluded from data processing. The relative gene expression of IFNγ was calculated using the comparative Ct method ($2^{-\Delta\Delta Ct}$).

Structural modeling

Missing loops in the IL-12 structure were modelled with Yasara Structure (www.yasara.org) and the final structure was energy-minimized.

3 The molecular basis of chaperone-mediated interleukin 23 assembly control

Susanne Meier[1], Sina Bohnacker[1], Carolin J. Klose[1], Abraham Lopez[1,2], Christian A. Choe[3], Philipp W. N. Schmid[1], Nicolas Bloemeke[1], Florian Rührnößl[1], Martin Haslbeck[1], Michael Sattler[1,2], Po-Ssu Huang[3] and Matthias J. Feige[1,4,*]

[1] Center for Integrated Protein Science at the Department of Chemistry, Technical University of Munich, Lichtenbergstr. 4, 85748 Garching, Germany

[2] Institute of Structural Biology, Helmholtz Center Munich, 85764 Neuherberg, Germany

[3] Department of Bioengineering, Stanford University, Stanford, California, USA

[4] Institute for Advanced Study, Technical University of Munich, Lichtenbergstr. 2a, 85748 Garching, Germany;

*Corresponding author: matthias.feige@tum.de

Author Contributions

MJF conceived the study. NMR experiments were performed by AL and analyzed by AL and MS. PWNS performed ultracentrifugation experiments, NB performed microscopy experiments, HDX experiments were performed by FR. All other experiments were performed by SM, SB and CJK. Protein design was performed by CAC and PSH. Data were analyzed by all authors and the paper was written by SM and MJF with input from all.

Submitted for publication

3.1 Introduction

In order to become functional, a large number of proteins depend on assembly into higher order complexes[249-251]. Assembly thus needs to be aided and scrutinized by molecular chaperones that surveil the multiple steps of protein biosynthesis from translation on the ribosome to adopting the final native structure[252]. In fact, unassembled proteins likely represent a major class of clients for the cellular quality control machinery[174,253] but also a particularly complicated one to assess: on the path from protein folding to assembly, the degree of structure in an immature protein can be expected to increase, as specific protein-protein interactions depend on specific interfaces. This simple notion, however, poses a conundrum: chaperones recognize non-native states of proteins and can target their clients for degradation if folding does not occur. Unassembled subunits, on the other hand, need to be stable and structured enough to allow for specific interactions, avoiding futile steps in the biosynthesis of proteins, but also allow the cellular quality control machinery to read their assembly state. Although specific assembly chaperones exist for particularly abundant and complex clients[254,255], most proteins can be expected to rely on the more generic chaperone machineries to survey their oligomerization state. In the cytoplasm, recent studies have shown that protein translation and assembly can be intimately coupled, increasing efficiency of these processes by spatial constraints[170,171] or translational pausing[172]. Such a scenario has not been described for secretory pathway proteins, which are produced in the endoplasmic reticulum (ER) and make up ca. 1/3 of all proteins produced in a typical mammalian cell[79]. For these, translation in the cytoplasm and assembly in the ER are spatially separated by the translocon. Cells still have to ensure that proteins correctly assemble before being transported to their final destination from the ER, at the same time avoiding premature degradation[173]. Furthermore, as opposed to the cytosol, quality control proteases or ubiquitin conjugating systems are absent from the lumen of the ER, rendering assembly control highly dependent on recognition by the generic ER chaperone machinery[174,175].

In order to better understand the cellular regulation and control of protein assembly processes in the relevant biological context of the cell[256], we thus need to refine our understanding of what chaperones recognize as signatures of unassembled proteins. Although structural insights into chaperone-client interactions exist in some cases[176,257-261], these remain very limited and are mostly absent *in vivo*. During this study we thus selected a protein model system where assembly control is particularly relevant to maintain proper

function of the immune system, the heterodimeric interleukin-23[39]. IL-23 is a key cytokine, composed of one α and one β subunit which is involved in inflammatory diseases as well as cancer and has become a major therapeutic target in the clinics[36,63,65,262]. We show that locally restricted incomplete folding of one subunit allows for reliable assembly control of the heterodimeric protein by ER chaperones while at the same time avoiding premature degradation of unassembled subunits. Structural insights into IL-23 biogenesis and chaperone recognition allow us to rationally engineer protein variants that can pass quality control checkpoints even while unassembled. Engineering such variants may provide proteins with new biological functions in cellular signaling.

3.2 Results

3.2.1 An assembly-induced folding mechanism regulates IL-23 formation

IL-23 is a heterodimeric cytokine composed of IL-23α and IL-12β (Fig. 3.1a). IL-23α alone is retained in cells and IL-12β induces its secretion[39] (Fig. 3.1b) as one well-defined, covalent IL-23α/IL-12β heterodimer[26,39] (Fig. 3.1c). In contrast, for unassembled, intracellular IL-23α we observed multiple species on non-reducing SDS-PAGE gels (Fig. 3.1c). Thus, IL-23α fails to fold into one defined native state in the absence of IL-12β and (some of) its cysteines remain accessible while unpaired with IL-12β.

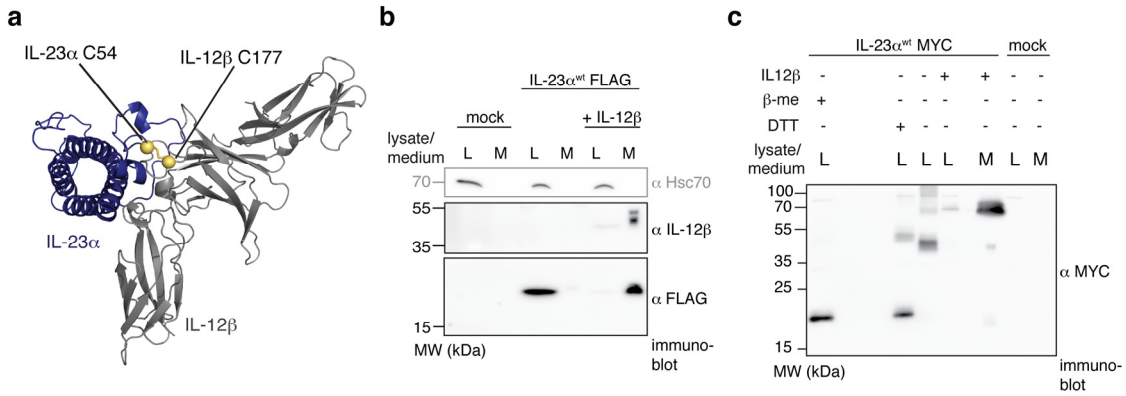

Figure 3.1 IL-23α misfolds *in vivo* in the absence of IL-12β. a Structure of heterodimeric IL-23. Cysteines in IL-23α (blue) and IL-12β (grey) that form an intermolecular disulfide bond are shown in yellow. **b** Secretion behavior of FLAG-tagged wild type IL-23α (IL-23α^{wt}) in the presence or absence of its interaction partner IL-12β. Hsc70 served as loading control. **c** IL-23α forms non-native disulfide bonds in isolation (lane 3) and IL-12β covalently heterodimerizes with IL-23α (lanes 4 and 5), concomitantly reducing misfolding of IL-23α. Samples were treated with β-Me post-lysis / DTT in cells for reduction where indicated and with NEM to conserve redox species.

A closer scrutiny of the IL-23α structure revealed three different types of cysteines within the protein: (1) C58 and C70, which form the single internal disulfide bond (2) C54, which engages with IL-12β upon complex formation, stabilizing the IL-23 heterodimer by a disulfide bond[26,39] and (3) two free cysteines (C14, C22) in the first helix of its four-helix bundle fold (Fig. 3.2a). Structure and sequence alignments of the IL-23α subunit with its homologs IL-6 and IL-12α revealed interesting features about the cysteine configurations in these three proteins: although the single internal disulfide bond was structurally conserved (Fig. 3.2b,c), the disulfide bonding pattern was quite different. In IL-23α, the disulfide bond was formed by residues in sequence proximity, C58 and C70, similar to IL-6 (Fig. 3.2d). In contrast, in IL-12α, residues more distant in the sequence (C63 and C101) formed the corresponding disulfide bond. This left C80 in IL-12 free to engage with C15 in its first α-helix, forming a second

disulfide bond (Fig. 3.2d) – unlike in IL-23α, where C14 and C22 in its first α-helix remained unpaired but are buried in the native structure of IL-23α in the IL-23 heterodimer (Fig. 3.2e).

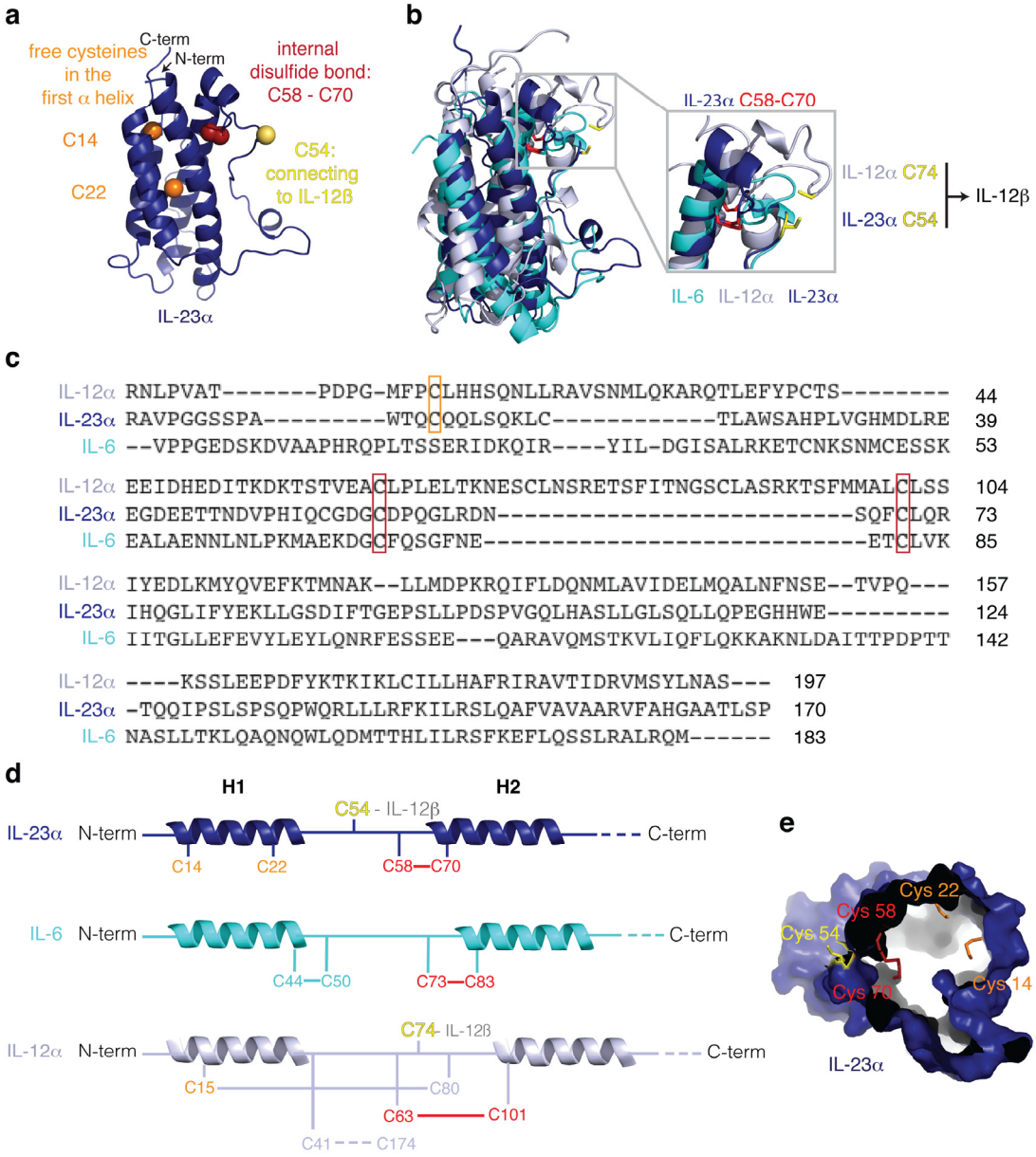

Figure 3.2 Cysteine conservation between IL-12α, IL-23α and IL-6. a Structure of IL-23α. Cysteines that form an intramolecular disulfide bond in IL-23α are shown in red, the one that engages with IL12β is highlighted in yellow, and free cysteines are shown in orange. **b** Structural alignment of IL-23α (blue), IL6 (cyan) and IL-12α (light grey). The conserved disulfide bond cysteines are shown in red and the IL-12β engaging free cysteines of IL-23α and IL-12α in yellow. **c** Sequence alignment of human IL-12α, IL-23α and IL-6. Cysteines forming a conserved disulfide bond are highlighted in red. The conserved IL-23α C14 and its corresponding cysteine in IL-12α are framed in orange. **d** Model of IL-23α, IL-6 and IL-12α illustrating cysteines and disulfide bonds. The same color code as in a) and b) was used. Numbering is without signal sequences. **e** Surface model of IL-23α (with the same color code as a) shows solvent-accessibility of indicated cysteines.

Cysteines are among the evolutionary most highly conserved amino acids and the presence of free cysteines in secretory pathway proteins is rare, as they may induce misfolding

and are often recognized by the ER quality control (ERQC) system[263]. This suggests that the unpaired C14 and C22 of IL-23α may play a functional role, e.g. in regulating IL-23 assembly. Based on these considerations we assessed the function of the different types of cysteines in IL-23α on its assembly-induced secretion by IL-12β. Mutating the disulfide bond-forming cysteines (IL-23$\alpha^{C58,70S}$) led to a drastically reduced efficiency of IL-12β-induced secretion of IL-23α, indicating a key structural role (Fig. 3.3). Replacement of C54 by Ser led to minimal secretion of unassembled IL-23α and otherwise had an intermediate effect on assembly-induced secretion by IL-12β (Fig. 3.3). Surprisingly, replacement of the two free cysteines in helix 1 of IL-23α by valines (IL-23$\alpha^{C14,22V}$) or serines (IL-23$\alpha^{C14,22S}$) did not have any strong effect on the efficiency of IL-12β-induced secretion of IL-23α (Fig. 3.3). The fact that the two unusual free cysteines in IL-23α are dispensable for efficient formation of the IL-23 heterodimer led us to characterize their molecular functions in more detail.

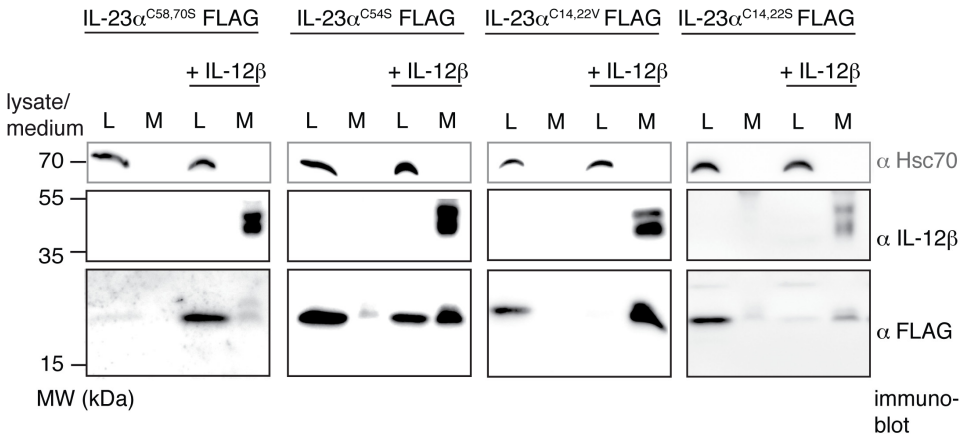

Figure 3.3 Secretion behavior of FLAG-tagged IL-23α mutants. Wild type and mutant IL-23α were transfected alone or co-transfected with IL-12β and analyzed for secretion. Hsc70 served as loading control.

3.2.2 Free cysteine residues in IL-23α function as chaperone anchors

We first assessed the influence of the different types of cysteine residues in IL-23α on its stability in cells. Wild-type IL-23α (IL-23α^{wt}) was degraded with a half-life of 63 ± 11 min (Fig. 3.4). In agreement with a key structural role, deleting the disulfide bond forming cysteines in IL-23$\alpha^{C58,70S}$ led to a faster degradation with a half-life of 30 ± 9 min (Fig. 3.4). Quite unexpectedly, however, the IL-23$\alpha^{C14,22V}$ and IL-23α^{C54S} mutants were degraded even faster with half-lives of only 20 ± 7 min and 17 ± 5 min, respectively (Fig. 3.4). Accordingly, the unpaired cysteines in helix 1 of IL-23α do not significantly promote IL-23 heterodimerization - but stabilize the protein while unassembled. This behavior can be explained by two

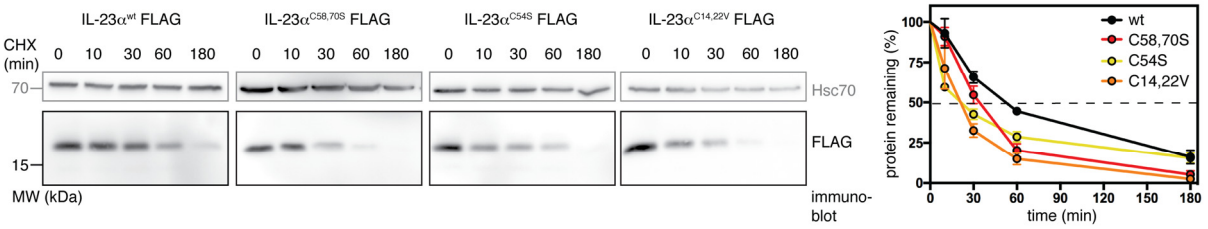

Figure 3.4 Degradation of IL-23α variants. Time course of degradation of IL-23α^{wt}, IL-23α^{C58,70S}, IL-23α^{C54S} and IL-23α^{C14,22V} upon inhibition of translation with cycloheximide (CHX) for up to 180 min. Hsc70 served as loading control. Right: Quantification of protein turnover is shown; data are the mean ±SEM of at least four independent experiments.

hypotheses: either these cysteines affected IL-23α misfolding in isolation and/or they are recognized differently by the ER quality control system. The latter could provide valuable insights into how protein folding states are recognized on a molecular level in the ER.

All IL-23α cysteine mutants showed a similar degree of misfolding and similar redox species like IL-23α^{wt} (Fig. 3.5). We thus proceeded to test the second hypothesis, that the cysteines are recognized differently by chaperones. Unpaired cysteines in secretory pathway proteins can be recognized by PDI family members in the ER[264]. Since we did not observe any significant difference in binding of PDI itself to IL-23α^{wt} *versus* IL-23α cysteine mutants (Fig. 3.6), we

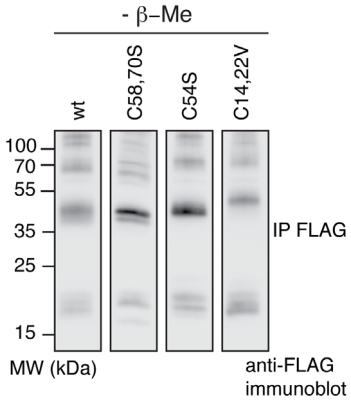

Figure 3.5 Redox status of FLAG-tagged IL-23α cysteine mutants. Samples were treated with NEM to conserve the redox species, immunoprecipitated and analyzed by non-reducing SDS-PAGE and anti-FLAG immunoblots.

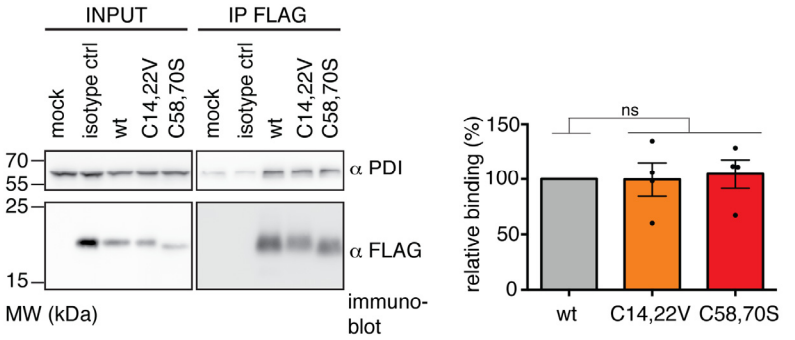

Figure 3.6 IL-23α interaction with PDI. Immunoblot analysis of co-immunoprecipitated endogenous protein disulfide isomerase (PDI) with FLAG-tagged IL-23α^{wt}, IL-23α^{C14,22V} and IL-23α^{C58,70S}. Relative intensities of each band (±SEM) were calculated for four independent experiments and normalized to the IL-23α^{wt} signal which was set to 100% relative binding. Statistical significance was calculated using a two-tailed unpaired t-test. ns = not significant.

assessed interaction with another PDI family member, ERp44. ERp44 serves as a recruitment chaperone from the ER-Golgi intermediate compartment (ERGIC) during protein assembly[265] and thus was an interesting candidate in terms of IL-23 assembly control. IL-23α^{wt} strongly bound to ERp44 (Fig. 3.7a) and co-localized with ERp44 in the ERGIC (Fig. 3.7b) indicating a biologically relevant interaction. Of note, binding of ERp44 was significantly reduced for IL-

23α^{C14,22V} and IL-23α^{C54S} *versus* IL-23α^{wt}, whereas binding to the IL-23α^{C58,70S} mutant was not affected (Fig. 3.7a). Single cysteine mutants in helix 1 of IL-23α (IL-23α^{C14S} and IL-23α^{C22S}) both also showed reduced binding to ERp44, suggesting that both cysteines can be recognized by ERp44 (Fig. 3.7c).

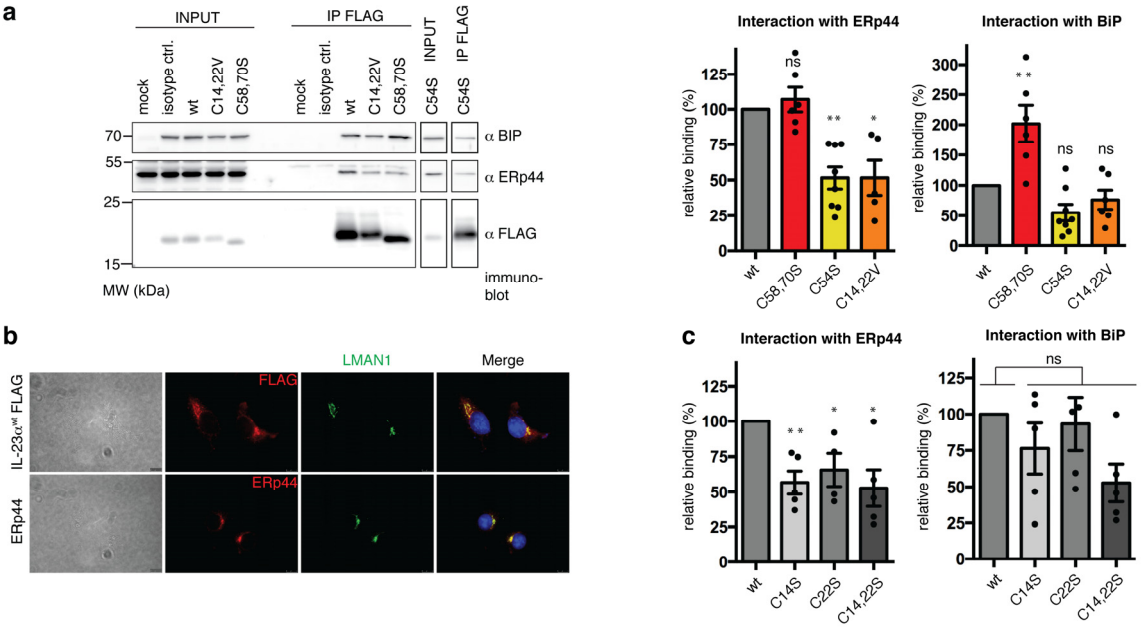

Figure 3.7 IL-23α is recognized by chaperones. **a** Immunoblot analysis of co-immunoprecipitated endogenous ERp44 or co-transfected hamster BiP with FLAG-tagged IL-23α^{wt}, IL-23α^{C58,70S}, IL-23α^{C54S} and IL-23α^{C14,22V}. Relative binding was determined from at least five independent experiments (shown ±SEM) and normalized to the IL-23α^{wt} signal, which was set to 100% relative binding. Statistical significance was calculated using a two-tailed unpaired t-test. ns = not significant; *p<0.05, **p<0.01 indicate statistically significant differences. **b** Immunofluorescence analysis of endogenous ERp44 and FLAG-tagged IL-23α^{wt}. Either COS-7 cells transfected with IL-23α^{wt} (top) or untransfected COS-7 cells (bottom) were immunostained for FLAG-tagged IL-23α^{wt} (red) or endogenous ERp44 (red), respectively. Additionally, cells were immunostained for LMAN1 (green) as an ER-Golgi intermediate compartment (ERGIC) marker, and nuclei were stained with DAPI (blue). ERp44 immunofluorescence and FLAG immunofluorescence signals from IL-23α^{wt} as well as LMAN1 and nuclei are displayed as central cell planes. Depicted images are representative of cells from at least three different biological replicates. Scale bars correspond to 10 µm. **c** Same as in a) but single cysteine mutants of IL-23α were analyzed.

Additionally, we assessed binding of the ER Hsp70 chaperone BiP to IL-23α and its cysteine mutants. BiP binds to exposed hydrophobic stretches in proteins and can thus serve as a good proxy to assess the folding status of a protein in the ER[110]. IL-23α^{C58,70S} bound significantly stronger to BiP than IL-23α^{wt} (Fig. 3.7a), corroborating a stabilizing structural role for the conserved disulfide bond in IL-23α. In contrast, mutating cysteines 14 and 22 or cysteine 54 led to unaltered BiP binding in comparison to IL-23α^{wt} (Fig. 3.7c), in agreement with the notion that replacing the free cysteines in IL-23α does not disrupt its structure formation. Taken together, our data suggest that free cysteines in IL-23α are bound by ERp44 and increase the protein's half-life. IL-23α^{C58,70S}, in contrast, loses structural stability provided

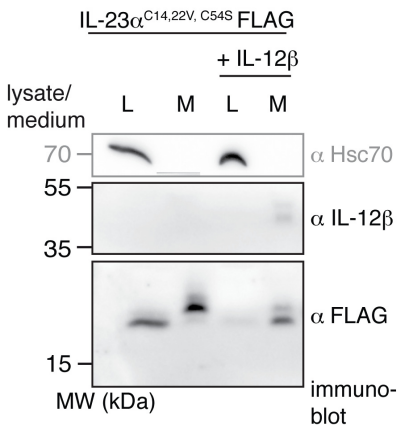

Figure 3.8 Secretion behavior of FLAG-tagged IL-23α^{C14,22V,C54S}. Mutant IL-23α was transfected alone or co-transfected with IL-12β and analyzed for secretion. Hsc70 served as loading control.

by the internal disulfide bond forming cysteines, is rapidly degraded and assembly-incompetent. If this hypothesis was correct, replacing all free cysteines in IL-23α should, in principle, lead to its secretion even while unpaired. Indeed, an IL-23α mutant where C14 and C22 were replaced by Val and C54 by Ser (IL-23α^{C14,22V,C54S}) was secreted even in the absence of IL-12β (Fig. 3.8). The fact that a significant amount of IL-23α^{C14,22V,C54S} was still retained in the cell, however, indicated the existence of a second quality control mechanism that acts on IL-23α maturation and heterodimerization.

3.2.3 Helix 1 in IL-23α is incompletely folded until heterodimerization with IL-12β

Our data show that all unpaired Cys in IL-23α function as a signal for its assembly status. Cysteines 14 and 22, however, are buried in the native structure of IL-23 (Fig. 3.2e) pointing towards structural changes occurring in IL-23α upon assembly. We reasoned that these changes might underlie the second quality control mechanism and could provide rare structural insights into protein assembly control in the ER. To analyze these further and complement our *in vivo* studies by structural analyses of IL-23 assembly control, we decided to study IL-23α *in vitro*. Based on our *in vivo* studies we proceeded with a mutant where all free cysteines were replaced and only the internal disulfide bond was retained, in order to understand the presumed second QC mechanism which acts independently of free cysteines. Consistent with our *in vivo* studies, C14 and C22 were replaced by valines and the IL-12β-connecting C54 by serine (IL-23α^{C14,22V,C54S}, denoted as IL-23α^{VVS} for simplicity in the following). IL-23α^{VVS} could be purified to homogeneity and formed its disulfide bond (Fig. 3.9a). Analytical ultracentrifugation (auc) experiments revealed a well-defined monomeric state ($MW_{monomer,\ calculated}$ = 18.9 KDa / MW_{auc} = 19.1 kDa) of IL-23α^{VVS} with a slightly elongated shape (f/f_0 = 1.5) as expected from the crystal structure of IL-23 (Fig. 3.9b)[26]. Far-UV CD spectroscopy showed that IL-23α^{VVS} possesses α-helical structure (Fig. 3.9c), although the overall intensity was low, which argues for flexible regions in the protein. Consistent with this notion, temperature-induced unfolding (Fig. 3.9d) and partial proteolysis experiments

(Fig. 3.9e) revealed an overall rather low stability for IL-23α^{VVS} with a melting point of 48 $\pm$ 0.2 °C and a half-life against proteolysis of 18 $\pm$ 2 min, respectively.

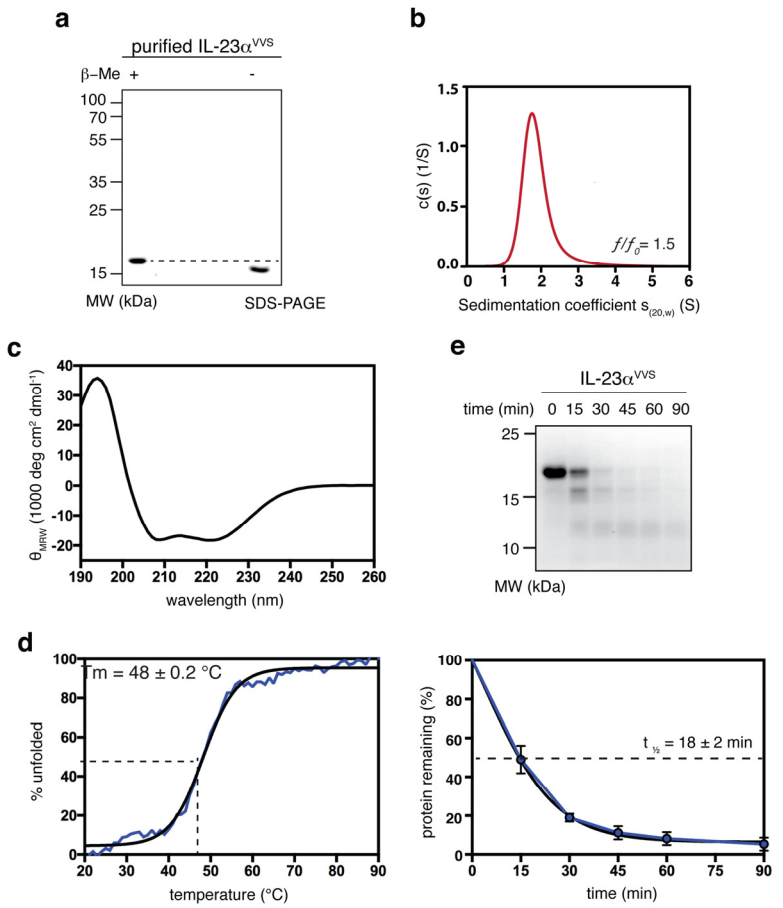

Figure 3.9 *In vitro* characterization of IL-23α^{VVS}. Analysis of recombinant IL-23α^{VVS} by (non-reducing) SDS-PAGE shows absence of covalent misfolding and formation of an internal disulfide bond. **b** Analytical ultracentrifugation confirms a monomeric state of purified IL-23α^{VVS} (MWmonomer, calculated = 18.9 KDa / MWauc = 19.1 kDa) and a slightly elongated shape (f/f0 = 1.5). **c** Far-UV CD spectrum of IL-23α^{VVS}. **d** IL-23α^{VVS} unfolds cooperatively with a melting temperature of 48±0.2°C **e** IL-23α^{VVS} is degraded with a half-life of 18 $\pm$ 2 min (SD) in partial proteolysis experiments with trypsin. Half-live from exponential fit (black) of the curve (blue, single data points ±SD, N= 3) is shown. d Analysis of recombinant IL-23$\alpha^{C14,22,54S}$ by (non-reducing) SDS-PAGE shows absence of covalent misfolding and formation of an internal disulfide bond.

To further understand the structural features of IL-23α and possible changes upon formation of the native heterodimer, we performed hydrogen/deuterium exchange (HDX) measurements on IL-23α in isolation and on the disulfide linked IL-23 heterodimer. HDX measurements revealed an overall higher flexibility of isolated IL-23α, in comparison to the heterodimer (Fig. 3.10). Interaction with IL-12β did not only stabilize helix 4, where the major interaction site is located[26], but also conferred rigidity to the rest of the protein (Fig. 3.10). Of note, the first helix of isolated IL-23α was the most flexible region within the unpaired subunit and became strongly stabilized upon interaction with IL-12β (Fig. 3.10). This first helix is exactly the region where the two free cysteines are located which we identified to be recognized by ERp44. Of note, when complexed with IL-12β, the different IL-23α mutants behaved like the wild type protein in a receptor activation assay testing for biological activity (Fig.3.11 a-c). Thus, the structural changes observed were fully consistent with formation of

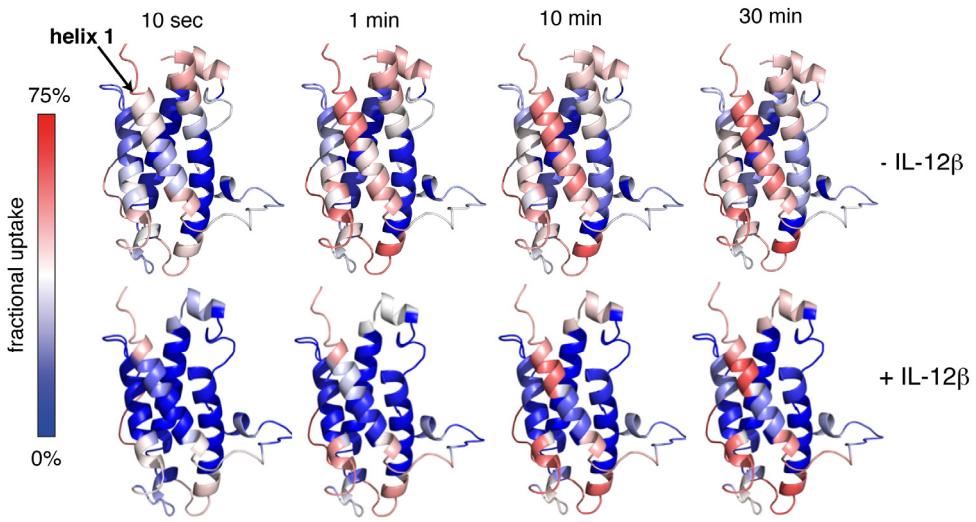

Figure 3.10 IL-23α stability. Helix one in IL-23α gains structure upon assembly with IL-12β. Hydrogen/ deuterium exchange (HDX) reveals helix 1 to be highly flexible in IL-23α^{VVS} and to be stabilized upon interaction with IL-12β. IL-23α is colored according to the measured HDX rates. Blue colors correspond to a lower (less flexible regions) and red colors to a higher (flexible regions) fractional uptake. Helix 4 in the IL-23 complex was not fully resolved.

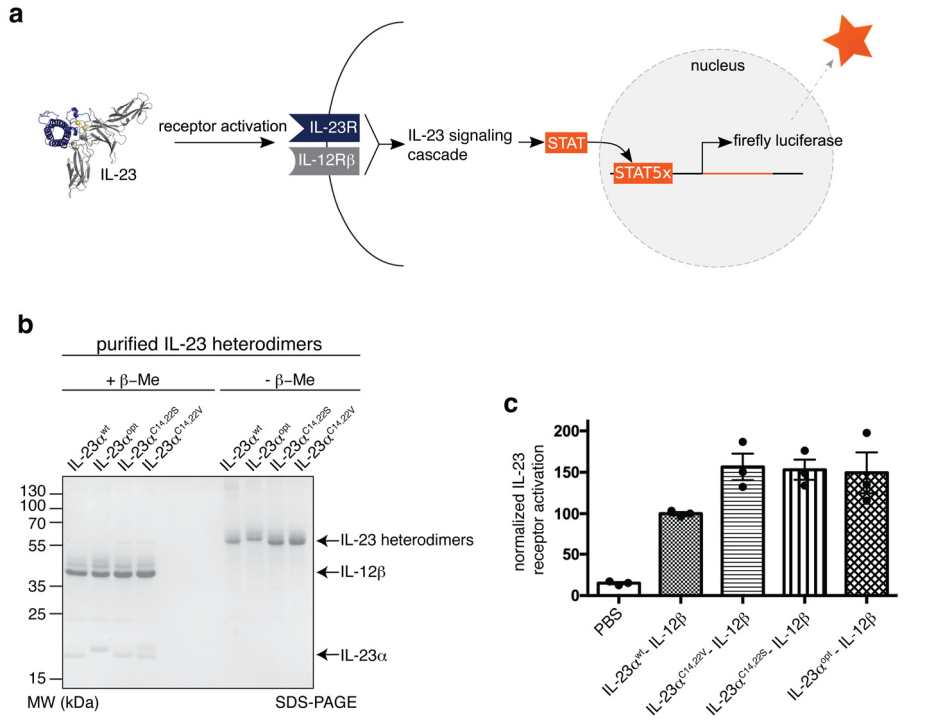

Figure 3.11 Biological activity of IL-23α variants. a Schematic of the iLite® IL-23 receptor activation assay. The assay is based on a genetically engineered reporter gene cell line, which expresses the IL-23 receptor (comprised of two receptor chains: IL-23R and IL-12Rβ1). IL-23 response is coupled to specific, proportional expression of Firefly Luciferase which serves as readout. A renilla luciferase reporter gene construct, under control of a constitutive promotor was used for normalization. **b** Analysis of recombinant IL-23 complexes purified from mammalian cells by (non-reducing) SDS-PAGE shows formation of the disulfide bridged complex. The double band pattern in IL-23$\alpha^{C14,22V}$ was due to incomplete Histag cleavage. **c** Biological activity of recombinant IL-23 complexes. Induction of IL-23 signaling by the indicated IL-23 complexes was assessed with a receptor activation assay as described in e). Relative receptor activation of each complex was calculated for at least three independent experiments (shown ±SEM) and normalized to the IL-23^{wt}-complex signal, which was set to 100%.

functional IL-23. NMR ^{1}H-^{15}N HSQC measurements confirmed the notion of IL-23α^{VVS} containing well-folded as well as flexible/disordered regions as we observed relatively low overall peak dispersion (Fig. 3.12a). Strikingly, we observed five signals corresponding to

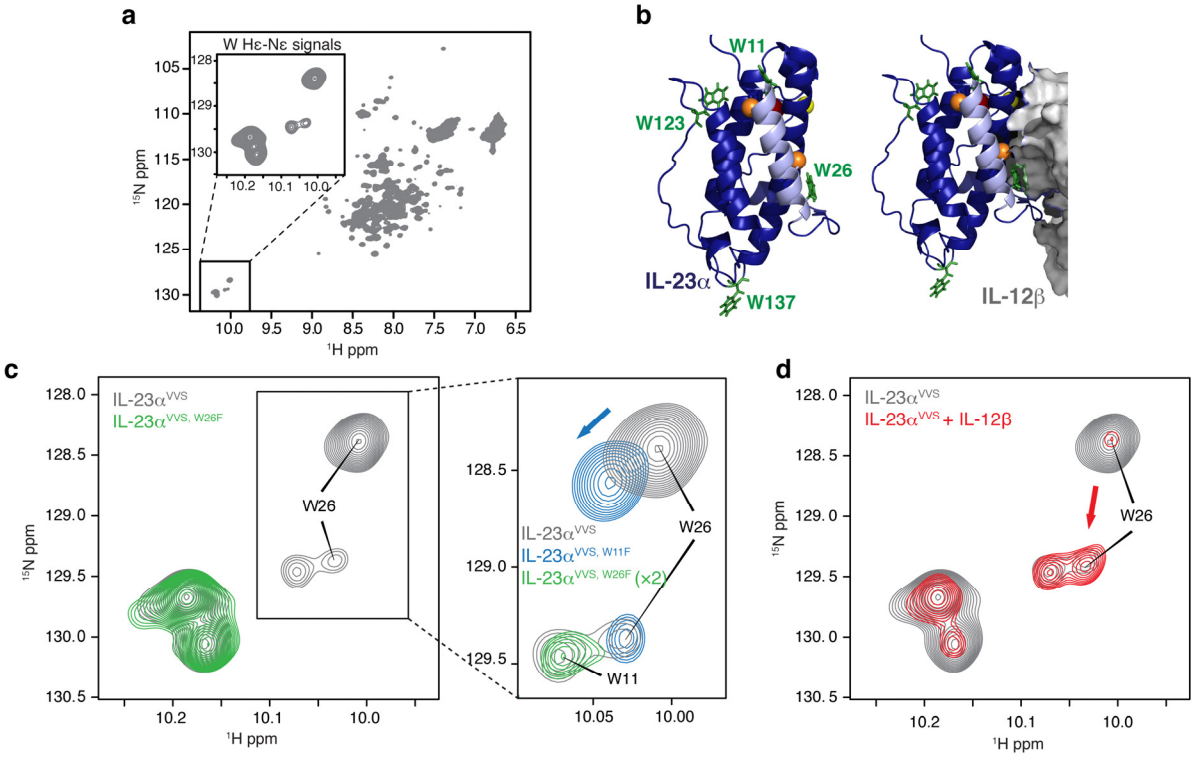

Fig. 3.12 Helix one in IL-23α gains structure upon assembly with IL-12β. a ^{1}H, ^{15}N HSQC experiment for IL-23α^{VVS}; the inset shows the downfield shifted tryptophan signals at greater magnification. **b** Structure of IL-23α (blue) with helix 1 in light blue and cysteine residues shown, using the same color code as in Fig. 3.2a) and IL-12β (grey). Trp residues are shown in green. **c** Trp indole side chain signals in ^{1}H,^{15}N HSQC experiments for IL-23α^{VVS} (black) and IL-23α^{VVS,W26F} (green). To unambiguously assign W26 from the two minor signals, the IL-23α ^{VVS,W26F} spectrum was scaled up by a factor of 2 (zoomed view), and an additional IL-23α $^{VVS, W11F}$ mutant was measured (blue). **d** Same as c) but for unpaired IL-23α^{VVS} (black) *versus* IL-23α^{VVS} in the presence of a 2-fold molar excess of unlabeled IL-12ß (red). The intensity of the bound spectrum was increased to compensate the gain in molecular weight of the complex.

tryptophan side chain indole amides groups in the ^{1}H, ^{15}N HSQC spectrum (Fig. 3.12a, inset), although IL-23α only contains four tryptophans (Fig. 3.12b). This argues for conformational heterogeneity and dynamics in IL-23α^{VVS} on the time scale of milliseconds or slower, indicating conformations with distinct chemical environments. In order to investigate this further, we assigned those resonances by single-point mutagenesis of individual tryptophan residues. This approach revealed that Trp26 gives rise to two signals in the NMR spectrum (Fig. 3.12c). Of note, Trp26 is located at the end of helix 1 of IL-23α and in the IL-12β binding interface (Fig 3.12b). Thus, our NMR measurements confirmed that helix 1 exchanges between two conformational states, where one may correspond to an incompletely folded form, as indicated by the HDX measurements. If indeed a folding transition of helix 1 was involved in

IL-23 assembly control, as suggested by our *in vivo* data and HDX measurements, the conformational transition should be detectable by NMR. In agreement with this idea, the presence of IL-12β caused the intensity of the major Trp26 indole signal to almost entirely shift towards the pre-existing minor conformation (Fig. 3.12d). This corroborates that IL-12β induces folding in helix 1 of IL-23α, and supports that its first α helix is mostly unfolded in the absence of IL-12β.

Taken together, our comprehensive analysis reveals an assembly-induced folding mechanism where IL-12β recognizes structured regions within IL-23α and subsequently induces further folding of the α subunit, in particular its first α helix. This reveals important information about what ER chaperones can recognize as signatures of an unassembled protein - without targeting their clients for rapid degradation.

3.2.4 Structural optimization of IL-23α overcomes ER quality control

Our structural studies revealed the first α helix in IL-23α to be unstructured while this subunit is unpaired, and to gain structure upon heterodimerization with IL-12β. Consequently, the two free cysteines that would otherwise be recognized by PDI chaperones get buried, pointing towards an intricate quality control mechanism that oversees IL-23 assembly. Building on these insights, we wondered if we could overcome ER quality control by selectively improving the stability of helix 1 in IL-23α. Towards this end we optimized helix 1 of IL-23α *in silico* using RosettaRemodel[266]. The native structure of IL-23 contains a number of non-ideal structural features[267]. Upon first inspection, we found that a few of the residues near the N-terminus can be improved from their native environment (see methods for details). For example, Pro28 is exposed with little structural support; Ser37 is completely buried, and likely interacts with its own helical backbone, which may reduce the rigidity of the structure. We thus redesigned all of the core-facing residues on helix 1, adjusted the buried polar residues to hydrophobic ones, extended the N-terminus of the crystal structure by two residues, and completely rebuilt the first six amino acids in order to create a stable N-terminus. Taken together, this led to three optimized models for IL-23α (Fig. 3.13a), out of which we proceeded with one that has a Met at the N-terminus of the rebuilt helix and one of the ERp44-binding cysteines (C22) still in place (Fig. 3.13b). This engineered protein is referred to as IL-23α^{opt} in the following. Strikingly, IL-23α^{opt} was now independently secreted from mammalian cells,

despite the presence of C22 in helix 1 of IL-23α^{opt} (Fig. 3.13c). Thus, optimization of the first helix in IL-23α makes IL-12β dispensable for its secretion. Of note, IL-23α^{opt} secreted in absence of IL-12β showed a slightly higher molecular weight than the non-secreted protein (Fig. 3.13c), which we had observed also for IL-23α^{VVS} (Fig. 3.8). We could attribute this increase in molecular weight to O-glycosylation of IL-23α^{opt} (Fig. 3.13d). O-glycosylation occurs in the Golgi, and hence IL-23α^{opt} correctly traverses the secretory pathway, indicating

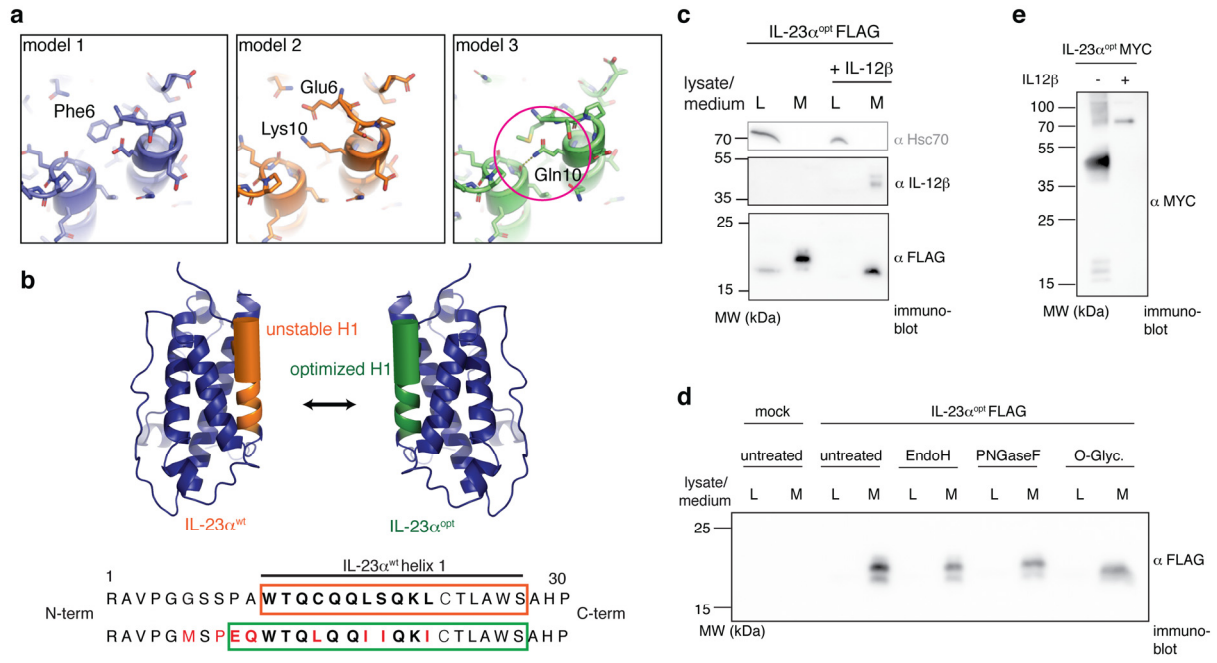

Figure 3.13 Optimization of helix 1 allows IL-23α to pass ER quality control in isolation. a *In silico* design of IL-23α^{opt} N-terminus. The three top models from the second design step where the N-terminus was extended by two residues are shown. We chose model 3 because it suggests a possibility that a hydrogen bond can form between residue Gln10 (magenta circle) and the neighboring helix. Model 1 has similar hydrophobic contacts as model 3, but Phe6 precluded the H-bond formation. Model 2 had a salt-bridge at the N-terminus, whereas hydrophobic packing would lead to more inter-helical stability. **b** Top: Model for IL-23α helix 1 optimization. Helices 1 in IL-23α^{wt} and IL-23α^{opt} are shown in orange and green, respectively. Filled helices indicate regions within helix 1 with amino acid exchanges for optimization. Bottom: Sequence comparison of the first 30 amino acids in IL-23α^{wt} and IL-23α^{opt}. Helical regions are framed in orange or green for wt and optimized protein, respectively. Amino acid exchanges in IL-23α^{opt} are highlighted in red and the optimized region within the helix is shown in bold. **c** Secretion behavior of FLAG-tagged IL-23α^{opt} in the presence and absence of IL-12β. Hsc70 served as a loading control. **d** IL-23α^{opt} becomes O-glycosylated upon independent secretion. Secreted FLAG-tagged IL-23α^{opt} from HEK 293T cells was treated with the indicated de-glycosylation enzymes (O-Glyc.: Mix of 0-Glycosidase and α2-3,6,8 Neuraminidase as described in method section) and detected on an immunoblot. **e** Oxidation state of IL-23α^{opt} in the presence and absence of IL-12β. Cells were treated with brefeldin A to retain proteins in cells.

proper folding. Apparently, interaction with IL-12β normally blocks this O-glycosylation site, which could be located within IL-23α or the GS-linker to the FLAG tag (see methods for details). Indeed, when IL-23α^{opt} was secreted in the presence of IL-12β, it did not become modified (Fig. 3.13c), again in agreement with data for IL-23α^{VVS} (Fig. 3.8). This also shows

that, although IL-23α^{opt} can be independently secreted, it is still able to very efficiently assemble into the heterodimeric IL-23 complex (Fig. 3.13e), further confirming correct folding of the optimized mutant. If indeed helix 1 was a major chaperone recognition site in the ER, IL-23α^{opt} should not only be secreted but also show reduced chaperone binding. In complete agreement with this hypothesis, chaperone interaction experiments revealed significantly less binding of ERp44 and BiP to IL-23α^{opt} (Fig. 3.14). To structurally characterize IL-23α^{opt} *in vitro*

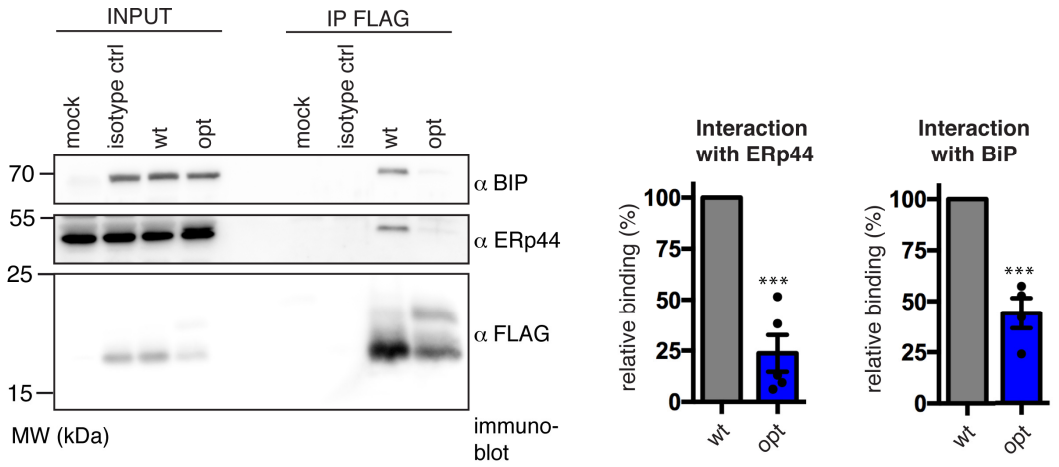

Figure 3.14 Chaperone interaction of IL-23α^{opt}. Immunoblot analysis of co-immunoprecipitated endogenous ERp44 or co-transfected hamster BiP with FLAG-tagged IL-23α^{opt}. Relative intensity of each band was calculated for at least four independent experiments (shown ±SEM) and normalized to the IL-23α^{wt} signal which was set to 100%. Statistical significance was calculated using a two-tailed unpaired t-test. ***p< 0.001 indicate statistically significant differences.

we created an IL-23α^{opt} mutant where the IL-12β-connecting C54 residue was additionally replaced by serine to minimize the aggregation potential of the protein (IL-23$\alpha^{opt,\ C54S}$). The purified protein formed its internal disulfide bond (Fig. 3.15a) and showed an α-helical conformation (Fig. 3.15b). Analytical ultracentrifugation experiments revealed the same slightly elongated shape for IL-23$\alpha^{opt,C54S}$ (ff_0 = 1.45) as for IL-23α^{VVS} and a predominantly monomeric state ($MW_{monomer,\ calculated}$ = 18.9 KDa / MW_{auc} = 22.6 kDa) with low percentage of dimer or trimer formation (MW_{auc} = 56.7 kDa) (Fig. 3.15c). Strikingly, IL-23$\alpha^{opt,C54S}$ had a melting point of 61 ± 0.7 °C (Fig. 3.15d), more than 10 °C higher than observed for the non-optimized protein (Fig. 3.9d). Unfolding, however, was less cooperative, which may be due to the strong stabilization of helix 1[268]. In agreement with these data, HDX measurements revealed the unpaired IL-23$\alpha^{opt,\ C54S}$ to be more stable, including the first optimized helix which was very labile in the non-optimized protein. Furthermore, helix 1 in IL-23$\alpha^{opt,\ C54S}$ was only slightly further stabilized upon complex formation with IL-12β (Fig. 3.16). Importantly, the IL-23α^{opt} - IL-12β heterodimer still showed biological activity excluding impaired receptor

binding by the stabilized IL-23α helix 1 (Fig. 3.11c). Taken together we identified the first helix of IL-23α as a major limiting factor in its folding process. Stabilization of this small region stabilizes the whole protein, enabling its escape from ER retention while preserving assembly-competency with IL-12β and biological activity.

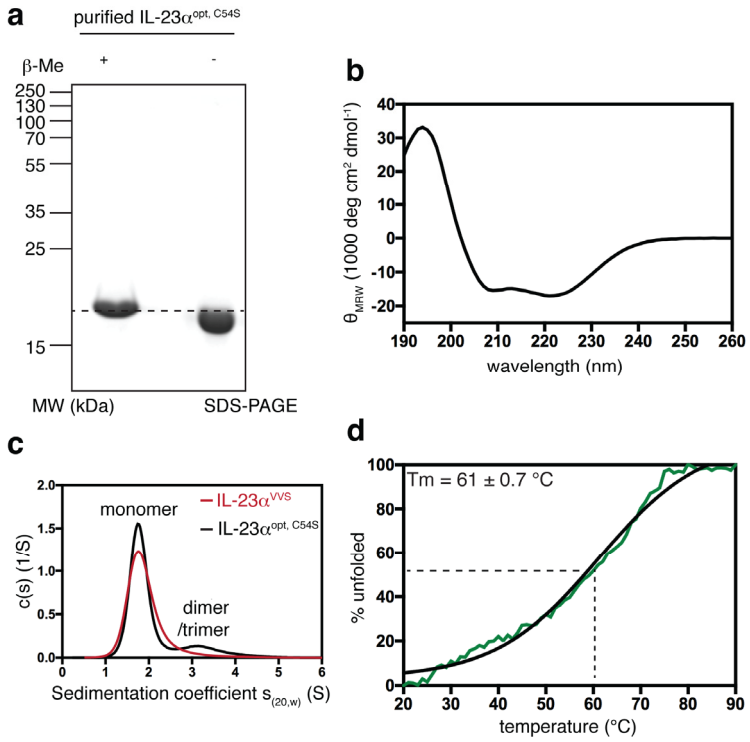

Figure 3.15 In vitro characterization of IL-23α$^{opt, C54S}$. **a** Analysis of recombinant IL-23α^{opt,C54S} by (non-reducing) SDS-PAGE shows absence of covalent misfolding and formation of an internal disulfide bond. **b** Far-UV CD spectrum of IL-23α^{opt,C54S}. **c** Analytical ultracentrifugation confirms a predominantly monomeric state of recombinant IL-23α^{opt,C54S} (MW $_{monomer, calculated}$= 18.9 KDa / MW$_{auc}$= 22.6 kDa) with low percentage of dimer or trimer formation (MW$_{auc}$= 56.7 kDa) and a slightly elongated shape (f/f_0 = 1.45). **d** IL-23α^{opt,C54S} unfolds with a melting temperature of 61 ± 0.7 °C.

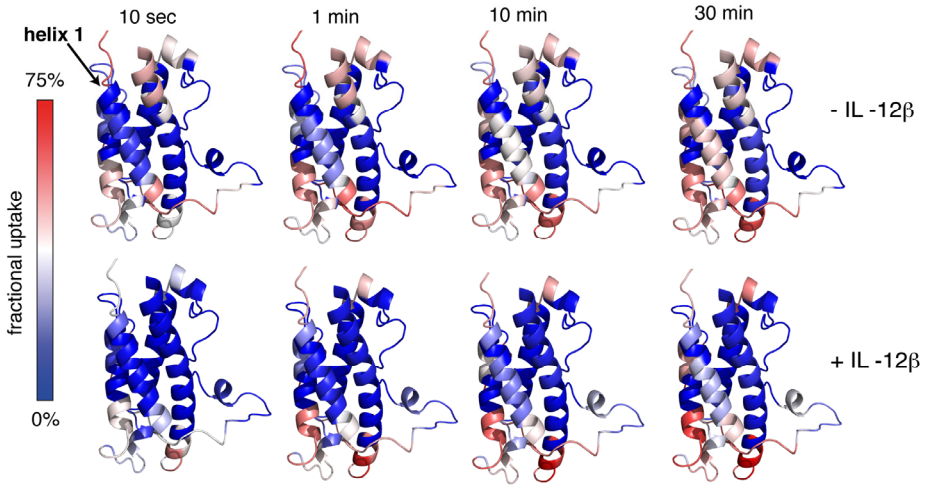

Figure 3.16 IL-23α^{opt} stability. Hydrogen/deuterium exchange (HDX) of unpaired IL-23α^{opt} *versus* IL-12β-paired IL-23α^{opt}. IL-23α^{opt} is colored according to the measured HDX rates. Blue colors correspond to a lower (less flexible regions) and red colors to a higher (flexible regions) fractional uptake.

3.3 Discussion

In this study we provide structural insights how ER chaperones can recognize unassembled proteins and aid their assembly into protein complexes - while at the same time preventing their premature degradation. We identified two structural features in IL-23α that synergistically guarantee proper ER quality control and assembly of the potent immune activator IL-23 (Fig. 5): (1) free cysteines recognized by the PDI family member ERp44 and (2) incomplete folding of its first α-helix detected by BiP. Intriguingly, these two motifs are located in the same region within IL-23α, but can be recognized at different stages of the secretory pathway. Whereas BiP is able to recognize hydrophobic stretches in partially unfolded proteins already as early as during co-translational import into the ER[112,123,269], ERp44 acts later inside the ER-Golgi intermediate compartment[270], preventing secretion of unassembled or incorrectly folded proteins[265]. Our structural analyses combined with *in vivo* studies thus allow us to understand, how ER protein assembly can be controlled with high fidelity by sequential quality control checkpoints, which is conceptually reminiscent although distinct on a molecular level to IgM assembly control[159,176,211,214]. Furthermore, it reveals how premature degradation of unassembled proteins may be avoided: The first α-helix of IL-23α, which we identified to be an incompletely folded chaperone recognition site, is devoid of any sequence patterns that would allow binding to ERdj4, ERdj5 or Grp170 (Fig. 3.17), BiP co-factors that can induce protein degradation[123,156,271-273]. Of note, a similar absence of such co-chaperone sites has been described for the antibody heavy chain C_H1 domain, which is permanently unfolded and only gains structure upon antibody heavy chain-light chain dimerization[123,176,211]. Since antibodies heavy chains are multidomain proteins, however, chaperone recognition sites can be spatially separated from domains that are well-folded and allow protein assembly. Such a separation is not possible for the single domain protein IL-23α, where local incomplete folding instead is used for chaperone recognition while preserving assembly-competency. This is conceptually reminiscent to IL-27 assembly control[73] and our study now provides a detailed structural underpinning for such a behavior.

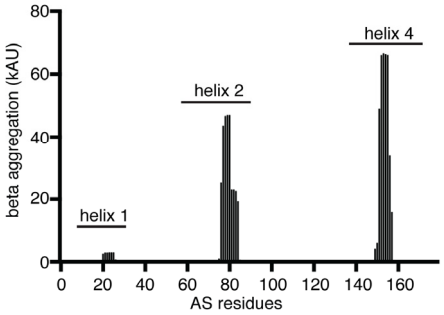

Figure 3.17 TANGO prediction for IL-23α. The TANGO algorithm was used to calculate the β-aggregation potential for IL-23α^{wt}, which correlates with binding of pro-degradative BiP co-chaperones.

Our results show that upon interaction with its interaction partner conformational changes occur in the first helix of IL-23α that subsequently prevent chaperone binding and retention. A mutant optimized *in silico*, IL-23α^{opt} stabilized in helix 1 gains structure independently of IL-12β but is still able to form a functional heterodimeric IL-23 complex. This finding suggests that incomplete folding of IL-23α has evolved for quality control and/or regulatory purposes and not for assembly *per se*. One possible explanation for such a behavior is the combinatorial complexity of the IL-12 family. Five subunits are used to build at least four different heterodimers, including extensive subunit sharing[6]. IL-12β is also part of heterodimeric IL-12, which itself is composed of IL-12α and IL-12β and produced by the same cells as IL-23[224]. ER quality control for IL-23 thus has to monitor the assembly status of IL-23α and at the same time allow for regulation of IL-23 *versus* IL-12 pairing, which share the same β-subunit. Thus, different quality control mechanisms may exist in immune cells helping to discriminate and regulate IL-12 and IL-23 formation to regulate immune functions. Indeed, IL-12α has no free cysteines (besides the IL-12β-interacting cysteine residue), whereas IL-23α exhibits two free cysteines in its first helix which strongly participate in its maturation, serving as chaperone anchors for the PDI family member ERp44. Interestingly, ERp44 can be activated by the lower pH in the ERGIC/Golgi compartment[159] but also by zinc ions[274]. Zinc plays pivotal roles in regulating the immune system[275]. Furthermore, it has been shown that zinc upregulates IL-23α mRNA expression[276]. Thus, zinc may not only affect IL-23α on a transcriptional level but could potentially also influence its maturation. Engineered cytokines are a powerful tool to modulate immune functions, as previously reported e.g. for IL-2, IL-15, IL-27 and others[73-76]. Directly engineering folding and quality control of interleukins provides one possible avenue to obtain immune signaling molecules not present in nature[73]. We detected no significant inhibition of IL-23 signaling by the IL-23α subunit (Fig. 3.18 a,b). Instead, unpaired IL-23α subunits could induce IL-23 signaling in our simplified reporter system (Fig. 3.18 c,d), similar to what has been observed for murine and human IL-27α subunits[73,277]. This possibly indicates more options for IL-23 receptor activation than a recent study has revealed for the IL-23 heterodimer[278]. Furthermore, our data reveal, that unpaired IL-23α is not able to engage and block its receptor and argue for a pronounced participation of IL-12β in initial receptor binding and/or changes in IL-23α structure that allow for receptor binding. Taken together, our study provides detailed structural insights into how protein assembly can be efficiently regulated and controlled in the ER even for single domain proteins:

chaperone recognition motifs may be localized in small structural areas, which are sequentially controlled in the secretory pathway and at the same time avoid motifs that would induce premature degradation. Using only small regions for control is compatible with formation of defined interaction surfaces. Molecular insights into these processes can be used to engineer proteins with altered quality control mechanisms.

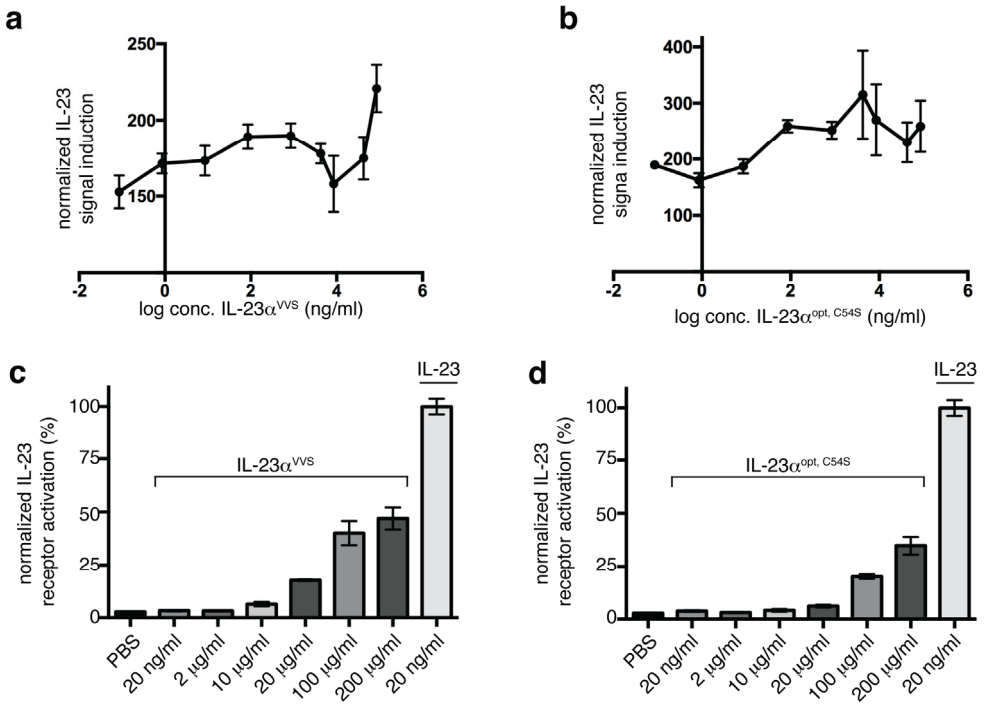

Figure 3.18 Assessing neutralizing effects of recombinant IL-23α^{VVS} on IL-23 signaling. **a** Molar ratios from 1:1 to 1:10000 of IL-23:IL-23α^{VVS} were tested. **b** Same as in a) but IL-23$\alpha^{opt,\ C54S}$ was used. **c** Assessing IL-23-like signaling by recombinant IL-23α^{VVS}. Indicated concentrations of unassembled recombinant IL-23α^{VVS} were compared to signal induction of commercially available IL-23. The IL-23α^{VVS} signal was normalized against signal induction by IL-23, which was set to 100%. **d** Same as in c) but IL-23$\alpha^{opt,\ C54S}$ was used.

3.4 Graphical summary

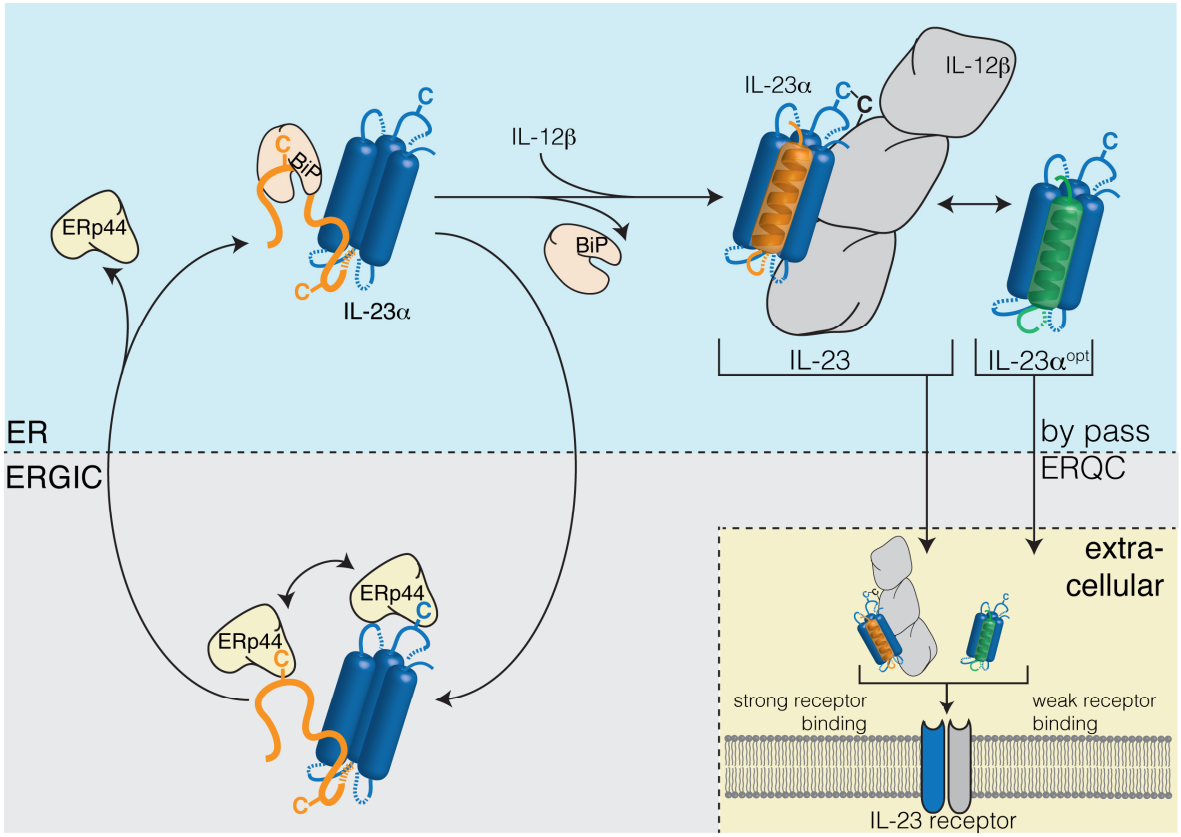

Fig. 3.19 A model for IL-23 assembly control in the cell. Incomplete folding of IL-23α^{wt} is recognized by chaperones along the secretory pathway. The first helix in IL-23α is incompletely structured and can be recognized by BiP during early biogenesis steps within the ER. ERp44, a member of the PDI-family supports BiP function by retrieving IL-23α from the ERGIC compartment to the ER. BiP and ERp44 act together, to slow down IL-23α degradation and maintain its assembly competency. Upon assembly with IL-12β, IL-23α completes folding of its first helix what inhibits chaperone interaction and results in secretion of the heterodimeric IL-23 complex, connected by a disulfide bond. Stabilization of the first helix renders IL-23α insensitive to chaperone interaction and allows independent folding and secretion. Despite independent secretion, IL-23α^{opt} is still able to interact with IL-12β. IL-23 induces strong signaling upon receptor binding, whereas IL-23α^{opt} shows weak receptor activation. Loops within the structure of IL-23α are indicated as dashed lines.

3.5 Experimental part

Constructs

Human interleukin cDNAs (Origene) were cloned into the pSVL (Amersham) or pcDNA 3.4 TOPO (Gibco) vectors for mammalian expression or the pET21a expression vector (Novagen) for protein production in *E. coli*. For mammalian expression hamster codon-optimized human interleukin cDNAs (Geneart) were used. The pMT-hamster BiP expression vector[279,280] was a kind gift of Linda Hendershot. Mutants were generated by site-directed mutagenesis. All constructs were sequenced.

Sequence analysis, structural modeling and analysis

Multiple sequence alignments were performed using Clustal Omega. Structural alignments were generated with PyMOL based on crystal structures from the PDB database (1F45 (IL-12), 3DUH (IL-23)). Missing loops were modelled with Yasara structure with a subsequent steepest descent energy minimization. Structures were depicted with PyMOL.

Cell culture and transient transfections

HEK293T cells were grown in Dulbecco's modified Eagle's medium (DMEM) containing L-Ala-L-Gln (AQmedia, Sigma-Aldrich) supplemented with 10% (v/v) fetal bovine serum (Biochrom or Gibco) at 37 °C and 5% CO_2. Medium was complemented with a 1% (v/v) antibiotic-antimycotic solution (25 µg/ml amphotenicin B, 10 mg/ml streptomycin, and 10,000 units of penicillin; Sigma-Aldrich). Transient transfections were carried out for 24 h either in p35 or p60 poly D-lysine coated dishes (VWR) using GeneCellin (BioCellChallenge) according to the manufacturer's protocol. Always 1 µg of IL-23α DNA and 2 µg of IL-12β DNA or mock vector (in absence of IL-12 β) were (co-)transfected for redox-, secretion- and degradation experiments and 3 µg IL-23α DNA for co-immunoprecipitation experiments. To analyze BiP-interactions, 1 µg hamster BiP DNA was co-transfected with IL-23α.

Immunoblotting experiments

For secretion and redox status experiments by immunoblotting, cells were transfected for 8 h in p35 dishes, washed twice with PBS and then supplemented with 0.5 ml fresh medium for another 16 h. For CHX chase assays cells were treated with 50 µg/ml CHX (Sigma-Aldrich) for

times indicated in the figures before lysis. Protein half-lives (±SD) were calculated from exponential fits of the curves. To analyze secreted proteins, the medium was centrifuged for 5 min, 300 g, 4 °C. Subsequently, samples were supplemented with 0.1 volumes of 500 mM Tris/HCl, pH 7.5, 1.5 M NaCl (and 200 mM NEM in the case of non-reducing SDS-PAGE) and protease inhibitor and centrifuged for 15 min, 20,000 g, 4 °C. Prior to lysis, if indicated, cells were treated with 10 mM DTT (Sigma-Aldrich) for the last hour or 1 µg/ml Brefeldin A (Sigma-Aldrich) for 2.5 hours, washed twice in ice cold PBS, supplemented with 20 mM NEM if samples were to be run on non-reducing SDS-PAGE gels. Cell lysis was carried out in RIPA buffer (50 mM Tris/HCl, pH 7.5, 150 mM NaCl, 1.0% Nonidet P40 substitute, 0.5% sodium deoxycholate, 0.1% SDS, 1x Roche complete Protease Inhibitor w/o EDTA; Roche Diagnostics) or Triton lysis buffer (50 mM Tris/HCl, pH 7.4, 150 mM NaCl, 1 mM EDTA, 1% Triton X-100, 1x Roche complete protease inhibitor w/o EDTA, supplemented with 10 U/ml Apyrase for BiP interaction studies (Sigma-Aldrich) or 20 mM NEM (Sigma) for PDI and Erp44 Co-IPs) in the case of co-immunoprecipitation experiments. Samples were supplemented with 0.2 volumes of 5x Laemmli containing either β-Me for reducing SDS-PAGE or 100 mM NEM for non-reducing SDS-PAGE. Deglycosylation assays with EndoH, PNGase F or a mix of O-glycosidase and α2-3,6,8 Neuraminidase (cleavage of O-glycosylations) were performed according to the manufacturer's protocols (New England Biolabs). Immunoprecipitations were performed with antibodies against the FLAG-tag, coupled to agarose beads (Sigma-Aldrich, A2220). For each cell lysate of one p60 dish, 30 µl of FLAG beads were used and rotated for 2 h at 4 °C. Immunoprecipitated proteins were washed three times with Triton buffer and eluted with Laemmli buffer for 5 min at 95°C. For immunoblots, samples were run on 12% SDS-PAGE gels, transferred to PVDF membranes and blotted with anti-myc (Merk Millipore 05-724, 1:1,000 in TBS, 0.05% Tween, 5% milk), anti-FLAG (Sigma-Aldrich F7425, 1:1,000 in TBS, 0.05% Tween, 5% milk), anti-ERp44 (B68)[270] (1:500 in TBS, 0.05% Tween, 5% milk), anti-hamster BiP[280] (1:500 in TBS, 0.05% Tween, 5% milk), anti-IL-12β (abcam ab133752, 1:500 in TBS, 0.05% Tween, 5% milk), anti-PDI (abcam ab2792, 1:1,000 in TBS, 0.05% Tween, 5% milk)or anti Hsc70 (Santa Cruz sc-1059, 1:1,000 in gelatin buffer (0.1% gelatin, 15 mM Tris/HCl, pH 7.5, 130 mM NaCl, 1 mM EDTA, 0.1% Triton X-100, 0.002% NaN_3). Species-specific HRP-conjugated secondary antibodies (in TBS, 0.05% Tween, 5% milk or gelatin buffer) were used to detect the proteins (Santa Cruz). Blots were detected using Amersham ECL prime (GE Healthcare) and a Fusion Pulse 6 imager (Vilber Lourmat).

Immunofluorescence

A total cell number of1.2 x 104 COS-7 cells were seeded in µ-slides VI0.4 (Ibidi) after transfection with 3.6 µg of DNA using Torpedo transfection reagent (Ibidi). According to manufacturer's instructions, medium was replaced 3 h after seeding. 24 h after transfection, cells were washed twice with PBS at room temperature (RT), and fixed with glyoxal59 (Sigma-Aldrich). Fixation was performed first for 30 min on ice, then for 30 min at RT. Subsequently samples were quenched for 20 min with NH4Cl (Sigma-Aldrich). In the following, permeabilization and blocking were performed for 15 min with PBS containing 2.5% BSA and 0.1% Triton- X 100. Primary antibody incubations using mouse monoclonal (M2) anti-FLAG 761 (Sigma-Aldrich, F1804) at 1:500, anti-LMAN1/ERGIC53 (abcam, ab125006) at 1:10 diluted in 2.5% BSA and 0.1% TritonX-100 in PBS or directly purified anti-ERp44 serum provided by Tiziana Anelli (UniSR, Milano) were carried out for 2 h at RT. Following incubation, samples were washed three times with PBS. Handling and usage of fluorophore-conjugated antibodies was performed in the dark. Secondary antibody incubations using anti-mouse-Alexa647 (Cell signaling, #4410S) at 1:1000 and anti-rabbit-Alexa568 (Thermo Fisher, #A-11011) at 1:1500 diluted in 2.5% BSA and 0.1% Triton X-100 in PBS were carried out for 1 h and samples subsequently washed with PBS once. Nuclei were stained for 2 min with 0.1 µg/ml DAPI (Sigma-Aldrich). Ultimately, samples were washed another three times with PBS before they were mounted with mounting medium (Ibidi) and imaged. Imaging was performed on Leica DMi8 CS Bino inverted widefield microscope using a 100x (NA = 1.4) oil immersion objective, and TXR (excitation/bandpass: 560/40 nm; emission/bandpass 630/75 nm), Y5 (excitation/bandpass: 620/660 nm; emission/bandpass 700/75 nm), or DAPI (excitation/bandpass: 350/50 nm; emission/bandpass 460/50 nm) dichroic filters. The LAS X (Leica) analysis software and ImageJ (NIH) where used for image analysis and processing, where adjustments were restricted to homogenous changes in brightness and contrast over each entire image.

Protein production and purification

Protein expression in *E. coli* of isolated IL-23α subunits (N-terminal Histag with TEV cleavage site, separated by a 2x GS linker) was performed for 4 h at 37 °C, and resulted in inclusion bodies. Inclusion bodies were solubilized in 50 mM sodium phosphate (pH 7.5), 250 mM NaCl, 10 mM ß-mercaptoethanol, and 6 M guanidine hydrochloride. Solubilized inclusion bodies

were centrifuged (20,000 g, 30 min, 20 °C). The supernatant was applied to a HisTrap HP column (GE Healthcare) in 50 mM sodium phosphate (pH 7.5), 250 mM NaCl, 1 mM ß-mercaptoethanol, 6 M guanidine hydrochloride supplemented with 20 mM imidazole. Elution was performed in 50 mM sodium phosphate (pH 4), 250 mM NaCl, 1 mM ß-mercaptoethanol, and 6 M guanidine hydrochloride. Subsequently, the eluate was supplemented with 100 mM DTT and 10 mM EDTA before applying to a HiPrep Sephacryl S-400 HR column (GE Healthcare) equilibrated in 50 mM sodium phosphate (pH 7.5), 6 M guanidine hydrochloride, 1 mM EDTA and 1 mM DTT. After gel filtration, the protein was diluted to 0.1 mg/ml in the same buffer, and then refolded overnight at 4 °C *via* dialysis against 250 mM Tris/HCl (pH 8.0), 500 mM L-arginine, 100 mM NaCl, 10 mM EDTA, 0.25 mM GSSG, and 0.25 mM GSH. IL-23α^{VVS} was pre-treated with 20 mM GSSG for at least 4 h before refolding. Directly after refolding, the redox status of the purified proteins was assessed by non-reducing SDS-PAGE in the presence of 20 mM NEM. After refolding, IL-23α proteins were dialyzed against 50 mM Tris/HCl (pH 8.0) and the Histag was cleaved by addition of TEV protease (TEV: IL-23α 1:10 (w/w)) overnight at 4 °C. After cleavage, the protein was applied to a HisTrap HP column (GE Healthcare) in 50 mM Tris/HCl (pH 8.0). The flow through was concentrated and applied to an EnrichSEC 70 gel filtration column (BioRad) equilibrated in 10 mM potassium phosphate buffer (pH 7.5). For NMR experiments proteins were purified following the same protocol except that protein producing bacteria were cultured in minimal M9 media supplemented with 1 g/l ^{15}N-ammonium chloride. IL-23 complexes were produced using the ExpiCHO Expression System (Gibco) according to the manufacturer's protocol. α (N-terminal Histag with TEV cleavage site, separated by a GS linker) and ß-subunits expressed from the pcDNA3.4 TOPO vector were co-transfected in a ratio of 2:1 for 5 days at 32 °C. After expression, medium was centrifuged (5,000 g, 30 min, 4 °C) and applied to a HisTrap HP column (GE Healthcare) in 10 mM potassium phosphate (pH 7.5), elution was performed in the same buffer with 500 mM imidazole. Subsequently the Histag was cleaved by addition of TEV protease (TEV: IL-23 complex 1:10 (w/w)) overnight at 4 °C and removed by a second HisTrap HP column in 10 mM potassium phosphate (pH 7.5). Final purification was performed using a HiLoad 26/60 Superdex 200 pg column (GE Healthcare) 10 mM potassium phosphate (pH 7.5). IL-12β was purified from transiently transfected ExpiCHO (Gibco) cell supernatant according to the manufacturer's protocol (max. titer). In total, 1 μg IL-12β in the pcDNA3.4 TOPO vector was transfected per 1 ml culture. The supernatant was purified using a HisTrap HP column (GE

Healthcare) in 10 mM potassium phosphate (pH 7.5) and eluted in the same buffer with 500 mM imidazole. The Histag was cleaved by addition of TEV protease (TEV: IL-12β, 1:10 (w/w)) overnight at 4 °C in the same buffer. After cleavage, the protein was applied to a HisTrap HP column (GE Healthcare) in the same buffer and the concentrated flow through was applied to an EnrichSEC 70 gel filtration column (BioRad) equilibrated in 10 mM potassium phosphate (pH 7.5).

Protein optical spectroscopy

Far-UV CD spectra were recorded with a Chirascan plus spectropolarimeter (Applied Photophysics) at 25 °C in 10 mM potassium phosphate, pH 7.5, in 0.2 mm quartz cuvette at a protein concentration of 50 μM. Spectra were recorded 10 times, averaged, and buffer-corrected. Temperature transitions were recorded in a 1 mm quartz cuvette at 10 μM protein concentration in 10 mM potassium phosphate, pH 7.5 at 222 nm. A heating rate of 60 °C/h was used from 25 °C to 95 °C.

HDX measurements

Hydrogen/deuterium exchange experiments (HDX) experiments were performed using an ACQUITY UPLC M-class system equipped with automated HDX technology (Waters, Milford, MA, USA). HDX kinetics were determined in technical triplicates, tacking data points at 0, 10, 60, 600, 1800 and 7200 s at 20°C. At each data point of the kinetic, 3 µl of a solution of 30 µM protein were diluted automatically 1:20 into 99.9% D_2O-containing 10 mM potassium phosphate, pH 7.5 (titrated with HCl) or the respective H_2O–containing reference buffer. The reaction mixture was quenched by the addition of 1:1 200 mM KH_2PO_4, 200 mM Na_2HPO_4, pH 2.3 (titrated with HCl), containing 4 M guanidine hydrochloride and 200 mM TCEP at 1°C and 50 µl of the resulting sample were subjected to on-column peptic digest on a Waters Enzymate BEH pepsin column 2.1x30 mm at 20°C. Peptides were separated by reverse phase chromatography at 0°C using a Waters Acquity UPLC C18 1.7 µm Vangard 2.1x5 mm trapping-column and a Waters Aquity UPLC BEH C18 1.7 µm 1x100 mm separation column. For separation a gradient increasing the acetonitrile concentration stepwise from 5-35% in 6 min, from 35-40% in 1 min and from 40-95% in 1 min was applied and the eluted peptides were analyzed using an in-line Synapt G2-S QTOF HDMS mass spectrometer (Waters, Milford, MA, USA). UPLC was performed in protonated solvents (0.1% formic acid), allowing deuterium to

be replaced with hydrogen from side chains and amino/carboxyl termini that exchange much faster than backbone amide linkages[281]. All experiments were performed in duplicate. Deuterium levels were not corrected for back exchange and are therefore reported as relative deuterium levels[282]. The use of an automated system handling all samples at identical conditions avoids the need for back exchange correction. MS data were collected over an m/z range of 100-2000. Mass accuracy was ensured by calibration with Glu-fibrino peptide B (Waters, Milford, MA, USA) and peptides were identified by MS^E ramping the collision energy automatically from 20-50 V. Data were analyzed in PLGS 3.0.3 and DynamX 3.0 software packages (Waters, Milford, MA, USA).

Analytical ultracentrifugation

Sedimentation velocity analytical ultracentrifugation (SV-AUC) experiments were performed on a ProteomeLab XL-I analytical ultracentrifuge (Beckman Coulter, Brea, CA, USA) equipped with absorbance optics. 350 µl of 10 µM IL-23α in 10 mM potassium phosphate buffer, pH 7.5 were loaded into a standard 12 mm double-sector epon-filled centerpiece, covered with quartz windows, alongside with 420 µl of the reference buffer solution. Samples were centrifuged at 34,000 rpm for IL-23α^{VVS} and 42,000 rpm for IL-23$\alpha^{opt,\ C54S}$ using an An-50 Ti rotor at 20 °C. Radial absorbance scans were acquired continuously at 230 nm for IL-23α^{VVS} and 235 nm for IL-23$\alpha^{opt,\ C54S}$ with a radial step size of 0.003 cm. The resulting sedimentation velocity profiles were analyzed using the SedFit software by Peter Schuck with a non-model based continuous Svedberg distribution method (c(s)), with time (TI) and radial (RI) invariant noise on[283]. The density (ρ), viscosity (η) and partial specific volume ($\bar{\nu}$) of the potassium phosphate buffer used for data analysis was calculated with SEDNTERP[284].

Partial Proteolysis

Stability against proteolytic digestion was assessed by partial proteolysis using trypsin (VWR). Trypsin was added at a concentration of 1:80 (w/w). Aliquots were withdrawn after different time points, and the proteolysis was terminated by the addition of Roche complete protease inhibitor without EDTA (Roche Applied Science), Laemmli buffer and boiling for 5 min at 90 °C. Proteins were separated on 15% SDS-PAGE gels. Gels were quantified using Fiji ImageJ.

IL-23α optimization

IL-23α was optimized using RosettaRemodel to improve stability. The structure of IL-23α was extracted from the chain B of PDB file 5MJ3. IL-23α monomer was first prepared following standard protocols (specified in the flag_relax file) to conform to the Rosetta forcefield. The HDX/NMR data suggested a flexible helix 1, and thus to stabilize the helical bundle, we focused on remodeling the first helix. We first rebuild the entire helix while allowing the sequence to vary. The first iteration of redocking the helix while redesigning the core is specified in the blueprint and flags file provided (remodel_1.bp and remodel_flags) to stabilize the helix bundle core residues on the first alpha helix, as well as to introduce a helix capping residue (Supplementary Fig. 4a). The top structure from 1000 independent trajectories from the first iteration was chosen based on improved helix core packing and minimal drifting of the first alpha helix. This resulted in mutations Q10A, C14L, L17I, S18I, L21I and C22L. Leucine on residue 22 impacts the interface with IL-12β, so it was kept as cysteine in the final design, also to preserve one ERp44 interaction site. Since Pro9 was unsupported in the IL-23α structure, we extended the N-terminus of the crystal structure by 2 residues, and completely rebuilt the first 6 amino acids in order to create a stable terminus. We incorporated N-capping motifs in residues 7 and 8, as Ser-Pro or Asp-Pro, and tested two different options for residue 6, either as a hydrophobic residue or as part of a salt-bridge with residue 10. This second iteration was run on the aforementioned top structure using remodel_2.bp and the same remodel_flags file but without the *-bypass_fragments true* flag. 1000 independent trajectories were sampled. After the completion of the two design steps, we crossreferenced by aligning the final design candidates to the crystal structure containing IL-12β and reverted cysteine 22 because the predicted leucine residue would potentially clash with a residue on IL-12β. All residue numbers refer to the IL-23α sequence without the signal peptide.

NMR spectroscopy

NMR experiments were performed using ^{15}N-labeled samples at a concentration of 100 µM in 10 mM KPi (pH 7.5) buffer containing 5% D2O. ^{1}H, ^{15}N heteronuclear single quantum coherence (HSQC) experiments using watergate water flip-back for solvent suppression were performed at 298 K on a Bruker Avance III spectrometers operating at 900 and 950 MHz proton Larmor frequency using cryogenically cooled probes. Spectra comprised 2046 X 256 complex data points for direct and indirect dimensions, respectively, with a spectral window

of 33 ppm centered at 117 ppm for the indirect dimension. All spectra were processed using Bruker Topspin 3.5 software (Bruker, Billerica, USA) using linear prediction and zero filling in the indirect dimension, and were analyzed using CcpNmr Analysis[285].

IL-23 receptor activation assay

The IL-23 receptor activation assay was performed using IL-23 iLite® reporter cells from Euro Diagnostica (BM4023), according to the supplier's instructions. To assess activity of recombinant IL-23 complexes a final concentration of 25 ng/ml was used. A final concentration of 25 ng/ml of recombinant human IL-23 (R&D systems, 1290-IL) was used to test IL-23α inhibition. The Firefly and Renilla luciferase signal was detected via the Dual-Glo Luciferase Assay System (Promega) in a Spark multimode microplate reader (Tecan group). Individual signals were normalized against the housekeeping renilla signal. To allow better comparisons between mutants, receptor activation of wild type IL-23 was set to 100%.

Quantification and statistics

Western blots were quantified using the Bio-1D software (Vilber Lourmat). Statistical analyses were performed using Prism (GraphPad Software). Where indicated, data were analyzed with two-tailed, unpaired Student's *t*-tests. Differences were considered statistically significant when $p<0.05$. Where no statistical data are shown, all experiments were performed at least three times, and one representative experiment was selected.

4 Conclusions and outlook

Since the discovery of IL-12, 30 years ago, the IL-12 family members have remained an interesting topic of investigations. This illustrates their important immunological functions and their prominent role human diseases. This work goes beyond the immunological aspects of IL-12 family members by examining biochemical and cellular features of IL-12/IL-23 folding and assembly. We show that assembly-induced folding is key in IL-12 and IL-23 biogenesis. Both IL-12 and IL-23 α subunits fail to adopt their native state in isolation but form non-native disulfide linked species instead. Further investigations will show, if those constitute functional intracellular proteins, as reported for IL-23α[19] or perform other roles e.g. in assembly control of IL-12 family members.

Only interaction with the shared β subunit induces complete folding and liberates the α subunits from retention by forming the heterodimeric, secreted IL complex. Further investigation is needed to answer the question if IL-12β is able to inhibit α subunit misfolding early during maturation or rescues non-natively folded α species. The latter is maybe more likely since the IL-12β interface is located close to the C-terminus of the α subunit and thus prevents early complex formation, already during co-translational import of IL-12α/IL-23α.

We identified one evolutionarily conserved disulfide bond, shared by IL-12α and IL-23α, which is a prerequisite for IL stability and assembly. This disulfide bond stabilizes the loop between helix one and two of IL-12α and IL-23α, respectively. Formation of this disulfide bond may provide an initial step in the formation of the 4-helix bundle topology of the α subunits, which can be subsequently recognized by IL-12β. Furthermore, this disulfide bond positions the IL-12β connecting cysteine residue. Although a covalent connection between α and β subunits is not necessary for IL-12 cytokine assembly, secretion and biological activity[208,223,286], it may influence assembly kinetics by inhibiting dissociation of the complex. On the other hand, a non-covalent IL complex could possess further extracellular functions. If α and β subunits get separated by harsh extracellular conditions they could function independently of each other. Interestingly, the immunoregulatory and anti-inflammatory members of the IL-12 family are not covalently connected and could function that way, adding another layer of complexity to the biological functions of IL-12 family members.

Another unanswered, yet very interesting question is, if or how IL-12β distinguishes between IL-12α and IL-23α. Interaction of IL-12β and its α subunits may simply be regulated kinetically and/or thermodynamically, favoring production of the more stable complex. Another possibility is that assembly is regulated by assistance of different sets of chaperones as this study suggests[150,287]. This would also allow for a fast adaptation in IL-production upon changed environmental conditions. Our detailed molecular studies on IL-23 biogenesis lays the basis of understanding differences in IL-12 and IL-23 maturation. For IL-23α we show that its first helix with two free cysteines is readily recognized by BiP and ERp44, whereas IL-12α possesses no unpaired cysteines. Free cysteines in IL-23α are recognized by ERp44 in the ERGIC compartment, which may implicate that IL-12β and IL-23α interaction occurs also outside the ER. Hence, IL-12 and IL-23 production may be spatially separated from each other. Another interesting point concerning different participation of chaperones in IL-12 and IL-23 biogenesis is N-glycosylation. Whereas IL-12α gets heavily glycosylated in the ER (Fig. 2.1b), there are no N-glycosylation sites predicted for IL-23α and no shift in molecular weight could be observed during secretion with IL-12β (Fig.3.1b) This points to a potential role of the CNX/CRT cycle in IL-12 maturation but not for IL-23. Since two N-glycosylation sites (Fig. 2.3a) are in close proximity to cysteine residues in IL-12α, glycosylation and oxidation, may be ultimately coupled, by the action of ERp57.

On a broader scale, this work provides insights into how small, single domain proteins combine different signals in order to regulate assembly, degradation and/or chaperone interaction. To date, *in vivo* data on assembly-induced protein folding are only available for multidomain proteins like IgG, IgM or the T cell receptor.

The major interaction site for IL-12β in IL-23α lies at helix four[286], opposite of helix one which we identified as unfolded and as the main chaperone anchor in IL-23α. This topology in principal allows for chaperone binding and interaction with the β subunit simultaneously. How interaction with IL-12β induces complete folding of a domain substructure which is only weakly involved in the IL-12β interface needs further investigation.

Our detailed investigation on IL-12 and IL-23 assembly control could provide the basis for a structural intervention of the assembly process. This could be ultimately used as a new therapeutic approach in regulating IL-12/IL-23 production. Furthermore, we showed that simplified, yet functional IL-12 and IL-23 variants are possible and designed a stable

unassembled IL-23α subunit. The optimized IL-23α subunit as well the simplified IL complexes could help in advancing in IL-12/IL-23-related therapies.

5 References

1 Chaplin, D. D. Overview of the immune response. *The Journal of allergy and clinical immunology* **125**, S3-S23, doi:10.1016/j.jaci.2009.12.980 (2010).

2 Iwasaki, A. & Medzhitov, R. Control of adaptive immunity by the innate immune system. *Nature immunology* **16**, 343-353, doi:10.1038/ni.3123 (2015).

3 Akdis, M. *et al.* Interleukins (from IL-1 to IL-38), interferons, transforming growth factor β, and TNF-α: Receptors, functions, and roles in diseases. *Journal of Allergy and Clinical Immunology* **138**, 984-1010, doi:https://doi.org/10.1016/j.jaci.2016.06.033 (2016).

4 Brocker, C., Thompson, D., Matsumoto, A., Nebert, D. W. & Vasiliou, V. Evolutionary divergence and functions of the human interleukin (IL) gene family. *Human genomics* **5**, 30-55, doi:10.1186/1479-7364-5-1-30 (2010).

5 Scapigliati, G., Buonocore, F. & Mazzini, M. Biological activity of cytokines: an evolutionary perspective. *Current pharmaceutical design* **12**, 3071-3081 (2006).

6 Vignali, D. A. & Kuchroo, V. K. IL-12 family cytokines: immunological playmakers. *Nature immunology* **13**, 722-728, doi:10.1038/ni.2366 (2012).

7 Wong, H. L. *et al.* Characterization of a factor(s) which synergizes with recombinant interleukin 2 in promoting allogeneic human cytolytic T-lymphocyte responses in vitro. *Cellular immunology* **111**, 39-54 (1988).

8 Wang, R. X., Yu, C. R., Mahdi, R. M. & Egwuagu, C. E. Novel IL27p28/IL12p40 cytokine suppressed experimental autoimmune uveitis by inhibiting autoreactive Th1/Th17 cells and promoting expansion of regulatory T cells. *The Journal of biological chemistry* **287**, 36012-36021, doi:10.1074/jbc.M112.390625 (2012).

9 Wang, X. *et al.* A novel IL-23p19/Ebi3 (IL-39) cytokine mediates inflammation in Lupus-like mice. *European journal of immunology* **46**, 1343-1350, doi:10.1002/eji.201546095 (2016).

10 Garbers, C. *et al.* Plasticity and cross-talk of interleukin 6-type cytokines. *Cytokine & growth factor reviews* **23**, 85-97, doi:10.1016/j.cytogfr.2012.04.001 (2012).

11 Hasegawa, H. *et al.* Expanding Diversity in Molecular Structures and Functions of the IL-6/IL-12 Heterodimeric Cytokine Family. *Frontiers in immunology* **7**, 479, doi:10.3389/fimmu.2016.00479 (2016).

12 Detry, S., Składanowska, K., Vuylsteke, M., Savvides, S. N. & Bloch, Y. Revisiting the combinatorial potential of cytokine subunits in the IL-12 family. *Biochemical Pharmacology*, doi:https://doi.org/10.1016/j.bcp.2019.03.026 (2019).

13 Jones, L. L. & Vignali, D. A. Molecular interactions within the IL-6/IL-12 cytokine/receptor superfamily. *Immunologic research* **51**, 5-14, doi:10.1007/s12026-011-8209-y (2011).

14 Langrish, C. L. *et al.* IL-12 and IL-23: master regulators of innate and adaptive immunity. *Immunological reviews* **202**, 96-105, doi:10.1111/j.0105-2896.2004.00214.x (2004).

15 Hunter, C. A. & Kastelein, R. Interleukin-27: balancing protective and pathological immunity. *Immunity* **37**, 960-969, doi:10.1016/j.immuni.2012.11.003 (2012).

16 Yoshida, H. & Hunter, C. A. The immunobiology of interleukin-27. *Annual review of immunology* **33**, 417-443, doi:10.1146/annurev-immunol-032414-112134 (2015).

17 Collison, L. W. *et al.* The inhibitory cytokine IL-35 contributes to regulatory T-cell function. *Nature* **450**, 566-569, doi:nature06306 [pii] 10.1038/nature06306 (2007).

18 Kastelein, R. A., Hunter, C. A. & Cua, D. J. Discovery and biology of IL-23 and IL-27: related but functionally distinct regulators of inflammation. *Annu Rev Immunol* **25**, 221-242, doi:10.1146/annurev.immunol.22.012703.104758 (2007).
19 Espígol-Frigolé, G. *et al.* Identification of IL-23p19 as an endothelial proinflammatory peptide that promotes gp130-STAT3 signaling. *Science signaling* **9**, ra28-ra28, doi:10.1126/scisignal.aad2357 (2016).
20 Frank, G. M., Divito, S. J., Maker, D. M., Xu, M. & Hendricks, R. L. A novel p40-independent function of IL-12p35 is required for progression and maintenance of herpes stromal keratitis. *Investigative ophthalmology & visual science* **51**, 3591-3598, doi:10.1167/iovs.09-4368 (2010).
21 Jana, M. & Pahan, K. IL-12 p40 homodimer, but not IL-12 p70, induces the expression of IL-16 in microglia and macrophages. *Molecular immunology* **46**, 773-783, doi:10.1016/j.molimm.2008.10.033 (2009).
22 Stumhofer, J. S. *et al.* A role for IL-27p28 as an antagonist of gp130-mediated signaling. *Nature immunology* **11**, 1119-1126, doi:10.1038/ni.1957 (2010).
23 Yan, J. *et al.* Interleukin-30 (IL27p28) alleviates experimental sepsis by modulating cytokine profile in NKT cells. *Journal of hepatology* **64**, 1128-1136, doi:10.1016/j.jhep.2015.12.020 (2016).
24 Muller, S. I. *et al.* A folding switch regulates interleukin 27 biogenesis and secretion of its alpha-subunit as a cytokine. *Proceedings of the National Academy of Sciences of the United States of America* **116**, 1585-1590, doi:10.1073/pnas.1816698116 (2019).
25 Floss, D. M., Schroder, J., Franke, M. & Scheller, J. Insights into IL-23 biology: From structure to function. *Cytokine & growth factor reviews* **26**, 569-578, doi:10.1016/j.cytogfr.2015.07.005 (2015).
26 Lupardus, P. J. & Garcia, K. C. The structure of interleukin-23 reveals the molecular basis of p40 subunit sharing with interleukin-12. *Journal of molecular biology* **382**, 931-941, doi:10.1016/j.jmb.2008.07.051 (2008).
27 Schroder, J. *et al.* Non-canonical interleukin 23 receptor complex assembly: p40 protein recruits interleukin 12 receptor beta1 via site II and induces p19/interleukin 23 receptor interaction via site III. *The Journal of biological chemistry* **290**, 359-370, doi:10.1074/jbc.M114.617597 (2015).
28 Bloch, Y. *et al.* Structural Activation of Pro-inflammatory Human Cytokine IL-23 by Cognate IL-23 Receptor Enables Recruitment of the Shared Receptor IL-12Rβ1. *Immunity* **48**, 45-58.e46, doi:10.1016/j.immuni.2017.12.008 (2018).
29 Trinchieri, G. Interleukin-12 and the regulation of innate resistance and adaptive immunity. *Nature Reviews Immunology* **3**, 133, doi:10.1038/nri1001 (2003).
30 Zundler, S. & Neurath, M. F. Interleukin-12: Functional activities and implications for disease. *Cytokine & growth factor reviews* **26**, 559-568, doi:10.1016/j.cytogfr.2015.07.003 (2015).
31 Becker, C., Wirtz, S. & Neurath, M. F. Stepwise regulation of TH1 responses in autoimmunity: IL-12-related cytokines and their receptors. *Inflammatory bowel diseases* **11**, 755-764 (2005).
32 Serafini, N., Vosshenrich, C. A. & Di Santo, J. P. Transcriptional regulation of innate lymphoid cell fate. *Nature reviews. Immunology* **15**, 415-428, doi:10.1038/nri3855 (2015).
33 Shafiani, S. *et al.* Pathogen-specific Treg cells expand early during mycobacterium tuberculosis infection but are later eliminated in response to Interleukin-12. *Immunity* **38**, 1261-1270, doi:10.1016/j.immuni.2013.06.003 (2013).

34 Gaffen, S. L. An overview of IL-17 function and signaling. *Cytokine* **43**, 402-407, doi:10.1016/j.cyto.2008.07.017 (2008).
35 Croxford, A. L., Mair, F. & Becher, B. IL-23: one cytokine in control of autoimmunity. *European journal of immunology* **42**, 2263-2273, doi:10.1002/eji.201242598 (2012).
36 Gaffen, S. L., Jain, R., Garg, A. V. & Cua, D. J. The IL-23-IL-17 immune axis: from mechanisms to therapeutic testing. *Nature reviews. Immunology* **14**, 585-600, doi:10.1038/nri3707 (2014).
37 McGeachy, M. J. *et al.* TGF-beta and IL-6 drive the production of IL-17 and IL-10 by T cells and restrain T(H)-17 cell-mediated pathology. *Nature immunology* **8**, 1390-1397, doi:10.1038/ni1539 (2007).
38 Amatya, N., Garg, A. V. & Gaffen, S. L. IL-17 Signaling: The Yin and the Yang. *Trends in immunology* **38**, 310-322, doi:10.1016/j.it.2017.01.006 (2017).
39 Oppmann, B. *et al.* Novel p19 protein engages IL-12p40 to form a cytokine, IL-23, with biological activities similar as well as distinct from IL-12. *Immunity* **13**, 715-725 (2000).
40 Li, Y., Wang, H., Lu, H. & Hua, S. Regulation of Memory T Cells by Interleukin-23. *International archives of allergy and immunology* **169**, 157-162, doi:10.1159/000445834 (2016).
41 Maurice K. Gately *et al.* THE INTERLEUKIN-12/INTERLEUKIN-12-RECEPTOR SYSTEM: Role in Normal and Pathologic Immune Responses. *Annual review of immunology* **16**, 495-521, doi:10.1146/annurev.immunol.16.1.495 (1998).
42 Shimozato, O. *et al.* The secreted form of the p40 subunit of interleukin (IL)-12 inhibits IL-23 functions and abrogates IL-23-mediated antitumour effects. *Immunology* **117**, 22-28, doi:10.1111/j.1365-2567.2005.02257.x (2006).
43 Jana, M., Dasgupta, S., Pal, U. & Pahan, K. IL-12 p40 homodimer, the so-called biologically inactive molecule, induces nitric oxide synthase in microglia via IL-12R beta 1. *Glia* **57**, 1553-1565, doi:10.1002/glia.20869 (2009).
44 Brahmachari, S. & Pahan, K. Suppression of regulatory T cells by IL-12p40 homodimer via nitric oxide. *Journal of immunology (Baltimore, Md. : 1950)* **183**, 2045-2058, doi:10.4049/jimmunol.0800276 (2009).
45 Gunsten, S. *et al.* IL-12 p80-dependent macrophage recruitment primes the host for increased survival following a lethal respiratory viral infection. *Immunology* **126**, 500-513, doi:10.1111/j.1365-2567.2008.02923.x (2009).
46 Khader, S. A. *et al.* Interleukin 12p40 is required for dendritic cell migration and T cell priming after Mycobacterium tuberculosis infection. *The Journal of experimental medicine* **203**, 1805-1815, doi:10.1084/jem.20052545 (2006).
47 Dambuza, I. M. *et al.* IL-12p35 induces expansion of IL-10 and IL-35-expressing regulatory B cells and ameliorates autoimmune disease. *Nature communications* **8**, 719-719, doi:10.1038/s41467-017-00838-4 (2017).
48 Espigol-Frigole, G. *et al.* Identification of IL-23p19 as an endothelial proinflammatory peptide that promotes gp130-STAT3 signaling. *Sci Signal* **9**, ra28, doi:10.1126/scisignal.aad2357 (2016).
49 Chen, D. & Nicholas, J. Structural requirements for gp80 independence of human herpesvirus 8 interleukin-6 (vIL-6) and evidence for gp80 stabilization of gp130 signaling complexes induced by vIL-6. *Journal of virology* **80**, 9811-9821, doi:10.1128/jvi.00872-06 (2006).
50 Kreymborg, K., Bohlmann, U. & Becher, B. IL-23: changing the verdict on IL-12 function in inflammation and autoimmunity. *Expert opinion on therapeutic targets* **9**, 1123-1136, doi:10.1517/14728222.9.6.1123 (2005).

51 Berraondo, P., Etxeberria, I., Ponz-Sarvise, M. & Melero, I. Revisiting Interleukin-12 as a Cancer Immunotherapy Agent. *Clinical cancer research : an official journal of the American Association for Cancer Research* **24**, 2716-2718, doi:10.1158/1078-0432.ccr-18-0381 (2018).
52 Smyth, M. J., Taniguchi, M. & Street, S. E. The anti-tumor activity of IL-12: mechanisms of innate immunity that are model and dose dependent. *J Immunol* **165**, 2665-2670 (2000).
53 Atkins, M. B. *et al.* Phase I evaluation of intravenous recombinant human interleukin 12 in patients with advanced malignancies. *Clinical cancer research : an official journal of the American Association for Cancer Research* **3**, 409-417 (1997).
54 Bajetta, E. *et al.* Pilot study of subcutaneous recombinant human interleukin 12 in metastatic melanoma. *Clinical cancer research : an official journal of the American Association for Cancer Research* **4**, 75-85 (1998).
55 Wu, C. J. *et al.* Combination of radiation and interleukin 12 eradicates large orthotopic hepatocellular carcinoma through immunomodulation of tumor microenvironment. *Oncoimmunology* **7**, e1477459, doi:10.1080/2162402x.2018.1477459 (2018).
56 Kamensek, U., Cemazar, M., Lampreht Tratar, U., Ursic, K. & Sersa, G. Antitumor in situ vaccination effect of TNFalpha and IL-12 plasmid DNA electrotransfer in a murine melanoma model. *Cancer immunology, immunotherapy : CII* **67**, 785-795, doi:10.1007/s00262-018-2133-0 (2018).
57 Strauss, J. *et al.* First-in-Human Phase I Trial of a Tumor-Targeted Cytokine (NHS-IL12) in Subjects with Metastatic Solid Tumors. *Clinical cancer research : an official journal of the American Association for Cancer Research* **25**, 99-109, doi:10.1158/1078-0432.ccr-18-1512 (2019).
58 Liu, X. *et al.* Modified nanoparticle mediated IL-12 immunogene therapy for colon cancer. *Nanomedicine : nanotechnology, biology, and medicine* **13**, 1993-2004, doi:10.1016/j.nano.2017.04.006 (2017).
59 Hutmacher, C. & Neri, D. Antibody-cytokine fusion proteins: Biopharmaceuticals with immunomodulatory properties for cancer therapy. *Advanced drug delivery reviews*, doi:10.1016/j.addr.2018.09.002 (2018).
60 Okamoto, S. *et al.* Anti-IL-12/23 p40 antibody attenuates experimental chronic graft-versus-host disease via suppression of IFN-gamma/IL-17-producing cells. *J Immunol* **194**, 1357-1363, doi:10.4049/jimmunol.1400973 (2015).
61 Kulig, P. *et al.* IL-12 protects from psoriasiform skin inflammation. *Nature communications* **7**, 13466-13466, doi:10.1038/ncomms13466 (2016).
62 Kim, J. & Krueger, J. G. Highly Effective New Treatments for Psoriasis Target the IL-23/Type 17 T Cell Autoimmune Axis. *Annual review of medicine* **68**, 255-269, doi:10.1146/annurev-med-042915-103905 (2017).
63 Benson, J. M. *et al.* Therapeutic targeting of the IL-12/23 pathways: generation and characterization of ustekinumab. *Nature biotechnology* **29**, 615-624, doi:10.1038/nbt.1903 (2011).
64 Machado, A. & Torres, T. Guselkumab for the Treatment of Psoriasis. *BioDrugs : clinical immunotherapeutics, biopharmaceuticals and gene therapy* **32**, 119-128, doi:10.1007/s40259-018-0265-6 (2018).
65 Langowski, J. L. *et al.* IL-23 promotes tumour incidence and growth. *Nature* **442**, 461-465, doi:10.1038/nature04808 (2006).
66 Calcinotto, A. *et al.* IL-23 secreted by myeloid cells drives castration-resistant prostate cancer. *Nature* **559**, 363-369, doi:10.1038/s41586-018-0266-0 (2018).

67 Yan, J., Smyth, M. J. & Teng, M. W. L. Interleukin (IL)-12 and IL-23 and Their Conflicting Roles in Cancer. *Cold Spring Harbor perspectives in biology* **10**, doi:10.1101/cshperspect.a028530 (2018).
68 Numasaki, M. *et al.* Interleukin-17 promotes angiogenesis and tumor growth. *Blood* **101**, 2620-2627, doi:10.1182/blood-2002-05-1461 (2003).
69 Chabaud, M. *et al.* Contribution of interleukin 17 to synovium matrix destruction in rheumatoid arthritis. *Cytokine* **12**, 1092-1099, doi:10.1006/cyto.2000.0681 (2000).
70 Hussain, S. M. *et al.* IL23 and TGF-ß diminish macrophage associated metastasis in pancreatic carcinoma. *Scientific Reports* **8**, 5808, doi:10.1038/s41598-018-24194-5 (2018).
71 Nie, W., Yu, T., Sang, Y. & Gao, X. Tumor-promoting effect of IL-23 in mammary cancer mediated by infiltration of M2 macrophages and neutrophils in tumor microenvironment. *Biochemical and biophysical research communications* **482**, 1400-1406, doi:10.1016/j.bbrc.2016.12.048 (2017).
72 Sieve, A. N., Meeks, K. D., Lee, S. & Berg, R. E. A novel immunoregulatory function for IL-23: Inhibition of IL-12-dependent IFN-gamma production. *European journal of immunology* **40**, 2236-2247, doi:10.1002/eji.200939759 (2010).
73 Muller, S. I. *et al.* A folding switch regulates interleukin 27 biogenesis and secretion of its alpha-subunit as a cytokine. *Proceedings of the National Academy of Sciences of the United States of America*, doi:10.1073/pnas.1816698116 (2019).
74 Moraga, I. *et al.* Synthekines are surrogate cytokine and growth factor agonists that compel signaling through non-natural receptor dimers. *eLife* **6**, doi:10.7554/eLife.22882 (2017).
75 Sockolosky, J. T. *et al.* Selective targeting of engineered T cells using orthogonal IL-2 cytokine-receptor complexes. *Science* **359**, 1037-1042, doi:10.1126/science.aar3246 (2018).
76 Rafei, M. *et al.* A granulocyte-macrophage colony-stimulating factor and interleukin-15 fusokine induces a regulatory B cell population with immune suppressive properties. *Nat Med* **15**, 1038-1045, doi:10.1038/nm.2003 (2009).
77 Wang, P. *et al.* Re-designing Interleukin-12 to enhance its safety and potential as an anti-tumor immunotherapeutic agent. *Nature communications* **8**, 1395-1395, doi:10.1038/s41467-017-01385-8 (2017).
78 Engelowski, E. *et al.* Synthetic cytokine receptors transmit biological signals using artificial ligands. *Nature communications* **9**, 2034-2034, doi:10.1038/s41467-018-04454-8 (2018).
79 Braakman, I. & Bulleid, N. J. Protein folding and modification in the mammalian endoplasmic reticulum. *Annual review of biochemistry* **80**, 71-99, doi:10.1146/annurev-biochem-062209-093836 (2011).
80 Wu, X., Cabanos, C. & Rapoport, T. A. Structure of the post-translational protein translocation machinery of the ER membrane. *Nature* **566**, 136-139, doi:10.1038/s41586-018-0856-x (2019).
81 Schuldiner, M. *et al.* The GET complex mediates insertion of tail-anchored proteins into the ER membrane. *Cell* **134**, 634-645, doi:10.1016/j.cell.2008.06.025 (2008).
82 Ast, T., Cohen, G. & Schuldiner, M. A network of cytosolic factors targets SRP-independent proteins to the endoplasmic reticulum. *Cell* **152**, 1134-1145, doi:10.1016/j.cell.2013.02.003 (2013).
83 Shan, S. O. & Walter, P. Co-translational protein targeting by the signal recognition particle. *FEBS letters* **579**, 921-926, doi:10.1016/j.febslet.2004.11.049 (2005).

84 Halic, M. & Beckmann, R. The signal recognition particle and its interactions during protein targeting. *Current Opinion in Structural Biology* **15**, 116-125, doi:https://doi.org/10.1016/j.sbi.2005.01.013 (2005).
85 Lakkaraju, A. K., Mary, C., Scherrer, A., Johnson, A. E. & Strub, K. SRP keeps polypeptides translocation-competent by slowing translation to match limiting ER-targeting sites. *Cell* **133**, 440-451, doi:10.1016/j.cell.2008.02.049 (2008).
86 Park, E. & Rapoport, T. A. Mechanisms of Sec61/SecY-mediated protein translocation across membranes. *Annual review of biophysics* **41**, 21-40, doi:10.1146/annurev-biophys-050511-102312 (2012).
87 Voorhees, R. M., Fernandez, I. S., Scheres, S. H. & Hegde, R. S. Structure of the mammalian ribosome-Sec61 complex to 3.4 A resolution. *Cell* **157**, 1632-1643, doi:10.1016/j.cell.2014.05.024 (2014).
88 Voorhees, R. M. & Hegde, R. S. Structure of the Sec61 channel opened by a signal sequence. *Science (New York, N.Y.)* **351**, 88-91, doi:10.1126/science.aad4992 (2016).
89 Gumbart, J., Trabuco, L. G., Schreiner, E., Villa, E. & Schulten, K. Regulation of the protein-conducting channel by a bound ribosome. *Structure (London, England : 1993)* **17**, 1453-1464, doi:10.1016/j.str.2009.09.010 (2009).
90 Pfeffer, S. *et al.* Dissecting the molecular organization of the translocon-associated protein complex. *Nature Communications* **8**, 14516, doi:10.1038/ncomms14516 (2017).
91 Sommer, N., Junne, T., Kalies, K. U., Spiess, M. & Hartmann, E. TRAP assists membrane protein topogenesis at the mammalian ER membrane. *Biochimica et biophysica acta* **1833**, 3104-3111, doi:10.1016/j.bbamcr.2013.08.018 (2013).
92 Hegde, R. S., Voigt, S., Rapoport, T. A. & Lingappa, V. R. TRAM Regulates the Exposure of Nascent Secretory Proteins to the Cytosol during Translocation into the Endoplasmic Reticulum. *Cell* **92**, 621-631, doi:https://doi.org/10.1016/S0092-8674(00)81130-7 (1998).
93 Dudek, J. *et al.* Protein transport into the human endoplasmic reticulum. *Journal of molecular biology* **427**, 1159-1175, doi:10.1016/j.jmb.2014.06.011 (2015).
94 Matlack, K. E., Misselwitz, B., Plath, K. & Rapoport, T. A. BiP acts as a molecular ratchet during posttranslational transport of prepro-alpha factor across the ER membrane. *Cell* **97**, 553-564 (1999).
95 Snapp, E. L. *et al.* Structure and topology around the cleavage site regulate post-translational cleavage of the HIV-1 gp160 signal peptide. *eLife* **6**, doi:10.7554/eLife.26067 (2017).
96 Tamura, T., Cormier, J. H. & Hebert, D. N. Characterization of early EDEM1 protein maturation events and their functional implications. *The Journal of biological chemistry* **286**, 24906-24915, doi:10.1074/jbc.M111.243998 (2011).
97 Daniels, R., Kurowski, B., Johnson, A. E. & Hebert, D. N. N-linked glycans direct the cotranslational folding pathway of influenza hemagglutinin. *Molecular cell* **11**, 79-90 (2003).
98 Bai, L., Wang, T., Zhao, G., Kovach, A. & Li, H. The atomic structure of a eukaryotic oligosaccharyltransferase complex. *Nature* **555**, 328-333, doi:10.1038/nature25755 (2018).
99 Schallus, T. *et al.* Malectin: a novel carbohydrate-binding protein of the endoplasmic reticulum and a candidate player in the early steps of protein N-glycosylation. *Molecular biology of the cell* **19**, 3404-3414, doi:10.1091/mbc.E08-04-0354 (2008).

100 Galli, C., Bernasconi, R., Solda, T., Calanca, V. & Molinari, M. Malectin participates in a backup glycoprotein quality control pathway in the mammalian ER. *PloS one* **6**, e16304, doi:10.1371/journal.pone.0016304 (2011).
101 Chen, Y. *et al.* Role of malectin in Glc(2)Man(9)GlcNAc(2)-dependent quality control of alpha1-antitrypsin. *Molecular biology of the cell* **22**, 3559-3570, doi:10.1091/mbc.E11-03-0201 (2011).
102 Frickel, E. M. *et al.* TROSY-NMR reveals interaction between ERp57 and the tip of the calreticulin P-domain. *Proceedings of the National Academy of Sciences of the United States of America* **99**, 1954-1959, doi:10.1073/pnas.042699099 (2002).
103 Kozlov, G. *et al.* Structural basis of cyclophilin B binding by the calnexin/calreticulin P-domain. *The Journal of biological chemistry* **285**, 35551-35557, doi:10.1074/jbc.M110.160101 (2010).
104 Solda, T., Garbi, N., Hammerling, G. J. & Molinari, M. Consequences of ERp57 deletion on oxidative folding of obligate and facultative clients of the calnexin cycle. *The Journal of biological chemistry* **281**, 6219-6226, doi:10.1074/jbc.M513595200 (2006).
105 Slominska-Wojewodzka, M. & Sandvig, K. The Role of Lectin-Carbohydrate Interactions in the Regulation of ER-Associated Protein Degradation. *Molecules (Basel, Switzerland)* **20**, 9816-9846, doi:10.3390/molecules20069816 (2015).
106 Williams, D. B. Beyond lectins: the calnexin/calreticulin chaperone system of the endoplasmic reticulum. *Journal of cell science* **119**, 615-623, doi:10.1242/jcs.02856 (2006).
107 Lamriben, L., Graham, J. B., Adams, B. M. & Hebert, D. N. N-Glycan-based ER Molecular Chaperone and Protein Quality Control System: The Calnexin Binding Cycle. *Traffic (Copenhagen, Denmark)* **17**, 308-326, doi:10.1111/tra.12358 (2016).
108 Gauss, R., Kanehara, K., Carvalho, P., Ng, D. T. & Aebi, M. A complex of Pdi1p and the mannosidase Htm1p initiates clearance of unfolded glycoproteins from the endoplasmic reticulum. *Molecular cell* **42**, 782-793, doi:10.1016/j.molcel.2011.04.027 (2011).
109 Avezov, E., Frenkel, Z., Ehrlich, M., Herscovics, A. & Lederkremer, G. Z. Endoplasmic reticulum (ER) mannosidase I is compartmentalized and required for N-glycan trimming to Man5-6GlcNAc2 in glycoprotein ER-associated degradation. *Molecular biology of the cell* **19**, 216-225, doi:10.1091/mbc.e07-05-0505 (2008).
110 Behnke, J., Feige, M. J. & Hendershot, L. M. BiP and its nucleotide exchange factors Grp170 and Sil1: mechanisms of action and biological functions. *Journal of molecular biology* **427**, 1589-1608, doi:10.1016/j.jmb.2015.02.011 (2015).
111 Blond-Elguindi, S. *et al.* Affinity panning of a library of peptides displayed on bacteriophages reveals the binding specificity of BiP. *Cell* **75**, 717-728 (1993).
112 Flynn, G. C., Pohl, J., Flocco, M. T. & Rothman, J. E. Peptide-binding specificity of the molecular chaperone BiP. *Nature* **353**, 726-730, doi:10.1038/353726a0 (1991).
113 Kityk, R., Kopp, J. & Mayer, M. P. Molecular Mechanism of J-Domain-Triggered ATP Hydrolysis by Hsp70 Chaperones. *Molecular cell* **69**, 227-237.e224, doi:10.1016/j.molcel.2017.12.003 (2018).
114 Misselwitz, B., Staeck, O. & Rapoport, T. A. J proteins catalytically activate Hsp70 molecules to trap a wide range of peptide sequences. *Molecular cell* **2**, 593-603 (1998).
115 Hendershot, L. M. The ER function BiP is a master regulator of ER function. *The Mount Sinai journal of medicine, New York* **71**, 289-297 (2004).

116 Kampinga, H. H. & Craig, E. A. The HSP70 chaperone machinery: J proteins as drivers of functional specificity. *Nature reviews. Molecular cell biology* **11**, 579-592, doi:10.1038/nrm2941 (2010).
117 Dudek, J. *et al.* ERj1p has a basic role in protein biogenesis at the endoplasmic reticulum. *Nature structural & molecular biology* **12**, 1008-1014, doi:10.1038/nsmb1007 (2005).
118 Blau, M. *et al.* ERj1p uses a universal ribosomal adaptor site to coordinate the 80S ribosome at the membrane. *Nature structural & molecular biology* **12**, 1015-1016, doi:10.1038/nsmb998 (2005).
119 Shen, Y. & Hendershot, L. M. ERdj3, a stress-inducible endoplasmic reticulum DnaJ homologue, serves as a cofactor for BiP's interactions with unfolded substrates. *Molecular biology of the cell* **16**, 40-50, doi:10.1091/mbc.e04-05-0434 (2005).
120 Jin, Y., Awad, W., Petrova, K. & Hendershot, L. M. Regulated release of ERdj3 from unfolded proteins by BiP. *The EMBO journal* **27**, 2873-2882, doi:10.1038/emboj.2008.207 (2008).
121 Petrova, K., Oyadomari, S., Hendershot, L. M. & Ron, D. Regulated association of misfolded endoplasmic reticulum lumenal proteins with P58/DNAJc3. *The EMBO journal* **27**, 2862-2872, doi:10.1038/emboj.2008.199 (2008).
122 Hassdenteufel, S. *et al.* Chaperone-Mediated Sec61 Channel Gating during ER Import of Small Precursor Proteins Overcomes Sec61 Inhibitor-Reinforced Energy Barrier. *Cell reports* **23**, 1373-1386, doi:10.1016/j.celrep.2018.03.122 (2018).
123 Behnke, J., Mann, M. J., Scruggs, F. L., Feige, M. J. & Hendershot, L. M. Members of the Hsp70 Family Recognize Distinct Types of Sequences to Execute ER Quality Control. *Molecular cell* **63**, 739-752, doi:10.1016/j.molcel.2016.07.012 (2016).
124 Preissler, S. *et al.* AMPylation targets the rate-limiting step of BiP's ATPase cycle for its functional inactivation. *eLife* **6**, doi:10.7554/eLife.29428 (2017).
125 Preissler, S. *et al.* Physiological modulation of BiP activity by trans-protomer engagement of the interdomain linker. *eLife* **4**, e08961, doi:10.7554/eLife.08961 (2015).
126 Wang, J. & Sevier, C. S. Formation and Reversibility of BiP Protein Cysteine Oxidation Facilitate Cell Survival during and post Oxidative Stress. *The Journal of biological chemistry* **291**, 7541-7557, doi:10.1074/jbc.M115.694810 (2016).
127 Wang, J., Pareja, K. A., Kaiser, C. A. & Sevier, C. S. Redox signaling via the molecular chaperone BiP protects cells against endoplasmic reticulum-derived oxidative stress. *eLife* **3**, e03496, doi:10.7554/eLife.03496 (2014).
128 Marzec, M., Eletto, D. & Argon, Y. GRP94: An HSP90-like protein specialized for protein folding and quality control in the endoplasmic reticulum. *Biochimica et biophysica acta* **1823**, 774-787, doi:10.1016/j.bbamcr.2011.10.013 (2012).
129 Huck, J. D., Que, N. L., Hong, F., Li, Z. & Gewirth, D. T. Structural and Functional Analysis of GRP94 in the Closed State Reveals an Essential Role for the Pre-N Domain and a Potential Client-Binding Site. *Cell reports* **20**, 2800-2809, doi:10.1016/j.celrep.2017.08.079 (2017).
130 Bloor, S., Maelfait, J., Krumbach, R., Beyaert, R. & Randow, F. Endoplasmic reticulum chaperone gp96 is essential for infection with vesicular stomatitis virus. *Proceedings of the National Academy of Sciences of the United States of America* **107**, 6970-6975, doi:10.1073/pnas.0908536107 (2010).

131 Randow, F. & Seed, B. Endoplasmic reticulum chaperone gp96 is required for innate immunity but not cell viability. *Nature cell biology* **3**, 891-896, doi:10.1038/ncb1001-891 (2001).
132 Wu, S. *et al.* The molecular chaperone gp96/GRP94 interacts with Toll-like receptors and integrins via its C-terminal hydrophobic domain. *The Journal of biological chemistry* **287**, 6735-6742, doi:10.1074/jbc.M111.309526 (2012).
133 Melnick, J., Aviel, S. & Argon, Y. The endoplasmic reticulum stress protein GRP94, in addition to BiP, associates with unassembled immunoglobulin chains. *The Journal of biological chemistry* **267**, 21303-21306 (1992).
134 Schopf, F. H., Biebl, M. M. & Buchner, J. The HSP90 chaperone machinery. *Nature reviews. Molecular cell biology* **18**, 345-360, doi:10.1038/nrm.2017.20 (2017).
135 Liu, B. *et al.* Folding of Toll-like receptors by the HSP90 paralogue gp96 requires a substrate-specific cochaperone. *Nat Commun* **1**, 79, doi:10.1038/ncomms1070 (2010).
136 Maharaj, K. A. *et al.* Exploring the Functional Complementation between Grp94 and Hsp90. *PloS one* **11**, e0166271-e0166271, doi:10.1371/journal.pone.0166271 (2016).
137 Sun, M., Kotler, J. L. M., Liu, S. & Street, T. O. The ER chaperones BiP and Grp94 selectively associate when BiP is in the ADP conformation. *The Journal of biological chemistry*, doi:10.1074/jbc.RA118.007050 (2019).
138 Fahey, R. C., Hunt, J. S. & Windham, G. C. On the cysteine and cystine content of proteins. Differences between intracellular and extracellular proteins. *Journal of molecular evolution* **10**, 155-160 (1977).
139 Wong, J. W., Ho, S. Y. & Hogg, P. J. Disulfide bond acquisition through eukaryotic protein evolution. *Molecular biology and evolution* **28**, 327-334, doi:10.1093/molbev/msq194 (2011).
140 Bechtel, T. J. & Weerapana, E. From structure to redox: The diverse functional roles of disulfides and implications in disease. *Proteomics* **17**, doi:10.1002/pmic.201600391 (2017).
141 Feige, M. J. & Hendershot, L. M. Disulfide bonds in ER protein folding and homeostasis. *Current opinion in cell biology* **23**, 167-175, doi:10.1016/j.ceb.2010.10.012 (2011).
142 Freedman, R. B., Klappa, P. & Ruddock, L. W. Protein disulfide isomerases exploit synergy between catalytic and specific binding domains. *EMBO reports* **3**, 136-140, doi:10.1093/embo-reports/kvf035 (2002).
143 Bekendam, R. H. *et al.* A substrate-driven allosteric switch that enhances PDI catalytic activity. *Nat Commun* **7**, 12579, doi:10.1038/ncomms12579 (2016).
144 Jansens, A., van Duijn, E. & Braakman, I. Coordinated nonvectorial folding in a newly synthesized multidomain protein. *Science (New York, N.Y.)* **298**, 2401-2403, doi:10.1126/science.1078376 (2002).
145 Ali Khan, H. & Mutus, B. Protein disulfide isomerase a multifunctional protein with multiple physiological roles. *Frontiers in chemistry* **2**, 70-70, doi:10.3389/fchem.2014.00070 (2014).
146 Walker, K. W. & Gilbert, H. F. Scanning and escape during protein-disulfide isomerase-assisted protein folding. *The Journal of biological chemistry* **272**, 8845-8848 (1997).
147 Araki, K. *et al.* Ero1-alpha and PDIs constitute a hierarchical electron transfer network of endoplasmic reticulum oxidoreductases. *The Journal of cell biology* **202**, 861-874, doi:10.1083/jcb.201303027 (2013).
148 Wang, C. *et al.* Structural insights into the redox-regulated dynamic conformations of human protein disulfide isomerase. *Antioxidants & redox signaling* **19**, 36-45, doi:10.1089/ars.2012.4630 (2013).

149 Cai, H., Wang, C. C. & Tsou, C. L. Chaperone-like activity of protein disulfide isomerase in the refolding of a protein with no disulfide bonds. *The Journal of biological chemistry* **269**, 24550-24552 (1994).
150 McLaughlin, S. H. & Bulleid, N. J. Thiol-independent interaction of protein disulphide isomerase with type X collagen during intra-cellular folding and assembly. *The Biochemical journal* **331 (Pt 3)**, 793-800 (1998).
151 Denisov, A. Y. *et al.* Solution structure of the bb' domains of human protein disulfide isomerase. *The FEBS journal* **276**, 1440-1449, doi:10.1111/j.1742-4658.2009.06884.x (2009).
152 Tu, B. P. & Weissman, J. S. The FAD- and O(2)-dependent reaction cycle of Ero1-mediated oxidative protein folding in the endoplasmic reticulum. *Molecular cell* **10**, 983-994 (2002).
153 Inaba, K. *et al.* Crystal structures of human Ero1alpha reveal the mechanisms of regulated and targeted oxidation of PDI. *The EMBO journal* **29**, 3330-3343, doi:10.1038/emboj.2010.222 (2010).
154 Tavender, T. J., Springate, J. J. & Bulleid, N. J. Recycling of peroxiredoxin IV provides a novel pathway for disulphide formation in the endoplasmic reticulum. *The EMBO journal* **29**, 4185-4197, doi:10.1038/emboj.2010.273 (2010).
155 Sato, Y. *et al.* Synergistic cooperation of PDI family members in peroxiredoxin 4-driven oxidative protein folding. *Sci Rep* **3**, 2456, doi:10.1038/srep02456 (2013).
156 Ushioda, R. *et al.* ERdj5 is required as a disulfide reductase for degradation of misfolded proteins in the ER. *Science (New York, N.Y.)* **321**, 569-572, doi:10.1126/science.1159293 (2008).
157 Ushioda, R. *et al.* Redox-assisted regulation of Ca2+ homeostasis in the endoplasmic reticulum by disulfide reductase ERdj5. *Proceedings of the National Academy of Sciences of the United States of America* **113**, E6055-e6063, doi:10.1073/pnas.1605818113 (2016).
158 Li, Y. & Camacho, P. Ca2+-dependent redox modulation of SERCA 2b by ERp57. *The Journal of cell biology* **164**, 35-46, doi:10.1083/jcb.200307010 (2004).
159 Vavassori, S. *et al.* A pH-regulated quality control cycle for surveillance of secretory protein assembly. *Molecular cell* **50**, 783-792, doi:10.1016/j.molcel.2013.04.016 (2013).
160 Watanabe, S., Harayama, M., Kanemura, S., Sitia, R. & Inaba, K. Structural basis of pH-dependent client binding by ERp44, a key regulator of protein secretion at the ER-Golgi interface. *Proceedings of the National Academy of Sciences of the United States of America* **114**, E3224-e3232, doi:10.1073/pnas.1621426114 (2017).
161 Yang, K. *et al.* Crystal Structure of the ERp44-Peroxiredoxin 4 Complex Reveals the Molecular Mechanisms of Thiol-Mediated Protein Retention. *Structure (London, England : 1993)* **24**, 1755-1765, doi:10.1016/j.str.2016.08.002 (2016).
162 Chai, Y. C., Ashraf, S. S., Rokutan, K., Johnston, R. B., Jr. & Thomas, J. A. S-thiolation of individual human neutrophil proteins including actin by stimulation of the respiratory burst: evidence against a role for glutathione disulfide. *Archives of biochemistry and biophysics* **310**, 273-281, doi:10.1006/abbi.1994.1167 (1994).
163 Birk, J. *et al.* Endoplasmic reticulum: reduced and oxidized glutathione revisited. *Journal of cell science* **126**, 1604-1617, doi:10.1242/jcs.117218 (2013).
164 van Lith, M., Tiwari, S., Pediani, J., Milligan, G. & Bulleid, N. J. Real-time monitoring of redox changes in the mammalian endoplasmic reticulum. *Journal of cell science* **124**, 2349-2356, doi:10.1242/jcs.085530 (2011).

165 Bulleid, N. J. & van Lith, M. Redox regulation in the endoplasmic reticulum. *Biochemical Society transactions* **42**, 905-908, doi:10.1042/bst20140065 (2014).
166 Tsunoda, S. *et al.* Intact protein folding in the glutathione-depleted endoplasmic reticulum implicates alternative protein thiol reductants. *eLife* **3**, e03421, doi:10.7554/eLife.03421 (2014).
167 Poet, G. J. *et al.* Cytosolic thioredoxin reductase 1 is required for correct disulfide formation in the ER. *The EMBO journal* **36**, 693-702, doi:10.15252/embj.201695336 (2017).
168 Depuydt, M. *et al.* A periplasmic reducing system protects single cysteine residues from oxidation. *Science (New York, N.Y.)* **326**, 1109-1111, doi:10.1126/science.1179557 (2009).
169 Babu, M. *et al.* Interaction landscape of membrane-protein complexes in Saccharomyces cerevisiae. *Nature* **489**, 585-589, doi:10.1038/nature11354 (2012).
170 Shiber, A. *et al.* Cotranslational assembly of protein complexes in eukaryotes revealed by ribosome profiling. *Nature* **561**, 268-272, doi:10.1038/s41586-018-0462-y (2018).
171 Shieh, Y. W. *et al.* Operon structure and cotranslational subunit association direct protein assembly in bacteria. *Science* **350**, 678-680, doi:10.1126/science.aac8171 (2015).
172 Panasenko, O. O. *et al.* Co-translational assembly of proteasome subunits in NOT1-containing assemblysomes. *Nat Struct Mol Biol* **26**, 110-120, doi:10.1038/s41594-018-0179-5 (2019).
173 Zhang, S., Xu, C., Larrimore, K. E. & Ng, D. T. W. Slp1-Emp65: A Guardian Factor that Protects Folding Polypeptides from Promiscuous Degradation. *Cell* **171**, 346-357.e312, doi:10.1016/j.cell.2017.08.036 (2017).
174 Juszkiewicz, S. & Hegde, R. S. Quality Control of Orphaned Proteins. *Molecular cell* **71**, 443-457, doi:10.1016/j.molcel.2018.07.001 (2018).
175 Christis, C., Lubsen, N. H. & Braakman, I. Protein folding includes oligomerization - examples from the endoplasmic reticulum and cytosol. *FEBS J* **275**, 4700-4727, doi:10.1111/j.1742-4658.2008.06590.x (2008).
176 Feige, M. J. *et al.* An unfolded CH1 domain controls the assembly and secretion of IgG antibodies. *Molecular cell* **34**, 569-579, doi:10.1016/j.molcel.2009.04.028 (2009).
177 Anelli, T. *et al.* Sequential steps and checkpoints in the early exocytic compartment during secretory IgM biogenesis. *The EMBO journal* **26**, 4177-4188, doi:10.1038/sj.emboj.7601844 (2007).
178 Fra, A. M., Fagioli, C., Finazzi, D., Sitia, R. & Alberini, C. M. Quality control of ER synthesized proteins: an exposed thiol group as a three-way switch mediating assembly, retention and degradation. *The EMBO journal* **12**, 4755-4761 (1993).
179 Appenzeller-Herzog, C., Roche, A. C., Nufer, O. & Hauri, H. P. pH-induced conversion of the transport lectin ERGIC-53 triggers glycoprotein release. *The Journal of biological chemistry* **279**, 12943-12950, doi:10.1074/jbc.M313245200 (2004).
180 Feige, M. J., Behnke, J., Mittag, T. & Hendershot, L. M. Dimerization-dependent folding underlies assembly control of the clonotypic alphabetaT cell receptor chains. *The Journal of biological chemistry* **290**, 26821-26831, doi:10.1074/jbc.M115.689471 (2015).
181 Christianson, J. C. & Ye, Y. Cleaning up in the endoplasmic reticulum: ubiquitin in charge. *Nature structural & molecular biology* **21**, 325-335, doi:10.1038/nsmb.2793 (2014).

182 Mehnert, M., Sommer, T. & Jarosch, E. ERAD ubiquitin ligases: multifunctional tools for protein quality control and waste disposal in the endoplasmic reticulum. *BioEssays : news and reviews in molecular, cellular and developmental biology* **32**, 905-913, doi:10.1002/bies.201000046 (2010).
183 Stefanovic-Barrett, S. *et al.* MARCH6 and TRC8 facilitate the quality control of cytosolic and tail-anchored proteins. *EMBO reports* **19**, e45603, doi:10.15252/embr.201745603 (2018).
184 Baldridge, R. D. & Rapoport, T. A. Autoubiquitination of the Hrd1 Ligase Triggers Protein Retrotranslocation in ERAD. *Cell* **166**, 394-407, doi:10.1016/j.cell.2016.05.048 (2016).
185 Carvalho, P., Stanley, A. M. & Rapoport, T. A. Retrotranslocation of a misfolded luminal ER protein by the ubiquitin-ligase Hrd1p. *Cell* **143**, 579-591, doi:10.1016/j.cell.2010.10.028 (2010).
186 Mehnert, M. *et al.* The interplay of Hrd3 and the molecular chaperone system ensures efficient degradation of malfolded secretory proteins. *Molecular biology of the cell* **26**, 185-194, doi:10.1091/mbc.E14-07-1202 (2015).
187 Stein, A., Ruggiano, A., Carvalho, P. & Rapoport, T. A. Key steps in ERAD of luminal ER proteins reconstituted with purified components. *Cell* **158**, 1375-1388, doi:10.1016/j.cell.2014.07.050 (2014).
188 Schoebel, S. *et al.* Cryo-EM structure of the protein-conducting ERAD channel Hrd1 in complex with Hrd3. *Nature* **548**, 352-355, doi:10.1038/nature23314 (2017).
189 Wiertz, E. J. *et al.* Sec61-mediated transfer of a membrane protein from the endoplasmic reticulum to the proteasome for destruction. *Nature* **384**, 432-438, doi:10.1038/384432a0 (1996).
190 Scott, D. C. & Schekman, R. Role of Sec61p in the ER-associated degradation of short-lived transmembrane proteins. *The Journal of cell biology* **181**, 1095-1105, doi:10.1083/jcb.200804053 (2008).
191 Mehnert, M., Sommer, T. & Jarosch, E. Der1 promotes movement of misfolded proteins through the endoplasmic reticulum membrane. *Nature cell biology* **16**, 77, doi:10.1038/ncb2882 (2013).
192 Bodnar, N. O. *et al.* Structure of the Cdc48 ATPase with its ubiquitin-binding cofactor Ufd1-Npl4. *Nature structural & molecular biology* **25**, 616-622, doi:10.1038/s41594-018-0085-x (2018).
193 Ernst, R. *et al.* Enzymatic blockade of the ubiquitin-proteasome pathway. *PLoS biology* **8**, e1000605, doi:10.1371/journal.pbio.1000605 (2011).
194 Bernardi, K. M., Williams, J. M., Inoue, T., Schultz, A. & Tsai, B. A deubiquitinase negatively regulates retro-translocation of nonubiquitinated substrates. *Molecular biology of the cell* **24**, 3545-3556, doi:10.1091/mbc.E13-06-0332 (2013).
195 Zhang, Z. R., Bonifacino, J. S. & Hegde, R. S. Deubiquitinases sharpen substrate discrimination during membrane protein degradation from the ER. *Cell* **154**, 609-622, doi:10.1016/j.cell.2013.06.038 (2013).
196 Harada, K., Kato, M. & Nakamura, N. USP19-Mediated Deubiquitination Facilitates the Stabilization of HRD1 Ubiquitin Ligase. *International journal of molecular sciences* **17**, doi:10.3390/ijms17111829 (2016).
197 Sato, B. K., Schulz, D., Do, P. H. & Hampton, R. Y. Misfolded membrane proteins are specifically recognized by the transmembrane domain of the Hrd1p ubiquitin ligase. *Molecular cell* **34**, 212-222, doi:10.1016/j.molcel.2009.03.010 (2009).

198 Gogala, M. *et al.* Structures of the Sec61 complex engaged in nascent peptide translocation or membrane insertion. *Nature* **506**, 107, doi:10.1038/nature12950 (2014).
199 Foresti, O., Ruggiano, A., Hannibal-Bach, H. K., Ejsing, C. S. & Carvalho, P. Sterol homeostasis requires regulated degradation of squalene monooxygenase by the ubiquitin ligase Doa10/Teb4. *eLife* **2**, e00953-e00953, doi:10.7554/eLife.00953 (2013).
200 Fleig, L. *et al.* Ubiquitin-dependent intramembrane rhomboid protease promotes ERAD of membrane proteins. *Molecular cell* **47**, 558-569, doi:10.1016/j.molcel.2012.06.008 (2012).
201 Greenblatt, E. J., Olzmann, J. A. & Kopito, R. R. Derlin-1 is a rhomboid pseudoprotease required for the dislocation of mutant alpha-1 antitrypsin from the endoplasmic reticulum. *Nature structural & molecular biology* **18**, 1147-1152, doi:10.1038/nsmb.2111 (2011).
202 Devergne, O., Birkenbach, M. & Kieff, E. Epstein-Barr virus-induced gene 3 and the p35 subunit of interleukin 12 form a novel heterodimeric hematopoietin. *Proceedings of the National Academy of Sciences of the United States of America* **94**, 12041-12046 (1997).
203 Gubler, U. *et al.* Coexpression of two distinct genes is required to generate secreted bioactive cytotoxic lymphocyte maturation factor. *Proceedings of the National Academy of Sciences of the United States of America* **88**, 4143-4147 (1991).
204 Jalah, R. *et al.* The p40 subunit of interleukin (IL)-12 promotes stabilization and export of the p35 subunit: implications for improved IL-12 cytokine production. *The Journal of biological chemistry* **288**, 6763-6776, doi:10.1074/jbc.M112.436675 (2013).
205 Pflanz, S. *et al.* IL-27, a heterodimeric cytokine composed of EBI3 and p28 protein, induces proliferation of naive CD4(+) T cells. *Immunity* **16**, 779-790, doi:S1074761302003242 [pii] (2002).
206 McLaughlin, M. *et al.* Inhibition of Secretion of Interleukin (IL)-12/IL-23 Family Cytokines by 4-Trifluoromethyl-celecoxib Is Coupled to Degradation via the Endoplasmic Reticulum Stress Protein HERP. *Journal of Biological Chemistry* **285**, 6960-6969, doi:10.1074/jbc.M109.056614 (2010).
207 Alloza, I., Baxter, A., Chen, Q., Matthiesen, R. & Vandenbroeck, K. Celecoxib inhibits interleukin-12 alphabeta and beta2 folding and secretion by a novel COX2-independent mechanism involving chaperones of the endoplasmic reticulum. *Mol Pharmacol* **69**, 1579-1587, doi:mol.105.020669 [pii] 10.1124/mol.105.020669 (2006).
208 Reitberger, S., Haimerl, P., Aschenbrenner, I., Esser-von Bieren, J. & Feige, M. J. Assembly-induced folding regulates interleukin 12 biogenesis and secretion. *The Journal of biological chemistry* **292**, 8073-8081, doi:10.1074/jbc.M117.782284 (2017).
209 Ellgaard, L., McCaul, N., Chatsisvili, A. & Braakman, I. Co- and Post-Translational Protein Folding in the ER. *Traffic* **17**, 615-638, doi:10.1111/tra.12392 (2016).
210 Hendershot, L., Bole, D., Kohler, G. & Kearney, J. F. Assembly and secretion of heavy chains that do not associate posttranslationally with immunoglobulin heavy chain-binding protein. *J Cell Biol* **104**, 761-767 (1987).
211 Lee, Y. K., Brewer, J. W., Hellman, R. & Hendershot, L. M. BiP and immunoglobulin light chain cooperate to control the folding of heavy chain and ensure the fidelity of immunoglobulin assembly. *Mol Biol Cell* **10**, 2209-2219 (1999).
212 Corper, A. L. *et al.* Structure of human IgM rheumatoid factor Fab bound to its autoantigen IgG Fc reveals a novel topology of antibody-antigen interaction. *Nat Struct Biol* **4**, 374-381 (1997).

213 Muller, R. *et al.* High-resolution structures of the IgM Fc domains reveal principles of its hexamer formation. *Proceedings of the National Academy of Sciences of the United States of America* **110**, 10183-10188, doi:10.1073/pnas.1300547110 (2013).
214 Sitia, R. *et al.* Developmental regulation of IgM secretion: the role of the carboxy-terminal cysteine. *Cell* **60**, 781-790 (1990).
215 Schamel, W. W. *et al.* A high-molecular-weight complex of membrane proteins BAP29/BAP31 is involved in the retention of membrane-bound IgD in the endoplasmic reticulum. *Proc Natl Acad Sci U S A* **100**, 9861-9866, doi:10.1073/pnas.1633363100 1633363100 [pii] (2003).
216 Feige, M. J. & Hendershot, L. M. Quality control of integral membrane proteins by assembly-dependent membrane integration. *Mol Cell* **51**, 297-309, doi:10.1016/j.molcel.2013.07.013 (2013).
217 Fayadat, L. & Kopito, R. R. Recognition of a single transmembrane degron by sequential quality control checkpoints. *Mol Biol Cell* **14**, 1268-1278, doi:10.1091/mbc.E02-06-0363 (2003).
218 Suzuki, C. K., Bonifacino, J. S., Lin, A. Y., Davis, M. M. & Klausner, R. D. Regulating the retention of T-cell receptor alpha chain variants within the endoplasmic reticulum: Ca(2+)-dependent association with BiP. *J Cell Biol* **114**, 189-205 (1991).
219 Manolios, N., Letourneur, F., Bonifacino, J. S. & Klausner, R. D. Pairwise, cooperative and inhibitory interactions describe the assembly and probable structure of the T-cell antigen receptor. *EMBO J* **10**, 1643-1651 (1991).
220 Call, M. E., Pyrdol, J., Wiedmann, M. & Wucherpfennig, K. W. The organizing principle in the formation of the T cell receptor-CD3 complex. *Cell* **111**, 967-979, doi:S0092867402011947 [pii] (2002).
221 Geisler, C., Kuhlmann, J. & Rubin, B. Assembly, intracellular processing, and expression at the cell surface of the human alpha beta T cell receptor/CD3 complex. Function of the CD3-zeta chain. *J Immunol* **143**, 4069-4077 (1989).
222 Gearing, D. P. & Cosman, D. Homology of the p40 subunit of natural killer cell stimulatory factor (NKSF) with the extracellular domain of the interleukin-6 receptor. *Cell* **66**, 9-10 (1991).
223 Yoon, C. *et al.* Charged residues dominate a unique interlocking topography in the heterodimeric cytokine interleukin-12. *The EMBO journal* **19**, 3530-3541, doi:10.1093/emboj/19.14.3530 (2000).
224 Dixon, K. O., van der Kooij, S. W., Vignali, D. A. & van Kooten, C. Human tolerogenic dendritic cells produce IL-35 in the absence of other IL-12 family members. *European journal of immunology* **45**, 1736-1747, doi:10.1002/eji.201445217 (2015).
225 Teng, M. W. *et al.* IL-12 and IL-23 cytokines: from discovery to targeted therapies for immune-mediated inflammatory diseases. *Nat Med* **21**, 719-729, doi:10.1038/nm.3895 (2015).
226 Trinchieri, G., Pflanz, S. & Kastelein, R. A. The IL-12 family of heterodimeric cytokines: new players in the regulation of T cell responses. *Immunity* **19**, 641-644, doi:S1074761303002966 [pii] (2003).
227 Kobayashi, M. *et al.* Identification and purification of natural killer cell stimulatory factor (NKSF), a cytokine with multiple biologic effects on human lymphocytes. *J Exp Med* **170**, 827-845 (1989).
228 Stern, A. S. *et al.* Purification to homogeneity and partial characterization of cytotoxic lymphocyte maturation factor from human B-lymphoblastoid cells. *Proceedings of the National Academy of Sciences of the United States of America* **87**, 6808-6812 (1990).

229 Ma, X. *et al.* Regulation of IL-10 and IL-12 production and function in macrophages and dendritic cells. *F1000Res* **4**, doi:10.12688/f1000research.7010.1 (2015).
230 Kulig, P. *et al.* IL-12 protects from psoriasiform skin inflammation. *Nat Commun* **7**, 13466, doi:10.1038/ncomms13466 (2016).
231 Wolf, S. F. *et al.* Cloning of cDNA for natural killer cell stimulatory factor, a heterodimeric cytokine with multiple biologic effects on T and natural killer cells. *Journal of immunology* **146**, 3074-3081 (1991).
232 Ling, P. *et al.* Human IL-12 p40 homodimer binds to the IL-12 receptor but does not mediate biologic activity. *Journal of immunology* **154**, 116-127 (1995).
233 Carra, G., Gerosa, F. & Trinchieri, G. Biosynthesis and posttranslational regulation of human IL-12. *Journal of immunology* **164**, 4752-4761, doi:ji_v164n9p4752 [pii] (2000).
234 D'Andrea, A. *et al.* Production of natural killer cell stimulatory factor (interleukin 12) by peripheral blood mononuclear cells. *J Exp Med* **176**, 1387-1398 (1992).
235 Aparicio-Siegmund, S. *et al.* Recombinant p35 from bacteria can form Interleukin (IL-)12, but Not IL-35. *PLoS One* **9**, e107990, doi:10.1371/journal.pone.0107990 (2014).
236 Braakman, I. & Hebert, D. N. Analysis of disulfide bond formation. *Curr Protoc Protein Sci* **Chapter 14**, Unit14 11, doi:10.1002/0471140864.ps1401s03 (2001).
237 Otero, J. H., Lizak, B. & Hendershot, L. M. Life and death of a BiP substrate. *Semin Cell Dev Biol* **21**, 472-478, doi:S1084-9521(09)00253-5 [pii] 10.1016/j.semcdb.2009.12.008 (2010).
238 Abdi, K. *et al.* Free IL-12p40 monomer is a polyfunctional adaptor for generating novel IL-12-like heterodimers extracellularly. *Journal of immunology* **192**, 6028-6036, doi:10.4049/jimmunol.1400159 (2014).
239 Mattner, F. *et al.* The interleukin-12 subunit p40 specifically inhibits effects of the interleukin-12 heterodimer. *European journal of immunology* **23**, 2202-2208, doi:10.1002/eji.1830230923 (1993).
240 Hurtley, S. M. & Helenius, A. Protein oligomerization in the endoplasmic reticulum. *Annu Rev Cell Biol* **5**, 277-307, doi:10.1146/annurev.cb.05.110189.001425 (1989).
241 Leitzgen, K., Knittler, M. R. & Haas, I. G. Assembly of immunoglobulin light chains as a prerequisite for secretion. A model for oligomerization-dependent subunit folding. *J Biol Chem* **272**, 3117-3123 (1997).
242 Kosuri, P. *et al.* Protein folding drives disulfide formation. *Cell* **151**, 794-806, doi:10.1016/j.cell.2012.09.036 (2012).
243 Qin, M., Wang, W. & Thirumalai, D. Protein folding guides disulfide bond formation. *Proceedings of the National Academy of Sciences of the United States of America* **112**, 11241-11246, doi:10.1073/pnas.1503909112 (2015).
244 Oka, O. B., Pringle, M. A., Schopp, I. M., Braakman, I. & Bulleid, N. J. ERdj5 is the ER reductase that catalyzes the removal of non-native disulfides and correct folding of the LDL receptor. *Mol Cell* **50**, 793-804, doi:10.1016/j.molcel.2013.05.014 (2013).
245 Tannous, A., Pisoni, G. B., Hebert, D. N. & Molinari, M. N-linked sugar-regulated protein folding and quality control in the ER. *Semin Cell Dev Biol* **41**, 79-89, doi:10.1016/j.semcdb.2014.12.001 (2015).
246 Hernandez-Alcoceba, R., Poutou, J., Ballesteros-Briones, M. C. & Smerdou, C. Gene therapy approaches against cancer using in vivo and ex vivo gene transfer of interleukin-12. *Immunotherapy* **8**, 179-198, doi:10.2217/imt.15.109 (2016).
247 Yeku, O. O. & Brentjens, R. J. Armored CAR T-cells: utilizing cytokines and pro-inflammatory ligands to enhance CAR T-cell anti-tumour efficacy. *Biochem Soc Trans* **44**, 412-418, doi:10.1042/BST20150291 (2016).

248 McLaughlin, M. & Vandenbroeck, K. The endoplasmic reticulum protein folding factory and its chaperones: new targets for drug discovery? *Br J Pharmacol* **162**, 328-345, doi:10.1111/j.1476-5381.2010.01064.x (2011).
249 Havugimana, P. C. *et al.* A census of human soluble protein complexes. *Cell* **150**, 1068-1081, doi:10.1016/j.cell.2012.08.011 (2012).
250 Krogan, N. J. *et al.* Global landscape of protein complexes in the yeast Saccharomyces cerevisiae. *Nature* **440**, 637-643, doi:10.1038/nature04670 (2006).
251 Gavin, A. C. *et al.* Proteome survey reveals modularity of the yeast cell machinery. *Nature* **440**, 631-636, doi:10.1038/nature04532 (2006).
252 Balchin, D., Hayer-Hartl, M. & Hartl, F. U. In vivo aspects of protein folding and quality control. *Science* **353**, aac4354, doi:10.1126/science.aac4354 (2016).
253 McShane, E. *et al.* Kinetic Analysis of Protein Stability Reveals Age-Dependent Degradation. *Cell* **167**, 803-815.e821, doi:10.1016/j.cell.2016.09.015 (2016).
254 Hauser, T., Popilka, L., Hartl, F. U. & Hayer-Hartl, M. Role of auxiliary proteins in Rubisco biogenesis and function. *Nature plants* **1**, 15065, doi:10.1038/nplants.2015.65 (2015).
255 Pena, C., Hurt, E. & Panse, V. G. Eukaryotic ribosome assembly, transport and quality control. *Nat Struct Mol Biol* **24**, 689-699, doi:10.1038/nsmb.3454 (2017).
256 Hartl, F. U. & Hayer-Hartl, M. Converging concepts of protein folding in vitro and in vivo. *Nat Struct Mol Biol* **16**, 574-581, doi:nsmb.1591 [pii] 10.1038/nsmb.1591 (2009).
257 Hagn, F. *et al.* Structural analysis of the interaction between Hsp90 and the tumor suppressor protein p53. *Nat Struct Mol Biol* **18**, 1086-1093, doi:10.1038/nsmb.2114 (2011).
258 Rodriguez, F. *et al.* Molecular basis for regulation of the heat shock transcription factor sigma32 by the DnaK and DnaJ chaperones. *Mol Cell* **32**, 347-358, doi:10.1016/j.molcel.2008.09.016 (2008).
259 Balchin, D., Milicic, G., Strauss, M., Hayer-Hartl, M. & Hartl, F. U. Pathway of Actin Folding Directed by the Eukaryotic Chaperonin TRiC. *Cell* **174**, 1507-1521.e1516, doi:10.1016/j.cell.2018.07.006 (2018).
260 Salmon, L. *et al.* Capturing a Dynamic Chaperone-Substrate Interaction Using NMR-Informed Molecular Modeling. *J Am Chem Soc* **138**, 9826-9839, doi:10.1021/jacs.6b02382 (2016).
261 Karagoz, G. E. *et al.* Hsp90-Tau complex reveals molecular basis for specificity in chaperone action. *Cell* **156**, 963-974, doi:10.1016/j.cell.2014.01.037 (2014).
262 Cua, D. J. *et al.* Interleukin-23 rather than interleukin-12 is the critical cytokine for autoimmune inflammation of the brain. *Nature* **421**, 744-748, doi:10.1038/nature01355 (2003).
263 Feige, M. J. *Oxidative Folding of Proteins: Basic Principles, Cellular Regulation and Engineering*. (RSC publishing, 2018).
264 Appenzeller-Herzog, C. & Ellgaard, L. The human PDI family: versatility packed into a single fold. *Biochim Biophys Acta* **1783**, 535-548, doi:10.1016/j.bbamcr.2007.11.010 (2008).
265 Anelli, T. *et al.* Thiol-mediated protein retention in the endoplasmic reticulum: the role of ERp44. *EMBO J* **22**, 5015-5022, doi:10.1093/emboj/cdg491 (2003).
266 Huang, P. S. *et al.* RosettaRemodel: a generalized framework for flexible backbone protein design. *PLoS One* **6**, e24109, doi:10.1371/journal.pone.0024109 (2011).
267 Desmet, J. *et al.* Structural basis of IL-23 antagonism by an Alphabody protein scaffold. *Nat Commun* **5**, 5237, doi:10.1038/ncomms6237 (2014).

268 Watters, A. L. *et al.* The highly cooperative folding of small naturally occurring proteins is likely the result of natural selection. *Cell* **128**, 613-624, doi:10.1016/j.cell.2006.12.042 (2007).
269 Lyman, S. K. & Schekman, R. Binding of secretory precursor polypeptides to a translocon subcomplex is regulated by BiP. *Cell* **88**, 85-96 (1997).
270 Anelli, T. *et al.* ERp44, a novel endoplasmic reticulum folding assistant of the thioredoxin family. *Embo j* **21**, 835-844, doi:10.1093/emboj/21.4.835 (2002).
271 Buck, T. M., Kolb, A. R., Boyd, C. R., Kleyman, T. R. & Brodsky, J. L. The endoplasmic reticulum-associated degradation of the epithelial sodium channel requires a unique complement of molecular chaperones. *Mol Biol Cell* **21**, 1047-1058, doi:10.1091/mbc.E09-11-0944 (2010).
272 Buck, T. M. *et al.* The Lhs1/GRP170 chaperones facilitate the endoplasmic reticulum-associated degradation of the epithelial sodium channel. *J Biol Chem* **288**, 18366-18380, doi:10.1074/jbc.M113.469882 (2013).
273 Dong, M., Bridges, J. P., Apsley, K., Xu, Y. & Weaver, T. E. ERdj4 and ERdj5 are required for endoplasmic reticulum-associated protein degradation of misfolded surfactant protein C. *Mol Biol Cell* **19**, 2620-2630, doi:10.1091/mbc.E07-07-0674 (2008).
274 Watanabe, S. *et al.* Zinc regulates ERp44-dependent protein quality control in the early secretory pathway. *Nat Commun* **10**, 603, doi:10.1038/s41467-019-08429-1 (2019).
275 Haase, H. & Rink, L. Zinc signals and immune function. *BioFactors (Oxford, England)* **40**, 27-40, doi:10.1002/biof.1114 (2014).
276 Doi, T., Hara, H., Kajita, M., Kamiya, T. & Adachi, T. Zinc regulates expression of IL-23 p19 mRNA via activation of eIF2alpha/ATF4 axis in HAPI cells. *Biometals : an international journal on the role of metal ions in biology, biochemistry, and medicine* **28**, 891-902, doi:10.1007/s10534-015-9874-4 (2015).
277 Garbers, C. *et al.* An interleukin-6 receptor-dependent molecular switch mediates signal transduction of the IL-27 cytokine subunit p28 (IL-30) via a gp130 protein receptor homodimer. *J Biol Chem* **288**, 4346-4354, doi:10.1074/jbc.M112.432955 (2013).
278 Bloch, Y. *et al.* Structural Activation of Pro-inflammatory Human Cytokine IL-23 by Cognate IL-23 Receptor Enables Recruitment of the Shared Receptor IL-12Rbeta1. *Immunity*, doi:10.1016/j.immuni.2017.12.008 (2017).
279 Hendershot, L. *et al.* Inhibition of immunoglobulin folding and secretion by dominant negative BiP ATPase mutants. *Proceedings of the National Academy of Sciences of the United States of America* **93**, 5269-5274 (1996).
280 Hendershot, L. M. *et al.* In vivo expression of mammalian BiP ATPase mutants causes disruption of the endoplasmic reticulum. *Mol Biol Cell* **6**, 283-296 (1995).
281 Englander, S. W. & Kallenbach, N. R. Hydrogen exchange and structural dynamics of proteins and nucleic acids. *Quarterly reviews of biophysics* **16**, 521-655 (1983).
282 Wales, T. E. & Engen, J. R. Hydrogen exchange mass spectrometry for the analysis of protein dynamics. *Mass spectrometry reviews* **25**, 158-170, doi:10.1002/mas.20064 (2006).
283 Dam, J., Velikovsky, C. A., Mariuzza, R. A., Urbanke, C. & Schuck, P. Sedimentation velocity analysis of heterogeneous protein-protein interactions: Lamm equation modeling and sedimentation coefficient distributions c(s). *Biophys J* **89**, 619-634, doi:10.1529/biophysj.105.059568 (2005).
284 Harding, S. E., Rowe, A. J. & Horton, J. C. (eds S. E. Harding, Arthur J. Rowe, & J. C. Horton) (Royal Society of Chemistry, Cambridge [England] :, 1992).

285 Vranken, W. F. *et al.* The CCPN data model for NMR spectroscopy: development of a software pipeline. *Proteins* **59**, 687-696, doi:10.1002/prot.20449 (2005).
286 Lupardus, P. J. & Garcia, K. C. The structure of interleukin-23 reveals the molecular basis of p40 subunit sharing with interleukin-12. *Journal of molecular biology* **382**, 931-941, doi:10.1016/j.jmb.2008.07.051 (2008).
287 McLaughlin, M. *et al.* Inhibition of secretion of interleukin (IL)-12/IL-23 family cytokines by 4-trifluoromethyl-celecoxib is coupled to degradation via the endoplasmic reticulum stress protein HERP. *The Journal of biological chemistry* **285**, 6960-6969, doi:10.1074/jbc.M109.056614 (2010).